UNIVERSITÀ
DEGLI STUDI
DI PADOVA

DIPARTIMENTO
DI INGEGNERIA
DELL'INFORMAZIONE

DIPARTIMENTO DI INGEGNERIA DELL'INFORMAZIONE

CORSO DI LAUREA MAGISTRALE IN BIOINGEGNERIA INDUSTRIALE

MECHANICAL VS KINEMATIC ALIGNMENT IN TOTAL KNEE ARTHROPLASTY: AN IN-SILICO BIOMECHANICAL ANALYSIS

Relatore: *Prof. Piero Pavan*
Correlatore: *Prof.ssa Silvia Todros*
Correlatore: *Prof. Bernardo Innocenti*

Laureando: *Filippo Carpanese*

ANNO ACCADEMICO 2022 - 2023

Data di laurea 20/10/2023

Abstract

Mechanical alignment is a method used to achieve a neutral hip-knee-ankle axis. Kinematic alignment, on the other hand, is an alternative technique in Total Knee Arthroplasty (TKA) that aims to preserve the natural kinematic axis and ligament balance of the patient's knee.

The purpose of this study is to biomechanically compare the effect of mechanical and kinematic alignment on a knee after TKA.

In-silico models are often used to study knee kinematics in healthy or pathological conditions.

An anatomical model of the native knee was created by segmenting CT images of the femur, patella and tibia. Additionally, the model incorporated the medial collateral ligament (MCL), lateral collateral ligament (LCL), medial patellofemoral ligament (MPFL), lateral retinaculum, and patellar tendon to achieve a comprehensive joint representation.

Ligaments of knee joint were modelled using two-dimensional shell elements.

Two three-dimensional knee models based on the native knee derived from segmentation were implemented to simulate the two different surgical techniques, mechanical alignment and kinematic alignment.

To evaluate the performance of the models, a squat movement from 0 to 120 degrees was simulated.

The study focused on the patellofemoral and tibiofemoral joints, analysing the kinematics of the two joints as well as the contact areas and contact forces in the two alignment approaches.

In conclusion, this study highlighted the potential benefits of achieving a joint line restoration closely aligned with its natural position, which may lead to superior clinical outcomes in kinematically aligned TKA. However, the persistence of patellofemoral complications remains a concern, especially when using conventional implants designed for mechanical alignment in the kinematic alignment approach.

Riassunto

L'allineamento meccanico è un metodo utilizzato per ottenere un asse anca-ginocchio-caviglia neutro. L'allineamento cinematico, invece, è una tecnica alternativa nell'artroplastica totale del ginocchio (TKA) che mira a preservare l'asse cinematico naturale e l'equilibrio legamentoso del ginocchio del paziente.

Lo scopo di questo studio è quello di confrontare biomeccanicamente l'effetto dell'allineamento meccanico e cinematico su un ginocchio dopo la TKA.

I modelli in-silico sono spesso utilizzati per studiare la cinematica del ginocchio in condizioni sane o patologiche.

È stato creato un modello anatomico del ginocchio nativo segmentando le immagini TC di femore, rotula e tibia. Inoltre, sono stati inclusi nel modello il legamento collaterale mediale (MCL), il legamento collaterale laterale (LCL), il legamento patellofemorale mediale (MPFL), il retinacolo laterale e il tendine rotuleo per ottenere una rappresentazione completa dell'articolazione.

I legamenti dell'articolazione del ginocchio sono stati modellati utilizzando elementi shell bidimensionali.

Sono stati implementati due modelli di ginocchio tridimensionali basati sul ginocchio nativo derivato dalla segmentazione per simulare le due diverse tecniche chirurgiche, l'allineamento meccanico e l'allineamento cinematico. Per valutare le prestazioni dei modelli, è stato simulato un movimento di squat da 0 a 120 gradi.

Lo studio si è concentrato sulle articolazioni patellofemorale e tibiofemorale, analizzando la cinematica delle due articolazioni oltre alle aree di contatto e le forze di contatto nei due approcci di allineamento.

In conclusione, questo studio evidenzia i potenziali vantaggi di ripristinare la *joint line*, allineandola alla sua posizione naturale, che può portare a risultati clinici superiori nella TKA ad allineamento cinematico. Tuttavia, la persistenza di complicazioni patellofemorali rimane un’incertezza, soprattutto quando si utilizzano impianti convenzionali progettati per l'allineamento meccanico applicati per mezzo dell'approccio di allineamento cinematico.

Summary

Introduction

Osteoarthritis is the prevailing joint disease in the elderly population, with a higher incidence observed in the knee compared to the hip and ankle joints. In contemporary medical practise, the primary approach for addressing severe joint conditions involves total knee arthroplasty (TKA), which aims to correct deformities, improve joint functionality, and alleviate joint pain. The 2022 annual report from the American Joint Replacement Registry presents comprehensive data collected between 2012 and 2021, encompassing over 2.8 million patients. In particular, 51.2% of these surgical procedures were related to TKA.

For over three decades, conventional mechanical alignment has been the prevailing technique employed in TKA, and it is still very common worldwide. This method consists of achieving a neutral alignment of the hip-knee-ankle axis, under the presumption that it is fundamental for achieving optimal postoperative functional recovery after TKA.

However, the evolution of multiple biomechanical researches has led many studies to question the completeness of mechanical alignment in restoring the natural lower limb alignment. Evidence suggests that it can alter the typical kinematics of knee movement, which could contribute to severe complications.

Kinematic alignment, introduced in 2006 by the studies of Howell et al., differs from mechanical alignment by predominantly focusing on the three-dimensional alignment of prosthetic components relative to the knee. The central objective is to manage the kinematics of the patella and tibia relative to the femur by restoring the three-dimensional alignment characteristic of the native articulation, rather than aiming for a neutral hip-knee-ankle angle.

Several studies have indicated that kinematic alignment is more likely to restore normal knee kinematics and yields favourable clinical outcomes compared to mechanical alignment. It may therefore result in an enhanced quality of life of the patients, an increased range of motion of the joint, and a decreased prevalence of pain, joint stiffness, and instability. However, it is important to acknowledge that kinematic alignment may present potential issues, including an elevated risk of patellar instability and polyethylene wear.

This study aims to compare these two surgical approaches from a biomechanical perspective by studying two models representing the two different surgical approaches using a finite elements method.

Chapter 1

Anatomy of the knee joint

The knee, considered the most complex synovial joint in the human body, is formed through the articulation of the femur, tibia, and patella bones of the lower limb. It can be conceptualised as comprising two distinct joints: the tibiofemoral joint and the patellofemoral joint [1].

The joint between the lateral tibial condyle and the proximal fibula (called the proximal tibiofibular joint) is a synovial plane joint (arthrodial joint); however, this joint is generally ignored when it comes to the biomechanics of the knee joint [2].

The tibiofemoral joint, which is the main load bearing joint of the knee, plays a key role in supporting body weight and facilitating the various movements of the lower limb. Its main function is to enable the transmission of forces between the femur and the tibia while providing stability and mobility to the knee joint. Furthermore, the tibiofemoral joint acts as a shock absorber, dispersing the impact forces generated during loading activities.

The main function of the patellofemoral joint, on the other hand, is to facilitate gliding and proper tracking of the patella during movement along the femoral groove during knee flexion and extension. It also acts as a pulley system, increasing the leverage of the quadriceps muscles and improving their ability to enable the knee to extend. It also helps to distribute evenly forces on the knee joint during activities such as walking, running, jumping, and climbing stairs.

In general, the knee joint is a complex structure that plays a critical role in weight bearing and locomotion. Its stability is maintained by a sophisticated system of ligaments, tendons, and muscles and is subject to various injuries and disorders that require careful management and treatment.

Articular cartilage that covers the surfaces of the femur and tibia helps reduce friction and provides a smooth sliding surface for the bones, minimising wear and tear. The knee joint is surrounded by a joint capsule consisting of an outer fibrous layer and an inner synovial membrane that has the main function of secreting synovial fluid to lubricate the articulation.

Several ligaments stabilise the knee joint, including the medial collateral ligament (MCL), lateral collateral ligament (LCL), anterior cruciate ligament (ACL), and posterior cruciate ligament (PCL). MCL and LCL provide medial and lateral stability to the joint, respectively, while ACL and PCL prevent anterior and posterior translation of the tibia relative to the femur.

In addition to ligaments, the knee joint is supported by several muscles, such as the quadriceps, hamstrings, and calf muscles. These muscles work together to provide dynamic stability to the joint during movement [2], [3].

1.1 Bones

1.1.1 Femur

The femur is the longest and strongest bone in the human body. This bone is articulated proximally with the pelvic bone and distally with the patella and the proximal portion of the tibia.

At the proximal epiphysis it has a spheroidal head that articulates with the acetabulum on the superomedial side of the bone (Fig. 1.1). Distally, the femur has two convex surfaces called condyles that allow it to articulate with the proximal epiphysis of the tibia. On the posterior surface, they are separated by the intercondylar fossa. However, anteriorly, the condyles converge in the trochlear groove, allowing the femur to articulate with the patella, guiding the latter between the two prominences during flexion movements.

Both condyles have a spheroidal conformation but differ in both profile and anatomical positioning. The medial condyle, compared to the lateral, is elliptical in shape and has a more distal position. The lateral has a smaller posterior offset compared to its respective medial. Distally, it has a less rounded conformation, whereas the posterior aspect has a more spherical conformation.

Each condyle has a convexity called the medial and lateral epicondyle, respectively, which provides the insertions for the respective collateral ligaments.

The groove and femoral condyles are covered with articular cartilage, which allows for proper interaction with the posterior surface of the patella and tibial condyles, respectively [2], [3].

1.1.2 Tibia

The tibia is located medially respect to the fibula and extends between its smaller distal end, which projects downward toward the medial malleolus, and its proximal end at the interface with the femur (Fig. 1.2).

The proximal epiphysis consists of two plateaus separated by the intercondylar eminence that includes the medial and lateral tibial tubercles, which serve as the insertion point for the cruciate ligaments.

Morphologically, both plateaus are concave in the mediolateral direction; in the anteroposterior direction, however, the medial plateau is concave, in contrast to the lateral plateau, which appears convex, facilitating mobility in the joint.

Congruent with the femoral condyle, the medial tibial condyle is also elliptical in shape, has a larger articular surface area, and is up to three times thicker. The lateral counterpart has a more rounded shape and a smaller and less thick surface area as a result of the lower laterally induced forces that affect the femur.

The anterior condylar surfaces join inferiorly to form the tibial tuberosity, divided into a wrinkled lower region and a smooth upper region.

When viewed from the side, the tibia is not orthogonal to the femur, but has a posterior slope. This feature facilitates translational movements of the lateral portion of the bone, preventing dislocation [2], [3].

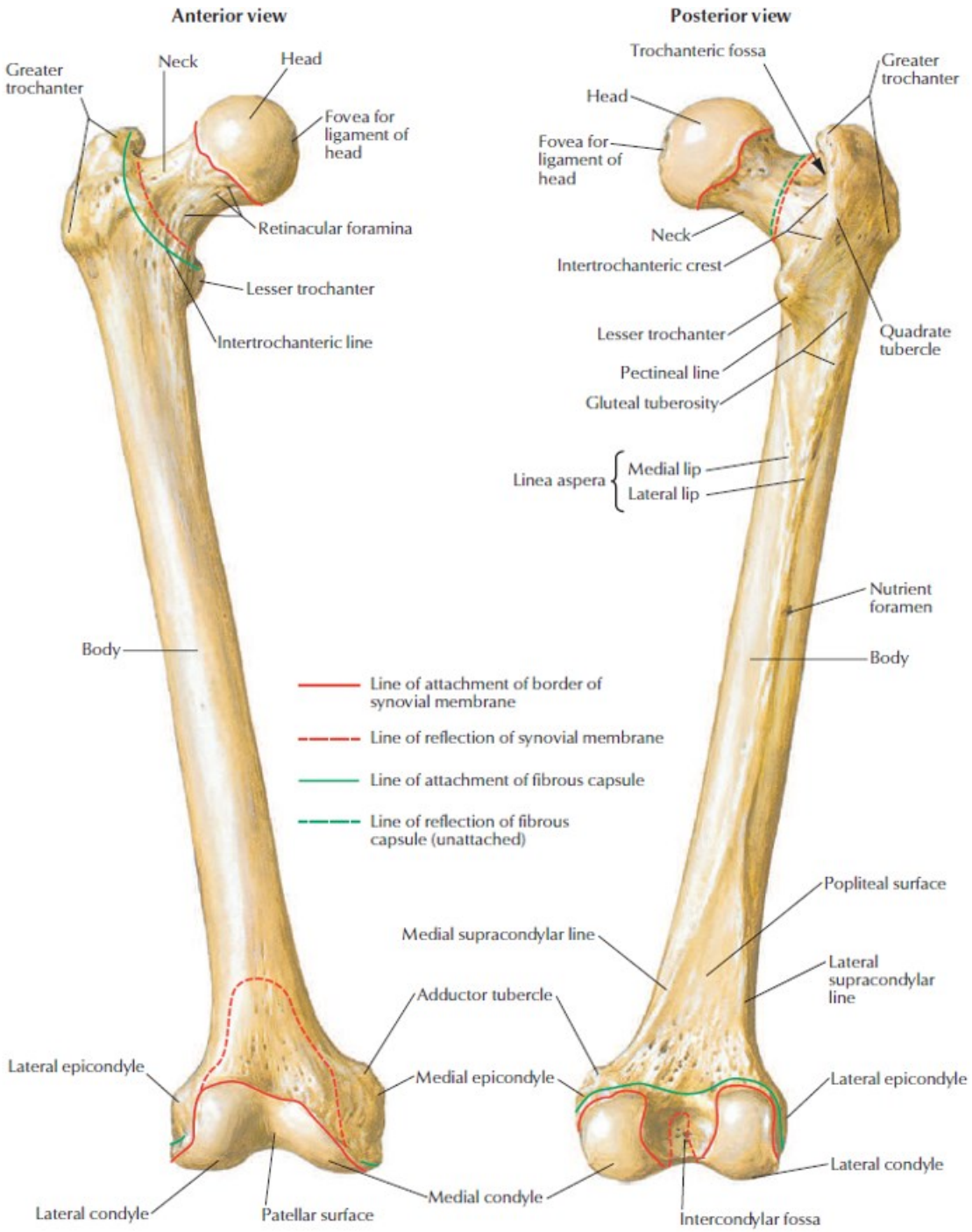

Figure 1.1: Anterior view and posterior view of the femoral bone [4].

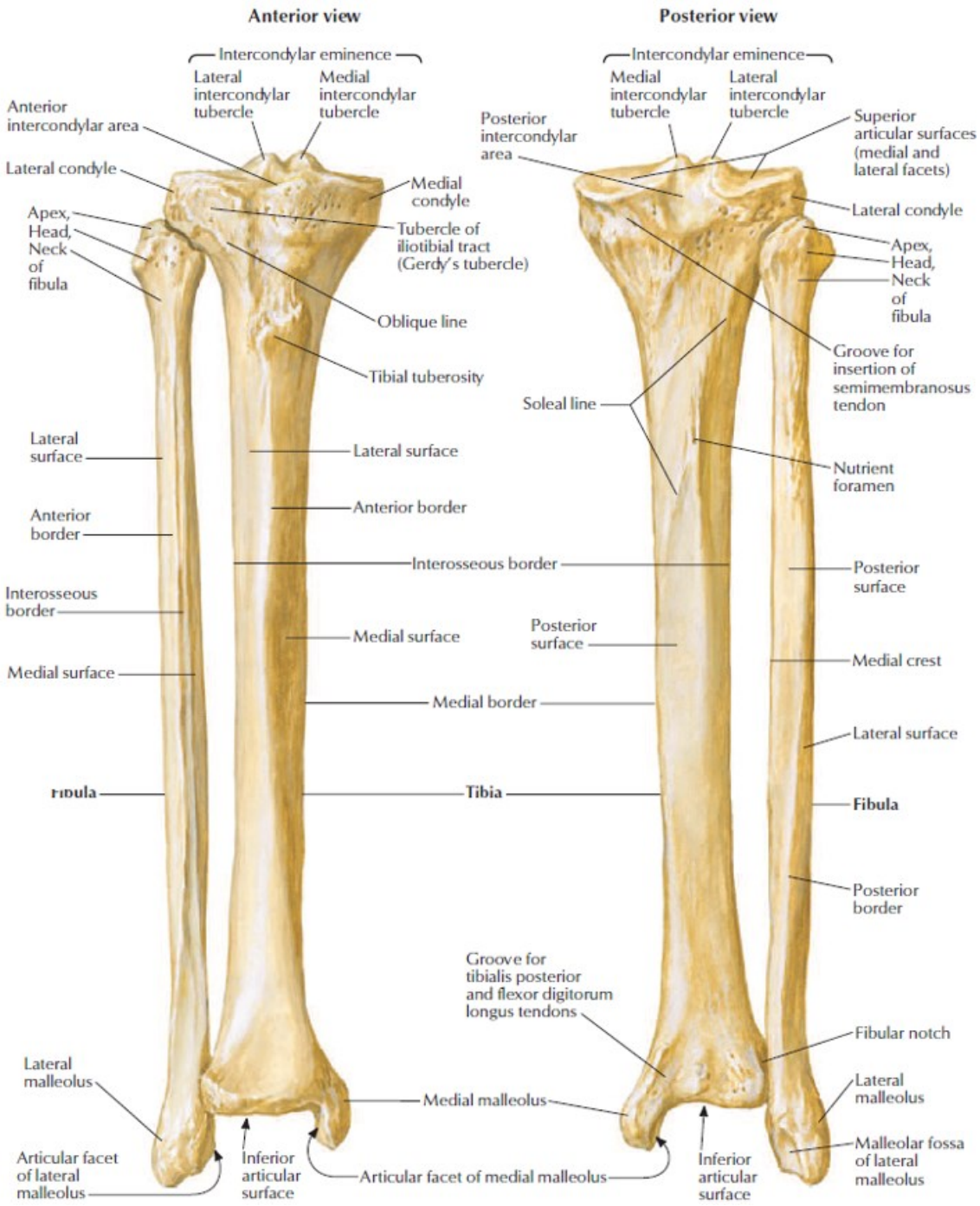

Figure 1.2: Anterior view and posterior view of the tibia [4].

1.1.3 Patella

The patella is the largest sesamoid bone in the human body and is anterior to the distal portion of the femur, the condyles. It can be roughly defined as triangular in shape because it has a proximal curved surface, which forms the upper aspect of the bone, and a distal termination consisting of its tapered apex (Fig. 1.3).

When the knee is extended, the inferior pole of the patella, also defined as the apex, is anteroproximal to the knee joint rhyme.

The anterior convex surface is embedded in the quadriceps femoris tendon, which extends distally into the patellar tendon (Fig. 1.4 A).

The posterior surface, covered by articular cartilage, is crossed by a vertical edge that divides the posterior surface into two facets, the medial and the lateral. This edge inserts into the intercondylar groove, articulating the patella with the femur.

The articular cartilage is the thickest in the body due to the high amount of stress it is subjected to.

The main function of the patella is to increase the moment arm of the quadriceps, therefore to improve the efficiency of the muscle during knee extension. The efficiency of the extensor mechanism increases 1.5 times because of the patella's presence. Another significant function of the patella is to protect the distal aspect of the femur from possible traumas and the quadriceps from tear or wear [2], [3].

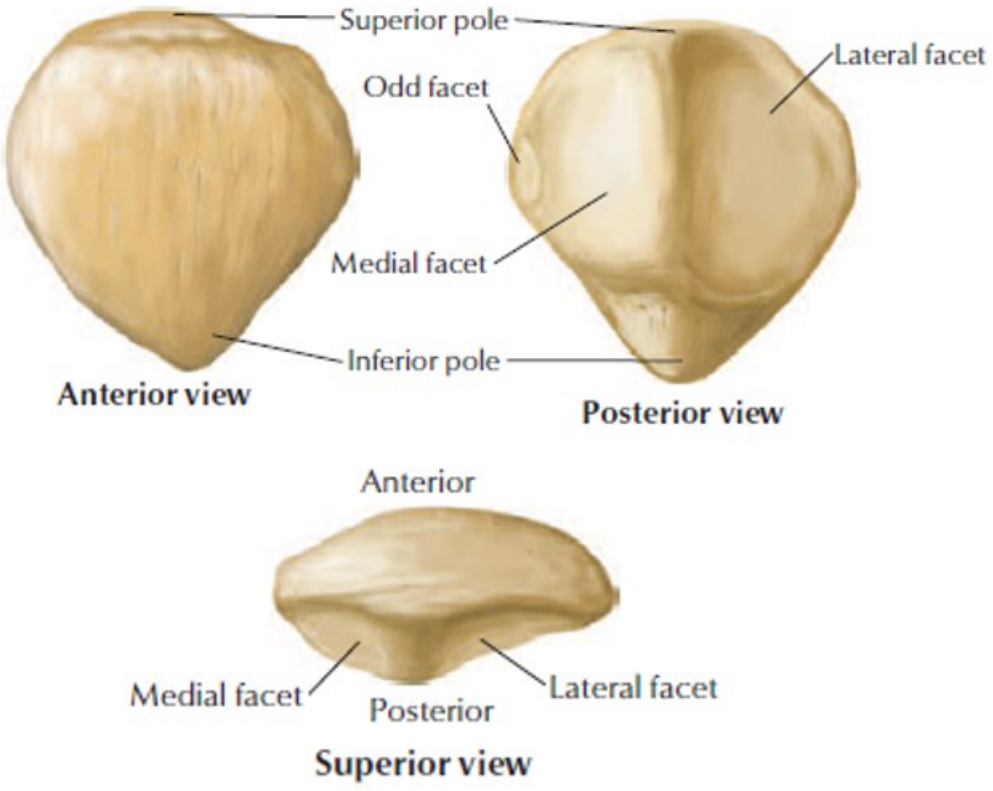

Figure 1.3: Patellar bone: anterior view, posterior view and superior view of the sesamoid bone [4].

1.2 Ligaments

The knee joint is supported by a complex network of ligaments that play a crucial role in maintaining its stability and function. Within this intricate network of connective tissues, several key ligaments stand out as the main contributors to knee stability. The main ligaments involved in providing stability to the tibiofemoral joint include the anterior cruciate ligament (ACL), the posterior cruciate ligament (PCL), the medial collateral ligament (MCL), and the lateral collateral ligament (LCL). Additionally, the medial patellofemoral ligament (MPFL), lateral patellar retinaculum (LR), patellar ligament, and quadriceps femoris tendon provide support and stability to the patellofemoral joint (Fig. 1.4). Understanding the anatomy and function of these ligaments is of paramount importance in various fields, such as biomechanical studies and ligament reconstruction for knee replacement [2].

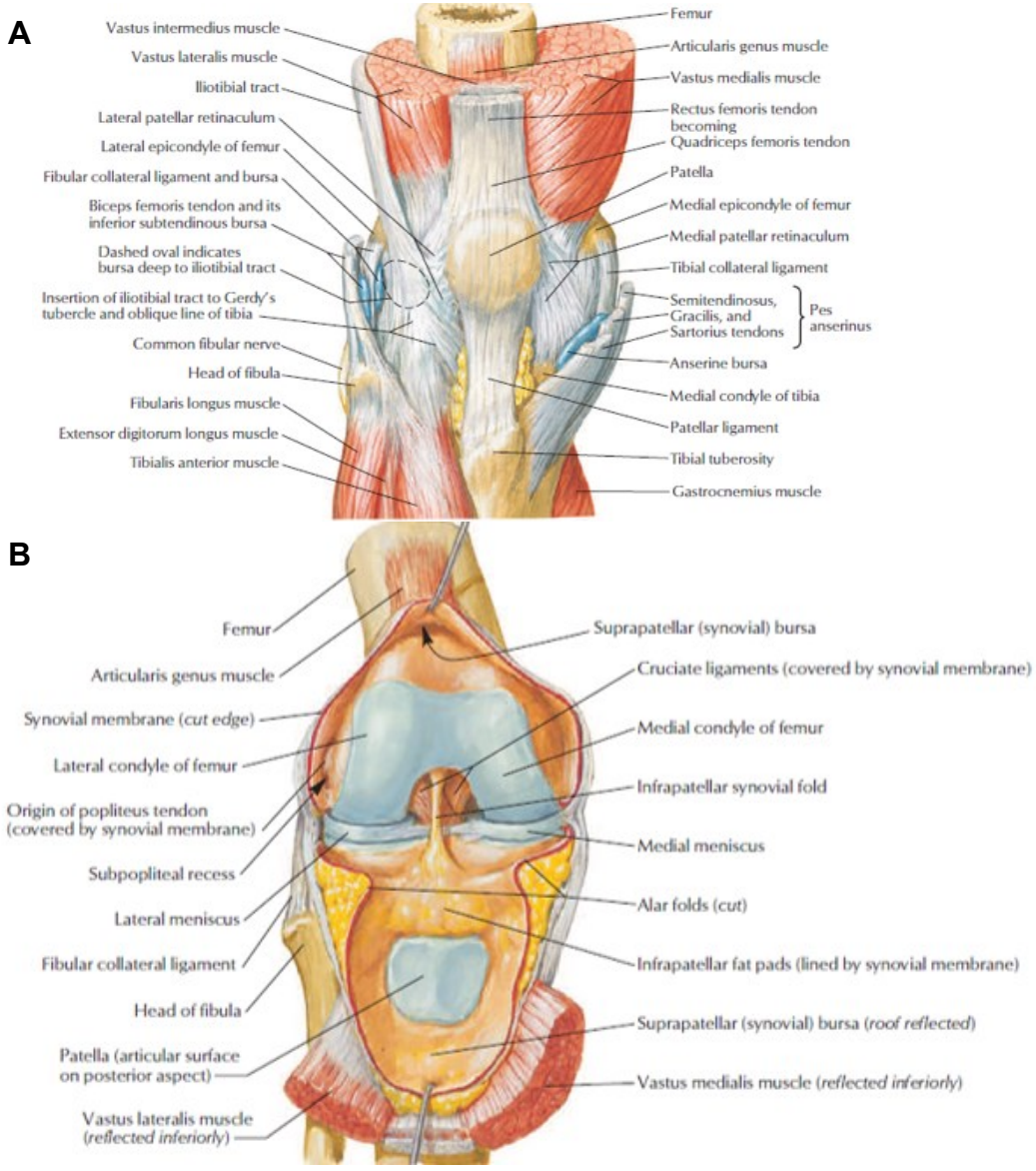

Figure 1.4: Anterior view of the extended knee (A) and of the open joint in slight flexion (B) [4].

1.2.1 Medial collateral ligament

The medial collateral ligament is wide and flat. It arises from the medial epicondyle of the femur, in continuation with the fibres of the adductor magnus tendon and inferiorly, it divides into two layers (Fig. 1.5).

The deep layer fuses with the underlying fibrous capsule and the medial meniscus and passes to the articular margin of the medial condyle of the tibia [5].

The superficial medial collateral ligament (sMCL) is the largest structure of the medial aspect of the knee, with one femoral and two tibial attachments. The superficial layer is embedded in the medial surface of the tibia, anterior to the insertions of the sartorius, gracilis, and semitendinosus. It is separated from the medial condyle of the tibia by vessels and the medial inferior geniculate nerve and by the insertion of the semimembranosus. The femoral attachment has a slightly oval shape and is located in a depression slightly proximal and posterior to the centre of the medial epicondyle. Its mean position is approximately 3.2 mm proximal and 4.8 mm posterior to the medial epicondyle. The sMCL has an overall length of 10-12 cm. When it extends distally, it divides into two separate tibial attachments. The proximal attachment involves primarily soft tissue rather than direct bony attachment, particularly the anterior arm of the semimembranosus tendon. The distal aspect of the sMCL attaches approximately 6 cm distal to the joint line. Its distal tibial attachment has a broad base and is located just anterior to the posteromedial crest of the tibia, primarily within the pes anserine bursa, contributing significantly to the posterior floor of the bursa. The posterior aspect of the tibial portion of the sMCL is fused with the distal tibial expansion of the semimembranosus tendon [5].

1.2.2 Medial patellofemoral ligament

The medial patellofemoral ligament (MPFL) plays a crucial role as a passive stabiliser of the patella, exerting approximately 50-60% of the restraining force on lateralisation between 0° and 30° of knee flexion.

Biomechanical studies have shown that the MPFL is the main medial static stabiliser, preventing external subluxation of the patella within the patellofemoral joint.

Anatomically, the medial patellofemoral ligament has a wide base of attachment at the superomedial aspect of the medial border of the patella (Fig. 1.5). The midpoint of attachment of the medial patellofemoral ligament was located 41.4% of the length from the proximal tip of the patella to the total length of the patella (proximal to distal). From that point on, the ligament heads medially towards the femoral attachments of the adductor magnus tendon and the superficial medial collateral ligament, attaching primarily to the soft tissues between these structures. On the femur, the MPFL attaches approximately 10.6 mm proximally and 8.8 mm posteriorly to the medial epicondyle, as well as 1.9 mm anteriorly and 3.8 mm distally to the adductor tubercle. The average length of the MPFL between the patellar and femoral attachment sites is 65.2 mm [5], [6].

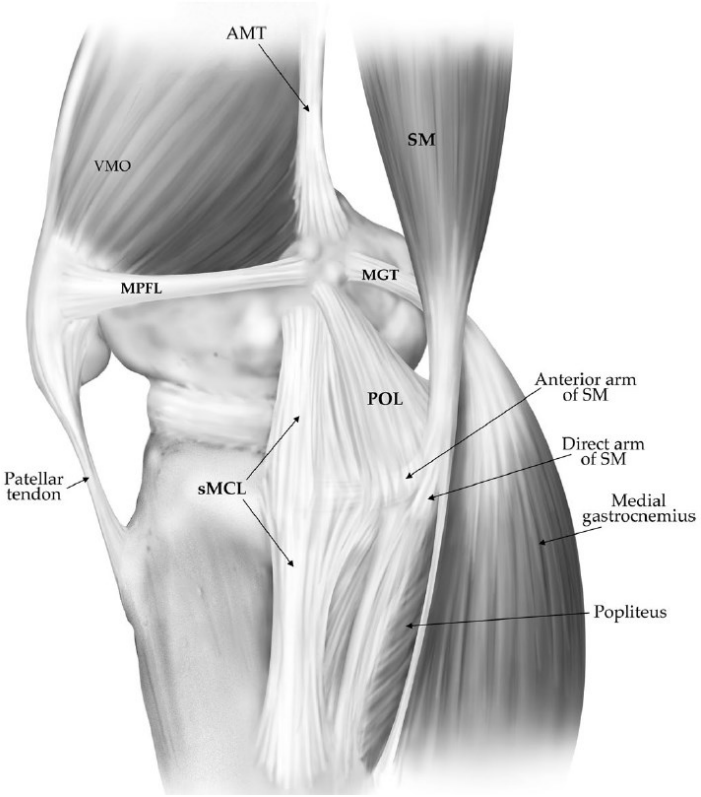

Figure 1.5: Main features of the the medial aspect of knee. VMO = vastus medialis obliquus muscle, MPFL = medial patellofemoral ligament, POL = posterior oblique ligament, sMCL = superficial medial collateral ligament, SM = semimembranosus muscle, MGT = medial gastrocnemius tendon, and AMT = adductor magnus tendon [7].

1.2.3 Lateral collateral ligament

The lateral collateral ligament (LCL), a cord-shaped structure, extends from the lateral aspect of the femur to the head of the fibula. It passes through the biceps femoris tendon and is separated from the fibrous capsule of the joint by adipose tissue (Fig. 1.6).

The femoral attachment of LCL is located in a small bony depression, approximately 1.4 mm proximal and 3.1 mm posterior to the lateral epicondyle. The distal attachment of the LCL is located in a small depression on the lateral side of the head of the fibula, approximately 8.2 mm posterior to the head of the anterior margin of the fibula and 28.4 mm distal to the tip of the fibular styloid. On average, the LCL has a length of 69.6 mm [8].

1.2.4 Lateral retinaculum

The lateral retinaculum, consisting of fibrous expansions of the vastus lateralis, surrounds the lateral side of the patellar bone. Its main function is to support the position of the patellar bone relative to the femur during knee movement. These fibrous expansions extend into the fibrous capsule on the lateral sides of the patellar tendon [2].

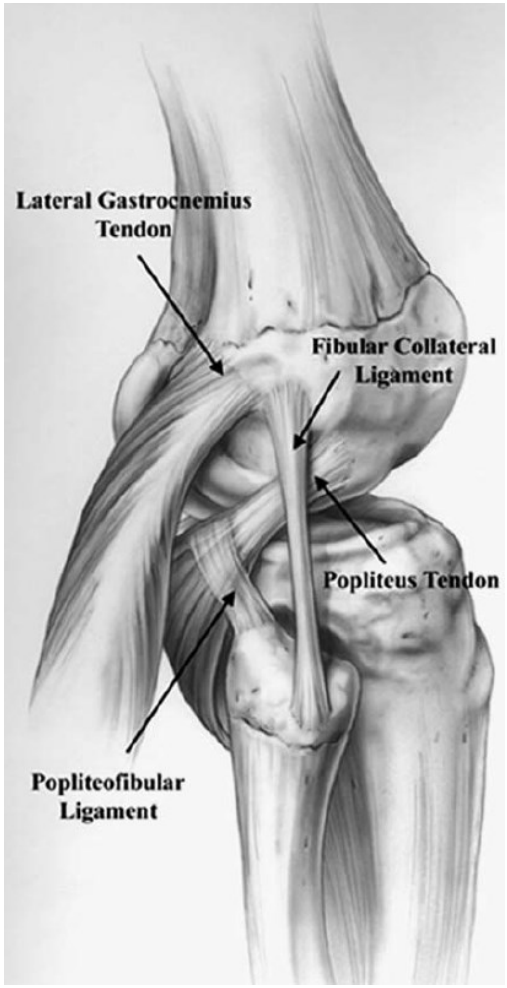

Figure 1.6: Main structures of the the lateral aspect of knee [9].

1.2.5 Cruciate ligaments

Cruciate ligaments are robust ligaments located within the joint capsule, extending from the head of the tibia to the intercondylar notch of the femur. These ligaments intersect each other in the shape of an 'X', which is the reason why they are called the cruciate ligaments (Fig. 1.4 B). They are called the anterior cruciate ligament (ACL) and the posterior cruciate ligament (PCL) based to their attachment points on the tibia: the ACL attaches to the anterior aspect of the intercondylar area, while the PCL inserts posteriorly to this latter anatomical feature.

Functionally, the cruciate ligaments play a crucial role in guiding the kinematics of the tibiofemoral joint and ensuring its anteroposterior stability. They limit the anteroposterior displacement of the tibia relative to the femur. Specifically, the ACL prevents excessive anterior translation of the tibia, while the PCL limits posterior translation. In addition, these ligaments contain sensory receptors that also contribute to the proprioceptive function of the joint [2].

1.2.6 Quadriceps tendon

The quadriceps tendon (QT) is formed by the confluence of the rectus femoris, vastus lateralis, vastus intermedius and vastus medialis tendons (Fig. 1.4 A). It inserts into the proximal pole of the patella and its dorsal, lateral, and medial surfaces along its path from proximal to distal. Tendon insertion is believed to consist of three distinct planes: the superficial plane includes the rectus femoris, the middle plane includes the vastus medialis and vastus lateralis, and the deep plane is formed by the vastus intermedius. The synovial membrane lies immediately deep in relation to this plane of insertion. The extensor mechanism has the function of transmitting forces from the quadriceps to the proximal tibia.

The deepest portion, separated by a thin layer of fat, is the vastus intermedius. The QT has an average length of 6 to 8 cm from the proximal pole of the patella to the myotendinous junction, with a width of 2.5 to 3 cm [10].

1.2.7 Patellar tendon

The patellar tendon (PT) is a powerful ligament, which is the distal continuation of the quadriceps tendon located under the patella, extending from the apex and lower portions of the patella to the smooth upper part of the tibial tuberosity (Fig. 1.4 A).

Two important structures are deep to the ligament. The upper part of the ligament is separated from the synovial membrane of the fat knee joint by the infrapatellar pad, while the lower part of the ligament is separated from the upper part of the tibia by the deep infrapatellar bursa (Fig. 1.7).

Proximally, the width of the tendon is equal to that of the patella and its thickness varies from 4 to 7 mm. As the tendon advances distally, it narrows in width but increases in thickness, with an average thickness of 5 to 6 mm at the tibial tubercle [10], [11].

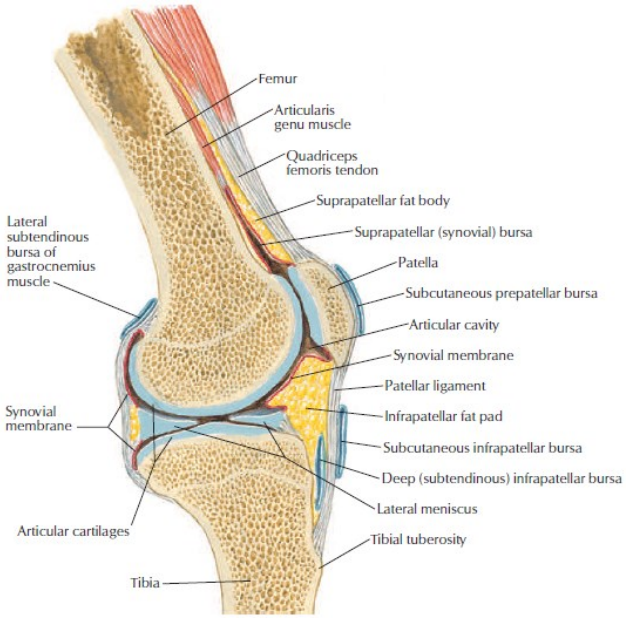

Figure 1.7: Sagittal section of the knee joint [4].

1.3 Cartilage

Synovial joints are distinguished by the presence of articular cartilage, which surrounds the bony interfaces (Fig. 1.7). Articular cartilage plays two key roles: attenuating the coefficient of friction between surfaces and increasing the contact area due to its elastic properties. Since contact pressure depends on the ratio of contact force to contact area, the presence of the cartilage layer facilitates the reduction of contact pressure within the joint to physiological levels, protecting its biological integrity [2].

1.4 Menisci

In the knee joint, contact forces can reach high levels under certain circumstances, making articular cartilage alone inadequate to reduce contact pressure to acceptable levels. As a result, an additional structural component, the menisci, is incorporated into the joint [12].

The menisci of the knees are two fibrocartilaginous discs that possess a unique composition and biochemical structure. These structures cover both the medial and lateral tibial plateaus and are anchored to the meniscal horns through bony attachments in the anterior and posterior aspects of the tibial plateau.

The lateral meniscus has a C-shaped configuration and covers 75% to 93% of the lateral tibial plateau, while the medial meniscus has a semicircular shape and covers 51% to 74% of the medial tibial plateau (Fig. 1.8) [13].

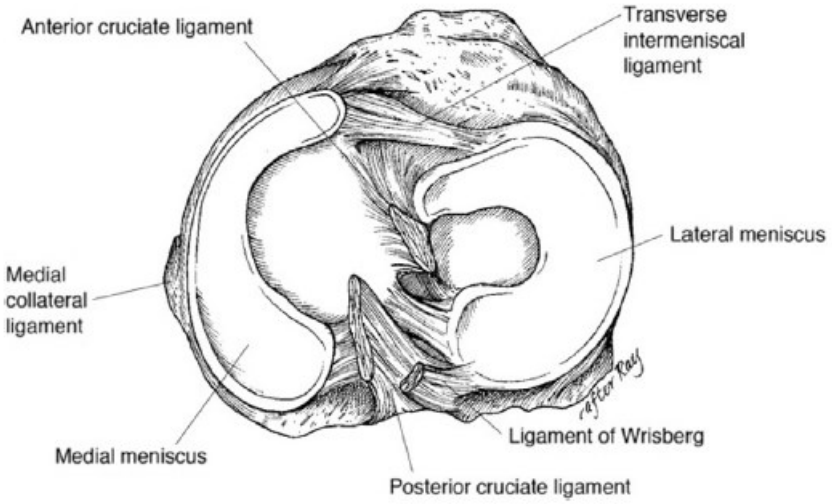

Figure 1.8: Transverse cut of a right knee, showing the medial and lateral menisci [4].

The menisci have primary functions that include improving the congruity and stabilisation of the joint, facilitating the transmission of load and shock. Without a medial meniscus, there is a discrepancy between the convexity of the medial femoral condyle and the slight concavity of the medial tibial plateau, resulting in a concentration of the contact area in the medial compartment of the knee (Fig. 1.9). In addition, they are involved in proprioception and joint lubrication [12].

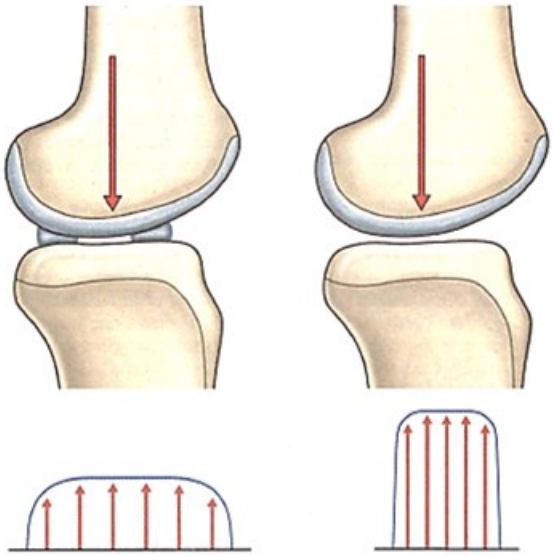

Figure 1.9: Function of the menisci in increasing articular congruity to distribute loads on a wider surface [12].

1.5 Muscles

The main muscle groups involved in knee flexion and extension are the quadriceps and hamstrings (Fig. 1.10). The quadriceps femoris muscle group, composed of rectus femoris, vastus medialis, vastus intermedius and vastus lateralis, acts as a powerful extensor of the knee joint (Fig. 1.10 A) [2]. These muscles insert into the patella and collectively exert their influence on the tibial tuberosity through the patella and patellar tendon. The quadriceps tendon, together with the patella and patellar tendon, forms the anterior segment of the fibrous joint capsule and comprises the suprapatellar bursa [5].

On the other hand, deriving their name from the tendons of the flexor muscles located in the popliteal region in the back of the thigh, the hamstrings consist of the semitendinosus, semimembranosus, and long head muscles of the biceps femoris (Fig. 1.10 B). These muscles arise from the ischial tuberosity and insert into the bones of the leg. Their main functions are the extension of the hip joint and the flexion of the knee joint [5].

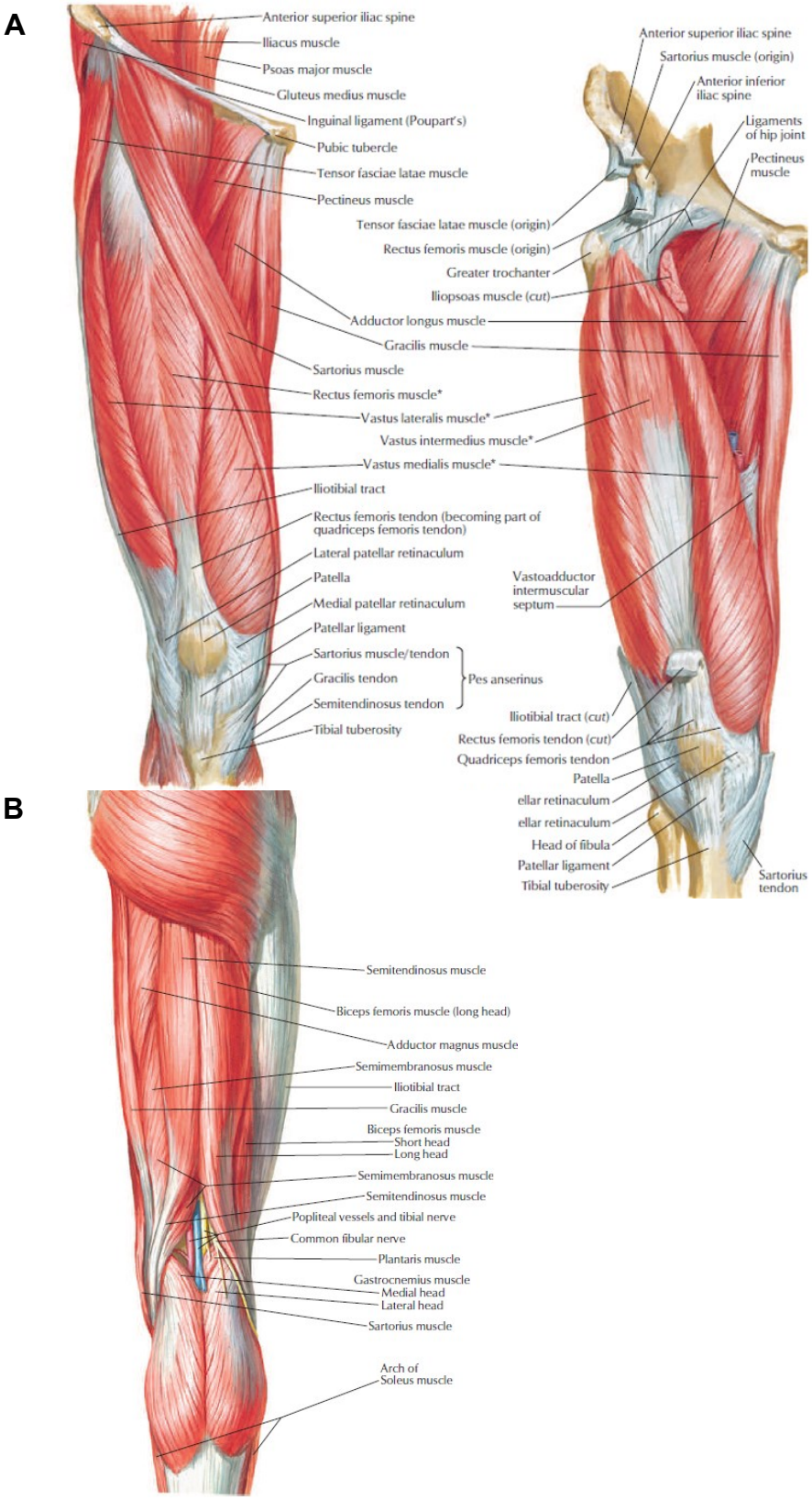

Figure 1.10: Muscles and thigh: anterior (A) and posterior (B) views [4].

Chapter 2

Biomechanics of the knee joint

2.1 Introduction to knee kinematics

The coordinate system is crucial for describing the relative position and its changes over time between two bodies. When establishing a coordinate system for a joint such as the knee, several factors must be specified. These factors include the Cartesian coordinate system for the geometry of each bone, the fixed axes of the body, and the reference axes of the joint coordinate system, which describe relative motion and the reference point for translation.

Grood and Suntay introduced an anatomical coordinate system that has become widely used to describe knee kinematics. This coordinate system is not fixed but consists of two segments attached to the tibial and femoral bones, respectively, along with a third floating axis that is always perpendicular to the other two.

To create such coordinate systems within each bone, two of their axes are aligned with the fixed reference axes of the body and the joint coordinate system. The origin of the coordinate system coincides with the reference point for translation. It is important to distinguish between the coordinate system within each bone and the joint coordinate system, which consists of the fixed axes of the body and their reciprocal perpendicular axes. The femoral coordinate system is represented by X, Y, Z with base vectors I, J, K, while the tibial coordinate system uses x, y, z with base vectors i, j, k (Fig. 2.1) [14].

The z-axis, associated with the movement of internal-external rotation, is chosen as the fixed axis for the tibial bone. It is located midway between the two intercondylar eminences proximally and through the centre of the ankle distally. The reference direction corresponds to the y-axis of the tibial, which is orientated anteriorly. The anterior direction is operationally defined as the cross product of the fixed axis and a line connecting the approximate centre of each plateau. The third axis of the tibial Cartesian coordinate system, the x-direction, completes the right-handed coordinate system. In the right knee, the x-axis is positive laterally, while in the left knee it is positive medially.

In the femur, the fixed axis of the body is chosen to correspond to the rotations associated with flexion-extension. This is achieved by selecting the fixed axis perpendicular to the femoral sagittal plane, known as the femoral Y-axis. To define the flexion axis within the femur, the mechanical axis (Z axis) must first be established. This axis passes through the centre of the femoral head and the most distal point of the posterior surface of the femur, between the medial and lateral condyles. The frontal plane of the femur, which contains the mechanical axis, is orientated so that the most posterior points of the femoral condyles are equidistant from the plane. The normal to the frontal plane, the femoral Y-axis, is obtained from the cross product of the mechanical axis and a line connecting the posterior points of the femoral condyles. The flexion axis, which lies within the frontal plane

of the femur, is determined as the cross product of the unit base vectors of the anteroposterior femoral axis and the mechanical axis. The fixed axes of the femoral body correspond to the Y axis with the base vector I, while the reference axis is chosen in the anterior direction [14].

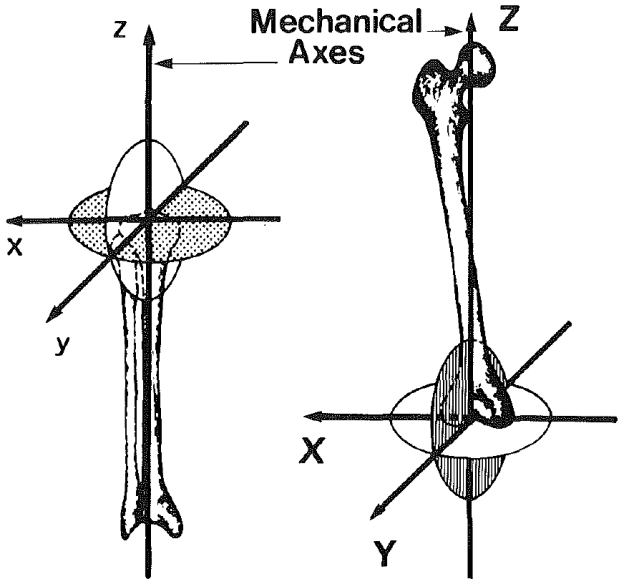

Figure 2.1: Cartesian coordinate systems are defined in each bone. Capitalised letters X, Y, Z denote the femoral system axes, while lower case letters, x, y, z denote the tibial system axes. For both bones, the z-axis is positive in the proximal direction, the y-axis is positive anteriorly, and the x-axis is positive to the right. The unit base vectors of these systems are I, J, K in the femur and i, j, k in the tibia [14].

Most joints in the body, including the knee joint, can fulfil movements in three dimensions; therefore, are characterized by six degrees of freedom (DOFs): three for translation and three for rotation.

Several techniques, such as the use of Grood-Suntay coordinate systems and other different approaches, have been employed to describe motion within the 6 DOF spatial joint. The six-degree-of-freedom spatial articulation model offers unlimited capabilities to capture motion between two bodies, encompassing both translation and rotation. It allows a complete description of the relative motion between these bodies. These methods define relative movement through consecutive displacements rather than instantaneous positions. However, a major limitation of the 6 DOF spatial articulation model is its inability to provide a spatial description and measurement of motion [2].

To allow one to describe more precisely the relative motion between the femur and the tibia, the movement for each of the six degrees of freedom is defined.

Internal and external rotations, commonly called longitudinal rotations, depend mainly on the tibial bone. Therefore, they are defined along the tibial mechanical axis (z-axis) as superior-inferior, or proximal-distal, translations.

Flexion-extension rotations and medio-lateral translations are designated along the femoral epicondylar axis.

Lastly, the varus-valgus rotations, also termed abduction-adduction, along with the anteroposterior translations are described along the fluctuating axis obtained from the cross product of the previous two axis.

Although the amplitude of the various movements can vary greatly from subject to subject due to anatomy, age, and training, we can consider the following average ranges of the different movements.

Rotations	Average range [deg]
Flexion - Extension	-15 - 140
Varus - Valgus	6 - 8
Internal - External	25 - 30

Translation	Range [mm]
Anterior - Posterior	10 - 15
Medial - Lateral	2 - 4
Superior - Inferior	2 - 5

Table 1: Average range of motion of the knee articulation along the six degrees of freedom of the joint [2].

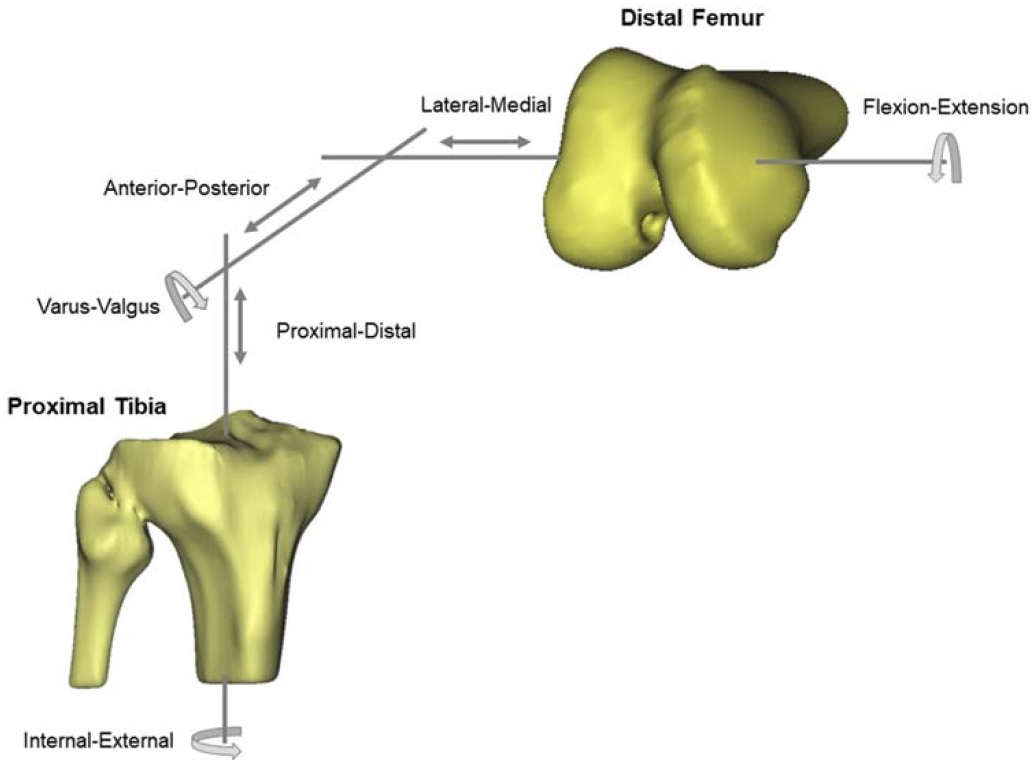

Figure 2.2: Description of the six degrees of freedom of the knee joint [15].

When defining the coordinate systems, a crucial aspect to consider is accuracy in identifying bony landmarks. Intra-operator and inter-operator variability can affect measurements. Depending on the techniques used, there may be differences in the identification of landmarks [2].

2.2 Tibiofemoral articular surface

In 1941, Bratingan and Voshell's studies on knee kinematics showed that the medial femoral condyle can act as the axis of rotation of the knee joint.

Since the late 1990s, numerous investigations have confirmed their conclusions. They have shown that, unlike the lateral condyle, which manifests an anteroposterior movement of approximately 20 mm, the medial condyle can be considered the centre of rotation. This is because medially, anteroposterior translations are negligible for flexion angles between 0 ° and 120 ° [16].

The motion with medial pivot and roll-back has been observed by several researchers. It can be seen that the traditional kinematic model of the human knee involves a progressive internal rotation of the tibia relative to the femur as flexion increases, followed subsequently by a posterior translation of the femoral condyles.

In the following paragraphs, these movements will be examined in detail to deepen the understanding of the biomechanical context of the human knee.

2.2.1 Medial articular surface

The sagittal section of the medial femoral condyle reveals a circular arc conformation, extending approximately 110 ° with an average radius of approximately 22 mm. However, this circular arc does not include the extreme posterior portion, which in fact has a smaller radius. During high flexion angles, this last section contacts only the horn of the medial meniscus; consequently, it cannot be considered an active part of the articular surface, as it is not directly in contact with the tibial surface.

Anteriorly, the femoral condylar surface subtends an arc of approximately 50 ° with an increased mean radius reaching 32 mm. This feature promotes better adaptation to the circular surface of the tibial condyle.

In fact, the anterior section of the medial tibial surface has an anterior inclination of approximately 11 ° on average, allowing greater congruence with the circular surface of the femoral condyle and promoting a better joint load distribution.

The medial surface of the tibia, dissected centrally, is flat posteriorly. This posterior portion maintains constant contact with the horn of the medial meniscus [17].

2.2.2 Lateral articular surface

The surface of the lateral femoral condyle has a configuration similar to that of the medial condyle, with a circular section at the posterior end forming an arc of approximately 114 °, with an average radius of 21 mm. Again, during flexion, the posterior end of the condyle contacts only the meniscus horn. However, compared to its medial counterpart, the anterior surface of the lateral femoral condyle is significantly shorter and may be difficult to distinguish.

The tibial articular surface, when analysed, appears relatively flat. However, it has downward curvatures in both the anterior and posterior regions, which serve as housings for the horns of the lateral meniscus. These characteristics help to

emphasise the concavity of the lateral component of the tibial surface and increase the anatomical complexity in this area (Fig. 2.3) [17].

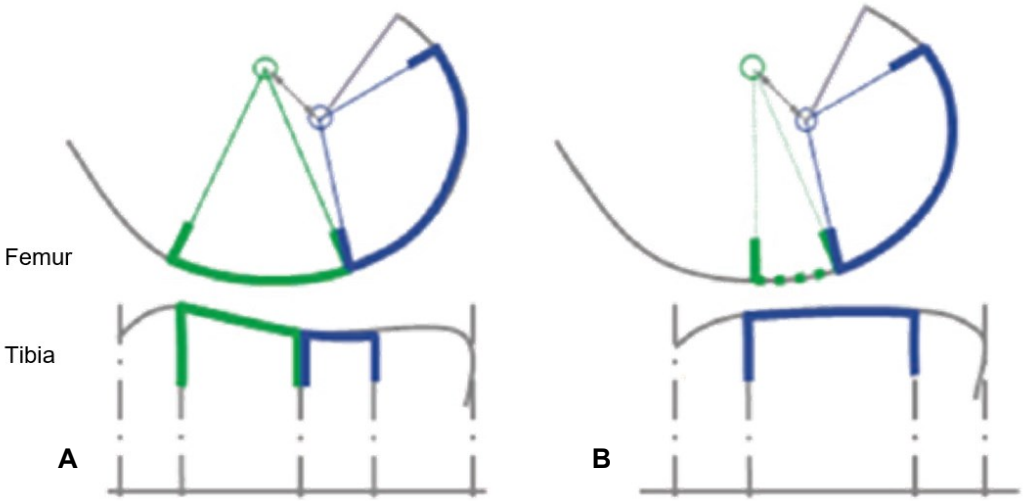

Figure 2.3: Sagittal sections through the centre of the medial (A) and lateral (B) compartments[17].

2.3 Tibiofemoral kinematics

The description of knee motion as to rotations and translations can be conducted by two approaches: determining the arrangement of contact areas or by evaluating condylar motion. The second approach will be detailed in the following paragraphs.

Knee flexion is divided into three distinct functional arcs, beginning with full extension, continuing with active flexion, and ending with the arc of passive flexion arc.

2.3.1 Terminal extension

This stretch is between, on average, 5 ° of hyperextension, the limit of passive extension, and 5 ° of flexion.

During this phase, the femur tends to rotate internally due to an anterior translation of the lateral condyle, while the medial condyle does not undergo anteroposterior movement.

At maximum extension, it can be seen that the medial condyle is in anterior contact with the inclined surface of the corresponding tibial condyle. On the contrary, the lateral condyle rolls forward on the flat surface of the tibial condyle (Fig. 2.4).

Finally, at the apex of the terminal extension, anteroposterior immobilization of both condyles is observed, which greatly contributes to the overall stability of the joint [17].

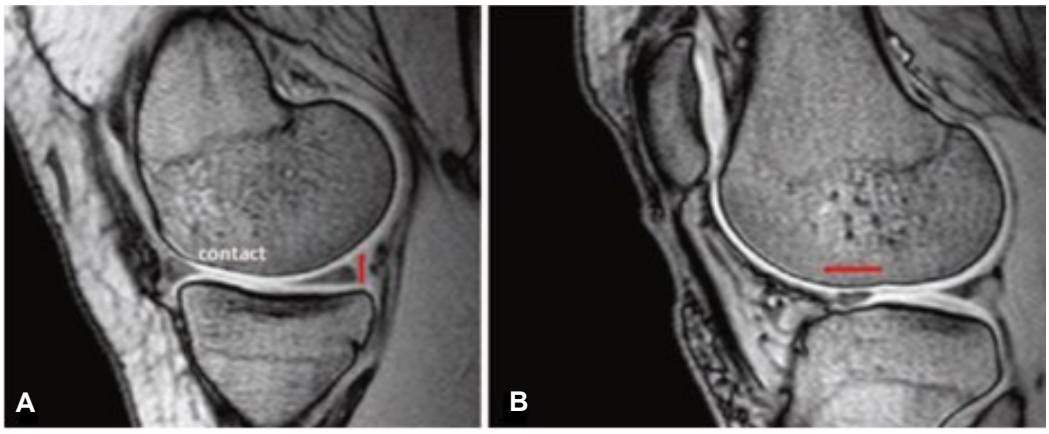

Figure 2.4: Sagittal view of the medial (A) and the lateral compartments (B) in hyperextension [17].

2.3.2 Arc of active flexion

The angular flexion between 10 ° and 120 ° is known as the active flexion. This designation reflects the fact that during this joint movement, the contraction of the surrounding muscles, particularly the hamstrings and quadriceps, plays a key role in its control.

At this stage, the medial component can be compared to a ball-and-socket joint, implying that translations are negligible. In fact, it can be seen that in this phase of movement, the knee undergoes mainly internal rotation movements in the medial region, accompanied by a slight varus. Thus, these rotations seem to act in synergy with the rotation of the flexors analysed in this section.

With respect to the lateral aspect, a set of movements is observed that involve rotations and translations in the anteroposterior direction. In particular, unlike the medial portion, the lateral condyle tends to translate posteriorly by about 15 mm on average. This allows the femur to perform an external rotation of about 30 ° around an axis centred on the medial condyle.

When performing a squat, the same principle applies; the movement follows the same criterion, although lateral translation may occur earlier [17].

2.3.3 Arc of passive flexion

Passive flexion refers to the movement of the joint that is not directly induced by muscle contraction, but is the result of the application of external forces. In the context of the knee, a transition zone is identified between 110° and 120°, followed by the passive flexion phase, which extends to 160°.

During this phase, the medial condyle translates 5 mm posteriorly on the tibial surface before adhering to the posterior horn of the respective meniscus. The latter, at the end of passive flexion, is compressed within the synovial recess between the femur and the tibia, limiting further flexion.

Similarly, it is observed that the lateral femoral condyle also undergoes posterior retraction in conjunction with retrograde translation of the posterior horn of the lateral meniscus (Fig. 2.5) [17].

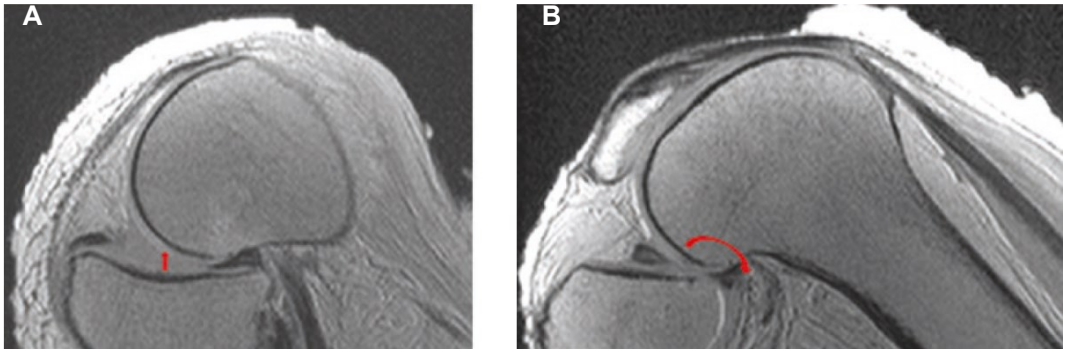

Figure 2.5: Sagittal of the medial (A) and lateral (B) compartments in 140 ° flexion [17].

2.3.4 Longitudinal rotation

In relation to rotation around the mechanical axis of the tibia, the initial reference position is where the femoral condyles are aligned at 0 degrees of flexion.

In the transition from the extended knee position to that of 120 degrees of flexion, it can be seen that the medial condyle does not show obvious anteroposterior displacement, while the lateral condyle shifts posteriorly by an average of about 18 mm.

Focussing on the terminal extension phase within the flexion arc, the femur tends to externally rotate about 7 °.

On the other hand, the tibia has a rotation freedom that varies between 20 ° and 30 °.

Finally, during passive flexion in the range of 120 ° to 160 °, due to posterior displacement of the medial femoral condyle by approximately 5 mm, a slight internal rotation of the femur can occur (fig. 2.6) [17].

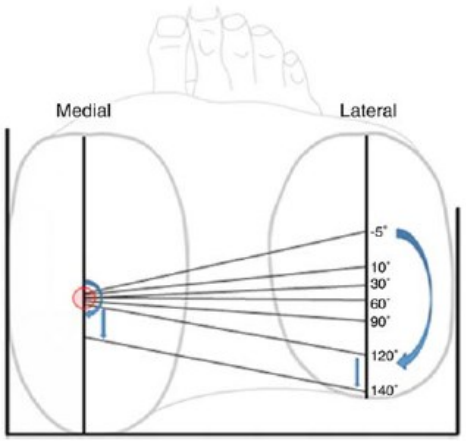

Figure 2.6: Medial and lateral femoral condylar centres plotted on the tibial plateaus for different flexion angles [17].

2.3.5 Varus and valgus rotation

Under conditions of complete knee extension, both collateral ligaments are tight, significantly limiting rotations in the varus or valgus.

However, when the knee flexes, the lateral collateral ligament loosens, allowing not only longitudinal rotation around the medial axis described above, but also varus rotation.

During the full flexion, movement in the valgus direction is negligible, while the lateral compartment moves up to 10 mm in the varus direction.

An appreciable asymmetry is observed between the lateral and medial joint spaces during flexion. This difference can be attributed both to the greater elasticity of the lateral collateral ligament and to the conformation of the articular bones themselves.

In fact, during the flexion process, the lateral joint space opens on average at about 7 °, a phenomenon known as "lift off." On the contrary, under stress in the valgus direction, the medial joint space shows a greater opening, averaging 2.1 mm [17].

2.4 Tibiofemoral kinetics

The forces transmitted in the knee joint have significant clinical implications. Within the context of normal ambulation, forces span a range approximately 2 to 3 times the individual's body weight. This phenomenon is imputable, in part, to the acceleration kinetics, the marked moments generated around the knee joint, and the concurrent engagement of multiple muscle groups. Some pathologies, such as obesity, increase the overall magnitude of loads in the knee. Therefore, each additional kilogramme of body mass leads to a multiplication of the forces exerted on the knee joint by a factor of 2 to 3 [18]. Furthermore, deviations from malalignment of the lower extremity can result in disproportionate loading of different compartments. In fact, modest deviations, as minimal as 3 to 5 ° in tibial varus alignment, can cause a substantial 50% surge in the force transmitted through the medial tibiofemoral compartment [2].

2.5 Patellofemoral kinematics

Within the context of knee articulation, the biomechanics of the patellofemoral joint is the most intricate to understand.

As stated previously, one of the principal functions attributed to the patella is to enhance the efficiency of the quadriceps contraption to ease knee extension. This is achieved by increasing the lever arm of the muscle by shifting the line of action anteriorly. Furthermore, the patella acts as a guide for the extensor mechanism by centralising the traction forces exerted by the quadriceps.

The kinematics of the patellofemoral joint is determined by multiple factors encompassing muscular contractile loads, the geometry of the articulating surfaces, and the characteristics of adjacent soft tissues that exert direct or indirect influences upon the patellar bone.

The predominant motion of the patella consists of its sliding upon the trochlear groove during knee flexion. It is important to acknowledge the multiplanar nature of joint motion, which extends beyond the sagittal plane to include also the coronal and axial planes.

At full extension of the knee, the femur and the patella remain unengaged. The contact occurs due to the repositioning of the patella in response to the vector forces resulting from the tension in the quadriceps and the tractive forces of the patellar tendon. This leads the patella to press against the contours of the trochlear groove.

As the arc of knee flexion, the patellofemoral force increases, resulting in the engagement between the two bones between 10 ° and 20 ° of flexion. As the flexion angle deepens, the contact area increases along with the contact force, as detailed in Smidt's 1973 study [19].

The area of contact is initially located in the inferior lateral margin of the surface. However, as flexion progresses beyond 30 degrees of flexion, the patella is stabilised by the loads of the quadriceps and patellar tendon that push it into the trochlear groove. Between the range comprised between 30 ° and 60 ° of flexion, the contact area is central to the articular surface of the patella. Upon achieving 90 degrees of flexion, it shifts proximally toward the superior pole of the bone. Beyond the previous cited point of flexion, a noticeable differentiation emerges; it is possible to distinguish two different areas of contact between the two bones, in particular medially and laterally, as it slides between the two femoral condyles.

In the coronal plane, the quadriceps strain force and the patellar tendon force draw an angle, which is generally called the Q angle (Fig. 2.7). This angle plays a determining role in the application of lateral forces on the patellar bone. During flexion, an increase in the Q angle corresponds to an increase in the lateral loads and thus a slight patellar lateral displacement. This displacement is geometrically limited by the femoral trochlear groove.

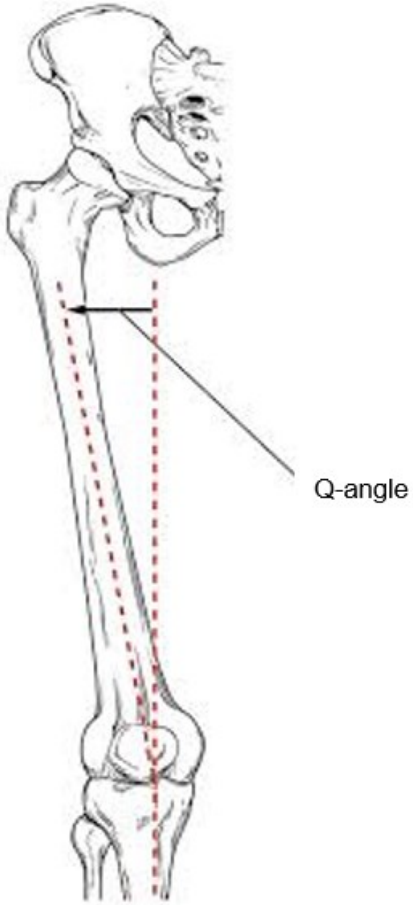

Figure 2.7: Angle Q described in the coronal plane of the lower extremity [20].

Studies have reported an average medial displacement of about 5mm in the coronal plane, mostly during the first 30 degrees of flexion. This displacement occurs because the patella is not relatively unanchored by the femoral condyles within the trochlear groove [21].

2.6 Patellofemoral kinetics

Convergence of the quadriceps muscle force on the patella occurs due to the attachment of its fibres along the medial, lateral, and proximal edges of the patella.

Considering the anatomical femoral axis, the vastus medialis and vastus lateralis orientation are not parallel to it, implying that these muscles exert medial and lateral forces on the patella.

In the sagittal plane, the resultant vector of the quadriceps strain force and the patellar tendon strain force is defined as the patellofemoral reaction force. As previously explained, the patellofemoral reaction force increases during knee flexion and decreases when the tibial tuberosity is anteriorly displaced (Fig. 2.8) [22].

Figure 2.8: Forces acting in the sagittal plane. The resultant vector between the quadriceps strain force (QF) and the patellar tendon strain force (PTF) is the patellofemoral reaction force (PRF). CG gravity centre [22].

Additionally, the lever arms of the femur increase, which requires greater quadriceps strength to resist the moment generated by body weight.

A pivotal factor in calculating patellar forces is the distance between the vertical line passing through the body's centre of gravity and the instantaneous axis of joint rotation. Alterations in posture, whether anterior or posterior, lead to changes in this distance, resulting in notable variations in patellar force[2].

In the coronal plane, the Q angle determines a lateral force vector known as the patellar lateral force, which peaks during full knee extension.

Within the axial plane, forces are influenced by knee flexion, trochlear and patellar anatomy, the balance of the patellofemoral ligaments, and the action of the quadriceps muscle.

Furthermore, the mechanical axis of the lower limb significantly affects patellofemoral biomechanics. Specifically, the valgus morphotype has negative implications for proper patellofemoral tracking, elevating the obliquity of the quadriceps force and subsequently increasing the Q angle and lateral force [22].

Chapter 3

Knee arthroplasty

3.1 Aetiology and implications of osteoarthritis in the knee joint

Multiple cellular components within tissue-specific cells are subjected to processes of ageing and degeneration. This affects the kinetics of their intracellular and intercellular forces and leads to dysregulation or diseases.

These alterations have a considerable impact on the mechanobiological aspect of the cellular environment, eventually resulting in an imbalance in the turnover of the extracellular matrix [23]. These events can contribute to a gradual degradation of tissue and weakening of mechanical properties and musculoskeletal structures, which can lead to a sensation of discomfort and diminished mobility.

Normally, the cellular response to these alterations induces tissue remodelling. However, under frequent and high mechanical stresses, their response can contribute to degenerative transformations and eventual tissue failure.

In particular, pathological reduction in bone density can contribute to the development of osteoporosis, and the reduction of cartilage thickness within synovial joints may progress to the outbreak of osteoarthritis [24].

Osteoarthritis (OA) is a common degenerative joint disease that affects cartilage, bones, and other tissues around joints. Patients are typically subjected to pain, stiffness, and reduced function in the affected joint. This chronic pathology occurs more frequently in knees, hips, hands and spine, but can nevertheless manifest in any joint (Fig. 3.1) [21].

Essentially, causes can be divided into two typologies: primary OA and secondary OA. The first leads to the bones being in direct contact and is caused by the degradation of the articular cartilage. In this scenario, the main risk factors consist of age, sex, and genetics. Secondary OA, instead, has a subsidiary aetiology, as cartilage results damaged by other circumstances, in addition to events that directly damage the articular cartilage. These latter conditions include excessive stress in the joints due to obesity, occupational factors, and varus or valgus alignment. Other risk factors are traumatic events such as joint injury or surgery and pathologies, for instance, rheumatoid arthritis [2].

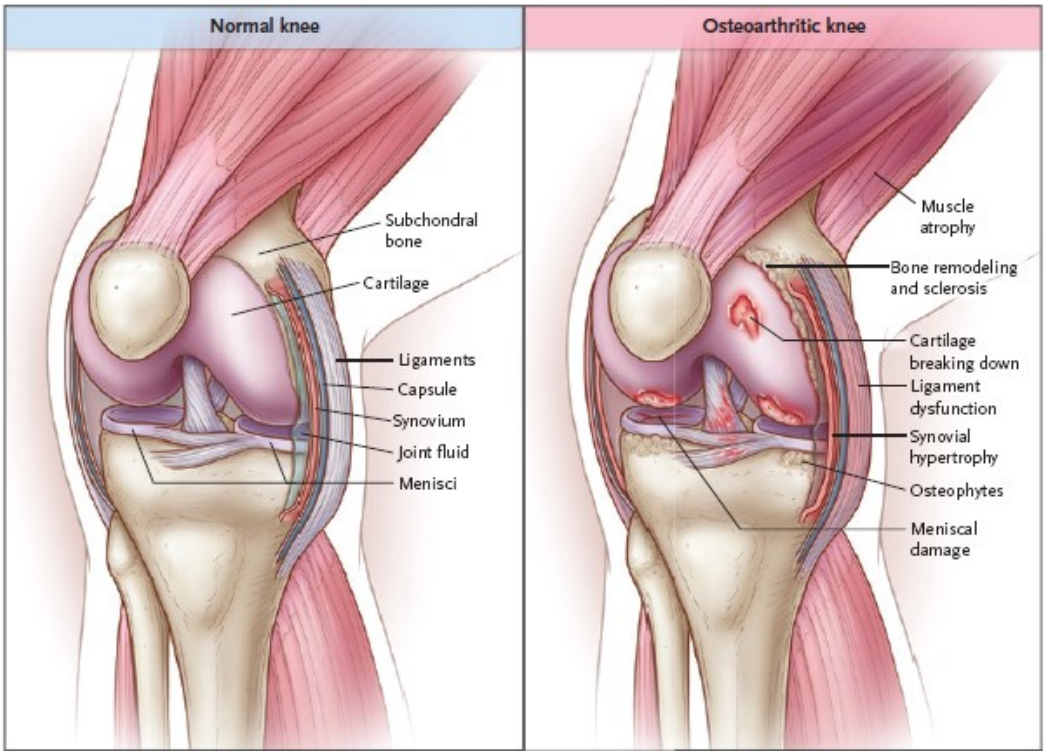

Figure 3.1: Comparison between healthy and osteoarthritic knees with a focus on the main articular issues [25].

All these factors result in friction through bone-to-bone contact that worsens the stages of OA and could induce a situation of continuous pain (Tab. 2) [26].

Pathogenesis of osteoarthritis
Aetiological factors
↓
Reversible matrix degradation
↓
Cellular attempts at repair
↓
Irreversible matrix degradation
↓
Loss of cartilage
↓
Misalignment/ loss of congruence
↓
Progressive osteoarthritis

Table 2: Evolution of the pathogenesis of osteoarthritis.

Knee OA is commonly associated with swelling, stiffness in the joint, and subsequent decreased mobility that dramatically reduces the patient's quality of life.

Currently, there is no cure for this pathology; however, there are various treatment options to decrease pain and restore mobility in the affected joint. Surgical knee insertion of knee replacement emerges as a long-established method for the effective treatment of severe OA in the case of less invasive techniques [25].

3.2 Introduction to knee replacement

Conservative treatments such as physical therapy, medications, and assistive devices are always preferred when dealing with degenerative knee diseases. However, when they no longer give the ability to provide proper relief to the pathologic condition, the implant of a knee prosthesis may be considered.

The primary objectives of knee replacement are to mitigate pain, restore articular function, and improve the patient's quality of life. The prosthesis is, in fact, designed to mimic the natural design of the knee joint and therefore reproduce the movement of a healthy articulation.

Based on the amount of articular degradation and the patient's specific requests, different prosthesis typologies could be considered, including partial or total knee replacements.

Knee implants are applied when joint damages are such that they significantly affect the patient's quality of life and conservative treatments are no longer effective.

Generally, a knee prosthesis consists of four different parts: two metallic components, one attached to the femur and the other to the tibial bone, called tibial tray; and two polyethylene components, the tibial insert, which is mechanically attached to the tibial tray and an optional patellar button that can be used in the patellofemoral joint to replace the patellar cartilage as shown in Figure 3.2.

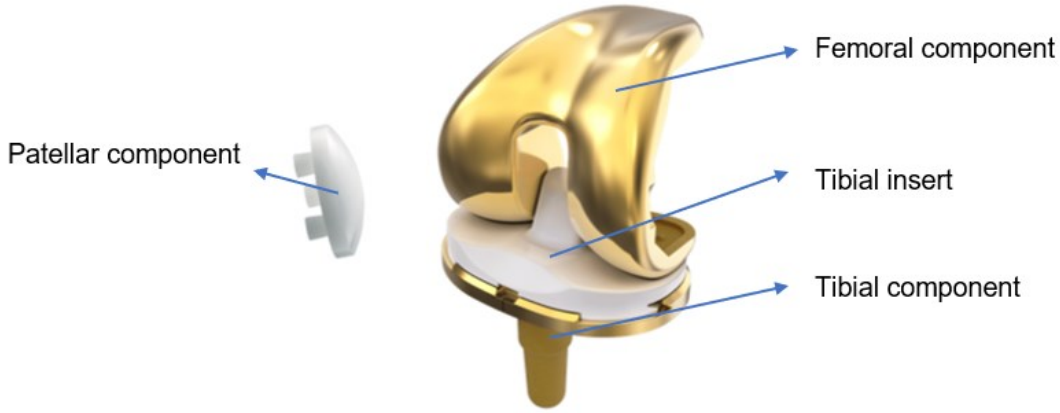

Figure 3.2: Generic components of a total knee implant (*Courtesy of Waldemar Link GmbH & Co. KG*).

There are many different designs of knee implants, and to describe the various typologies, it is important to consider some main distinctions [2]:

- total knee arthroplasty (TKA) and partial knee arthroplasty;

- cruciate retaining (CR) or posterior stabilised (PS) implant;

- cemented implant and press-fit implant;

- fix bearing and mobile-bearing;

- primary and revision TKA.

3.3 Design of knee prostheses

Cruciate ligaments are responsible for the stability of the knee joint, mainly related to anteroposterior translation. During the implantation of a knee prosthesis, the surgeon could adopt the solution of resecting them for multiple reasons. As a consequence, surgically, the decision to resect only the ACL, inserting a cruciate retaining implant, (CR) implant or to embrace the choice of posterior stabilised design, resecting both of them could be considered.

Academically, PS TKA should be used in patients with non-functional PCL. When the PCL is still functional, the surgeon makes a decision, usually, on preference, experience, and training.

In terms of range of motion, the PS design is superior to the CR. However, clinically there are no significant differences considering complications, clinical and functional outcomes [27].

The design of a posterior stabilised prosthesis provides anteroposterior support after resection of the ligaments. The post-cam system is projected to offer mechanical reinforcement, limiting anteroposterior translation through a metal cam placed in between the two condyles of the prosthesis. This characteristic during flexion engages a polyethylene post that arises from the tibial insert, which limits the translation mentioned above (Fig. 3.2) [2].

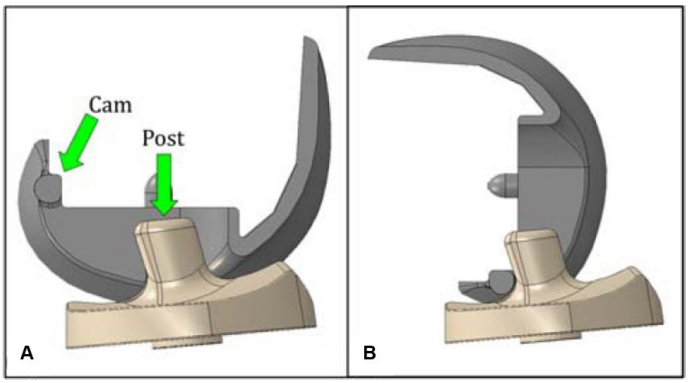

Figure 3.3: Post-cam system in a section of a PS implant: full extension configuration (A) and knee 90 degrees of flexion (B) [2].

A press fit can be used to fix the prosthesis to the bone; alternatively, bone cement called polymethyl methacrylate (PMMA) can be used. This material does not possess adhesive properties, in fact, it acts as a space filler in the cavity between bone and prosthesis, holding the implant in contact with the bone.

To promote bone growth in press-fit implants, the surfaces of the tibial and femoral components can be texturised. These may include, for example, a porous coating or hydroxyapatite layer with the aim of reducing stress conditions and motion at the interfaces between the two materials [28].

With respect to the relative movement that can exist between the tibial insert and the tibial metal component, the concept of fixed and mobile bearings emerges. The former, as the name suggests, is restricted to the tibial plateau, while the latter is free to rotate on the tibial component around a vertical axis.

Mobile bearing prostheses induce fewer rotational forces, since they have fewer degrees of freedom, thus reducing the risk of implant loosening. In addition, due to this peculiarity, the latter design is able to reduce the shear forces transmitted to the bone [29].

However, considering the negative aspects induced by this design, it must be taken into account that the tibial insert has two surfaces that interact with other components, thus inducing a greater possibility of wear. However, both scenarios have similar ROM, survival rate, and clinical score, as well as patient satisfaction rate [30].

The main aspects of the design of the femoral component of a knee prosthesis concern the geometry of the condyles. These can be symmetrical or not, thus distinguishing the medial from the lateral one. A peculiarity concerns the sagittal section of this part. The condyles can be designed to present a homogeneous curvature, therefore following the arc of a circumference with constant radius, or presenting a J-curved section. This involves a multiradii curvature, where the condyles present an arching that follows a larger radius in extension and a smaller radius in flexion. This design has recently been implemented by introducing the concept of a radius that continuously varies in size as the flexion angle increases.

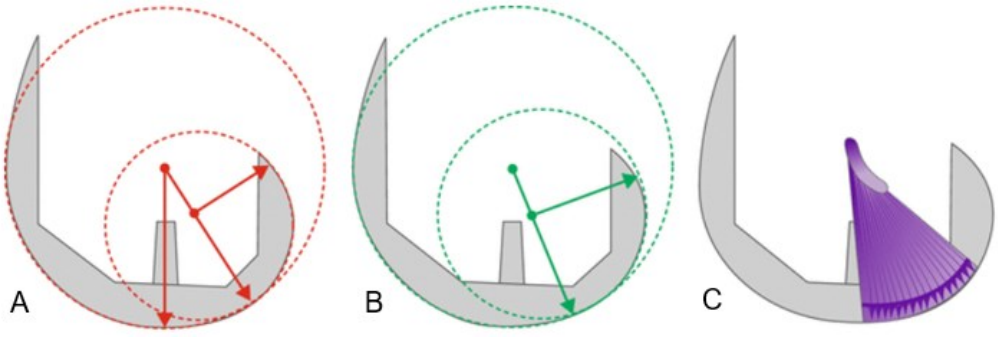

Figure 3.4: Femoral condylar design: multiradii of curvature (A), single radius of curvature (B), and gradually reduced radius design (ATTUNE GRADIUS™) (C) [31].

Although some designs are characterised by clearly improved knee kinematics, it is not possible to report evidence of improved clinical outcomes [2].

The design of the anterior aspect of the femoral surface of the prosthesis is also considered of great importance. In fact, the trochlear geometry was improved with the aim of recreating a joint surface more similar to the anatomical one in order to avoid inducing patellofemoral complications and to facilitate the kinematics of this joint [32].

The main design features of the tibial component that differentiate various models are related to the symmetry of the part. Implants with symmetric geometry allow for lower inventory costs, but present more difficulties during implantation. Asymmetrical prostheses, on the other hand, allow for better precision in covering the bone cut and easier application.

A special design of the component involves the tibial component and the tibial insert being joined into a single component made entirely of polyethylene. This reduces costs, and it allows it to be applied to patients with metal allergies [2].

With regard to tibial inserts, those with a symmetric design, the medial and lateral plateaus are both concave in the anteroposterior direction. On the other hand, in asymmetrical models, the lateral surface is less concave, simulating the anatomical lateral surface of the tibia.

Asymmetry can also be introduced within the frontal plane to simulate the 3-degree inclination of a native joint line, thus increasing the thickness in the lateral section [2].

3.4 Implant alignment in total knee arthroplasty

To date, no standardised approach to implant alignment has been established, which means how a surgeon decides to place a knee implant in a specific position and orientation. Therefore, this also determines how the surgeon manages the soft tissue envelope around the joint.

One major objective of total knee arthroplasty is to obtain homogeneous, symmetrical, and balanced flexion and extension gaps. These are described as the gaps that separate the femoral and proximal cuts of the tibia during joint flexion and extension.

Depending on whether the surgeon places the primary focus on ‘tension gaps’ or bone cuts, there are two different currents of thought. Following the first technique, through ligament tensioners, the surgeon chooses an appropriate amount of tension on the ligaments themselves and consequently cuts the bones.

Taking advantage of the second approach, called ‘measured resection’, the surgeon uses bone landmarks to perform bone cuts and determine the best position of the femoral component. The joint is stabilised only at a later stage by the soft tissues that balance it [33].

Regarding the measured resection, various procedures can be implemented based on the different orientations of the implant with respect to the longitudinal axes of the lower extremities.

Traditionally, the golden standard in TKA was to achieve neutral alignment postoperatively. This is possible by means of the so-called mechanical alignment, which involves positioning the femoral and tibial components orthogonally with respect to their corresponding mechanical axes, thus resecting the distal femur and proximal tibia.

Measured resection or gap balancing techniques are used to achieve proper extension and flexion gaps, as well as proper patellar tracking. Specifically, adjust the rotation of the femoral component, the thickness of the bony resections, and the proper balance of the ligament. For this reason, factors such as the flexion gap and rotation of the tibial component are of considerable importance [34].

Mechanical alignment, however, does not allow us to restore a native alignment of the lower limb; it may, in fact, alter the kinetics of the knee. Rather, this technique aims to equalise the loads in the implant, between the medial and lateral compartments, to decrease wear and loosening [35]. In Minoda's study [35] it emerges that a substantial correction in alignment of one component of the joint to compensate for the malalignment of the other component, to achieve a neutral alignment situation in TKA, should be fundamentally avoided due to the high failure rate. Therefore, it refers to a situation in which a tibial varus or femoral valgus alignment occurs [35].

As a result of the mechanical alignment, it can be observed that the volume of bone excised is asymmetric between the medial and lateral regions of the bones involved, this as a result of the natural inclination of the joint line of about 3 degrees. In order to avoid this problem, orthopaedic surgeons Hungerford and Krackow in the 1980s introduced a new surgical technique that mimicked the patient's native joint line. It was named "anatomical alignment" and involves cutting the tibia and femur at a 3-degree angle to their mechanical axes, thus regardless of the actual patient-specific inclination. Taking into account this last aspect, even this technique did not provide complete symmetry in resection [36].

On the contrary, kinematic alignment (KA) is more likely to restore normal knee kinematics, significantly improving the patient's quality of life. KA aims to restore the prearthritic anatomy of the knee joint, increasing ROM, and reducing the incidence of pain, joint stiffness, and instability. In contrast to the two techniques outlined above, the latter is patient-specific; indeed, it depends on each patient's joint line. A downside of this surgical approach is the potential increased risk of patellar instability and polyethylene wear.

This technique seeks to bring into alignment the joint line and three kinematic axes in the knee represented by a transverse one through which the tibia extends and flexes, one through which the patella can make the same rotations, and finally one around which the tibia rotates internally and externally (Fig. 3.5).

The three axes just described are thus either parallel or orthogonal to the knee joint line.

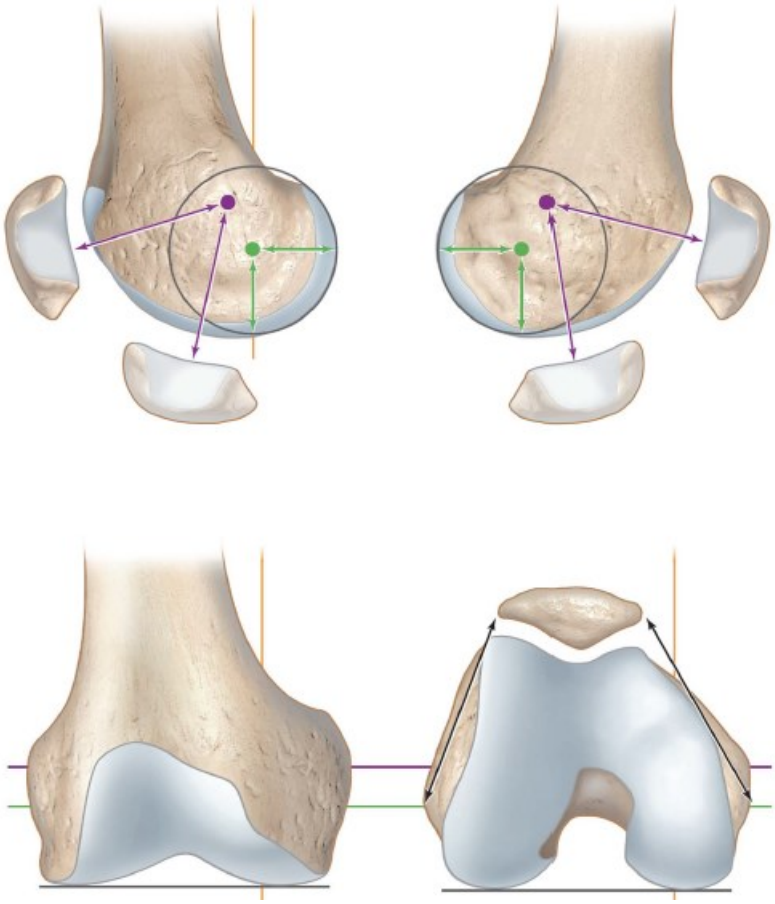

Figure 3.5: Transverse femoral axis about which the tibia extends and flexes (green line). The transverse femoral axis about which the patella extends and flexes (violet line). The longitudinal axis about which the tibia rotates externally and internally on the femur passes through the medial femorotibial compartment (yellow line) [34].

This surgical technique also returns the lengths of the native ligaments, by not creating a gap imbalance and consequently minimizing the need for release.

In this technique, the first cut is made on the distal femoral section, which is why it is called "femur first." This resection is performed parallel to the patient's joint line, and only then is accomplished the cut of the posterior femur. Finally, the surgeon completes the cut of the proximal portion of the tibia, parallel to the joint line. Unlike the other approaches, if there is a joint imbalance characterised by excessive laxity or tension, no ligament releases are performed; in fact, the soft tissue envelope is preserved intact, but in this technique, it is preferred to proceed with an additional cut of the tibia to compensate [34].
A similar approach of TKA concerns "inverse kinematic alignment".

The latter is a "tibia first" approach, so the surgeon initially cuts the tibia and only then maintaining the native inclination of the joint line. Only then is gap balancing performed through the distal and posterior cut in the femur [2].

Sappey-Marinier et al. performed a review study of clinical and radiological outcomes after TKA with KA versus MA at 2 years of follow-up [37].

They reported that 80% of the randomised controls did not show particular differences between the two groups for the main functional and clinical scores.

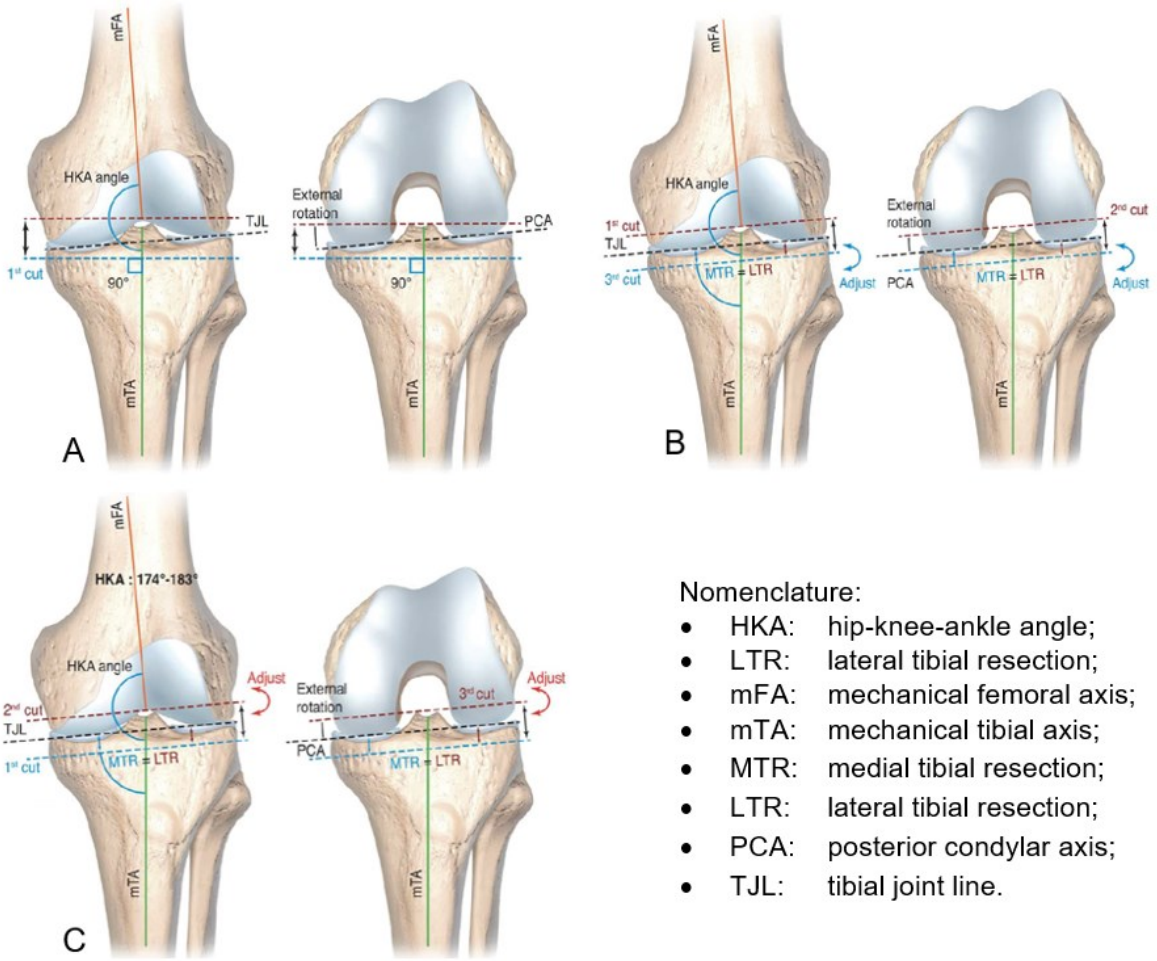

Only one study reported that kinematic alignment had markedly better pain range of motion and better scores than patients undergoing MA [37].

Figure 3.6: Mechanical alignment (A), kinematic alignment (B), and inverse kinematic alignment (C) [34].

In the context of total knee arthroplasty, the use of a sizing guide (sizer) serves as a fundamental component in the determination of both the accurate size and the positioning of the femoral component. Within this procedural framework, two distinct methodologies are used to establish the reference position of the sizing guide, specifically the anterior reference (AR) and the posterior reference (PR).

In scenarios where the anteroposterior dimension of the femoral condyle is precisely with that of the component, the extent of bone resection remains consistent regardless of the reference method employed. However, when the

anteroposterior dimension of the femoral condyle falls within the size spectrum of the component, the choice of component size and the magnitude of bone resection become variable, dependent on the reference method selected. In cases where the size of the component is smaller than the femoral condyle, the adoption of the AR methodology results in a more extensive bone resection and the consequent widening of the flexion gap. On the contrary, opting for the PR methodology increases the risk of creating an anterior notch. Thus, this study conducts a comprehensive analysis of the implications and clinical significance associated with the selection of reference methods during total knee arthroplasty [38].

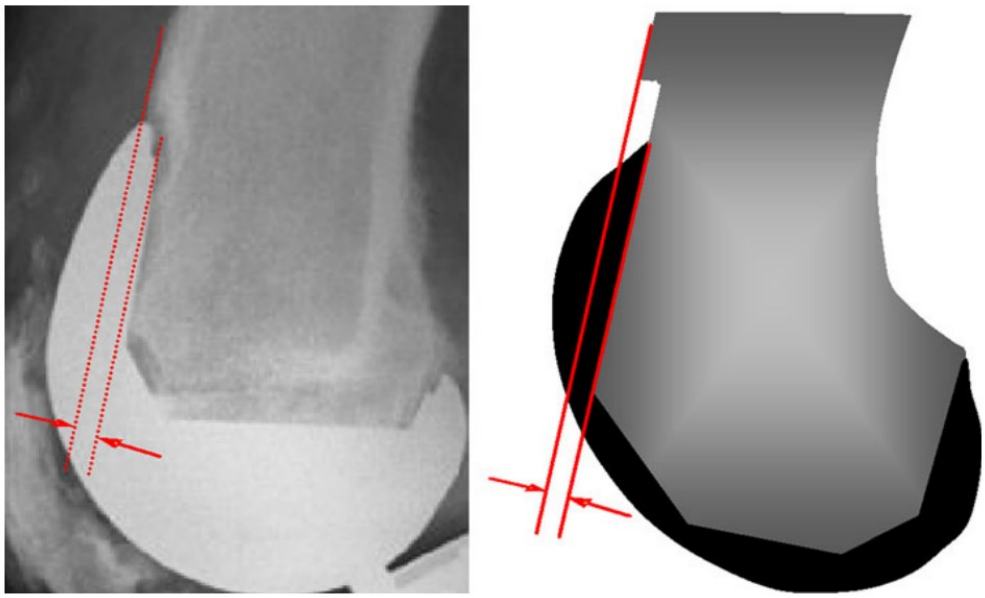

Figure 3.7: Radiograph of the knee after TKA with anterior femoral notching (left) and schematic representation of notch depth (right) [39].

Chapter 4

Material properties and constitutive models

Mathematical models have been shown to be an essential tool for the analysis and study of multiple phenomena, including the mechanical and physical aspects of biological structures.

These models find solid foundations in classical or Euclidean geometry along with the dimension given by the concept of time.

In the early stages of constructing a model for a molecule, object, or tissue, it is essential to therefore project that object into Euclidean space. Moreover, frequently, the space that such an object occupies three-dimensionally in Euclidean dimensions closely replicates those corresponding in the real world.

A notable advantage of employing a model is that it assigns Cartesian coordinates to all points within the real object. This means that every point in the object can be precisely located using a triplet of Cartesian coordinates (x1, x2, x3) within the Euclidean space, allowing quantitative measurements between different points [40].

However, the main advantage lies in the ability to define physical parameters and functions with respect to the coordinates established in the reference system. The essential point to be emphasised is that the creation of a Euclidean spatial model of an object gives the possibility of using the robust computational tools of classical geometry, integral calculus, and differential calculus to calculate quantities of extreme importance in the fields of physics and biology [40].

The way in which the material properties vary with respect to the direction at a fixed point in a material determines the material symmetry. If the properties of the material are the same in all directions, they are said to be isotropic. If the material properties are not isotropic, they are said to be anisotropic. There are different types of anisotropic symmetry. Those of most interest defined as orthotropic and transversely isotropic.

A orthotropic symmetry has three mutually perpendicular planes of reflective symmetry.

A material symmetry characterised by a single plane of isotropy is called transverse isotropy. Isotropic symmetry is characterised by the fact that each plane is a plane of isotropy.

The equations that characterise the physical properties of materials in a system are called "constitutive equations." Each material has a different constitutive equation to describe each of its physical properties [40].

In this regard, the finite element method (FEM) is a numerical technique for modelling complex geometries and loading systems. In fact, it is used to perform finite element analysis (FEA) of a given physical phenomenon.

The first step describes the geometry of the model when modelling with finite elements. This means choosing finite elements, determining material properties, and identifying stress conditions. The second phase involves simulating various stress conditions for the modelled material and concludes with the parametric study. This method is needed, for example, in the field of orthopaedics, to simulate or predict conditions that could lead to complications or failure and to react to increase the longevity of TKA [41].

To successfully develop an FE model for the study of joint mechanics, an accurate anatomical description of the joint and a detailed mathematical description of the material behaviour of all structures and tissues involved are required.

The following sections will review the most common constitutive models found in the literature used in FE models for each of the materials considered in the study.

4.1 Constitutive models of the bone

Bone is an important and extremely complex connective tissue. Its main functions are to provide mechanical support and protection to the body. This tissue differs from other tissues in the human body due to its higher stiffness and strength, donated mainly by the high percentage of minerals in its composition. In fact, bone is largely composed of apatite or hydroxyapatite in a collagen-based frame.

Analysing the structure of this tissue macroscopically, two different configurations are evident, cortical bone and trabecular bone.

4.1.1 Cortical bone

Cortical bone, also called compact bone, is a dense material that constitutes most of the outer envelope of a long bone with varying thickness.

Cortical bone is bounded by an outer layer, a dense specialised membrane of collagen fibres and fibroblasts, called the periosteum, and an inner surface called the endosteum. The latter does not contain the extensive collagenous structure of the periosteum; however, it delimits the central longitudinal tubular passage present in all long bones, called the medullary canal.

Lamellar bone consists of a series of laminae arranged concentrically with an axis parallel to that of the long bone in which they are located; between each lamina, there is a network-like system of blood vessels, with an occasional large radial vessel crossing a lamina and connecting two of the two-dimensional tangential networks. The bone is made up of quasi-cylindrical elements called osteons, consisting of the set of concentric laminae. This structure is organised to accommodate small arteries, arterioles, capillaries, and venules of the microcirculation.

As the macroscopic appearance of the cortical bone suggests, it has a shape-intrinsic orthotropic elastic symmetry. The degree of anisotropy of bone tissue can vary according to anatomical site, so cortical bone could also occasionally be considered transversely isotropic or even isotropic.

Recalling that the selection of a reference coordinate system is of considerable importance for anisotropic symmetry, we choose a coordinate system for the femur and the tibia as described in Chapter 2.
We then define the three ordered orthogonal directions: the first coincident with the longitudinal direction of the osteons, which is locally the most rigid direction; the second and third directions are mutually orthogonal in the plane perpendicular to the direction of the osteons.

Some research has assumed that cortical bone is transversely isotropic (TI), and others have assumed that it is an orthotropic (ORTH) material [42]. The choice of material symmetry for an elastic model of bone depends largely on the researcher's intended application of the elastic model. An example is the study of Norman et al. [43] that indicates that the stress analysis of a human femur is adequately satisfied by a transversely isotropic elastic model.
Therefore, if the intended use of elastic constants is the stress analysis of a particular bone, the assumption of greater symmetry of TI can be easily justified. However, if the physiological behaviour of bone tissue as a composite material is considered in a study, the difference in the assumption of ORTH or TI could be significant.
The constants determined using the ORTH and TI assumptions are slightly dissimilar; however, the difference is always consistent in the fact that the stiffness in the circumferential direction is always greater than that in the radial direction. If the bone were considered transversely isotropic, these two elastic constants would be equal. Blood normally flows from the medullary canal to the periosteum, that is, in the radial outward direction. This suggests that lower stiffness in the radial direction is associated with higher permeability in that direction [40].

	Pianigiani et al. (2017)	Yoon et al (1976)	Norman et al. (2001)	Knets et al. (1977)	Ashman et al. (1984)
Symmetry	ISO	TI	TI	ORTH	ORTH
E_x (GPa)	20.0	18.8	11.5	6.91	12.0
E_y (GPa)	20.0	18.8	11.5	8.51	13.4
E_z (GPa)	20.0	27.4	17.0	18.4	20.0
G_{xy} (GPa)	-	7.17	3.60	2.41	4.53
G_{xz} (GPa)	-	8.71	3.30	3.56	5.61
G_{yz} (GPa)	-	8.71	3.30	4.91	6.23
ν_{xy}	0.3	0.31	0.51	0.49	0.38
ν_{xz}	0.3	0.19	0.31	0.12	0.22
ν_{yz}	0.3	0.19	0.31	0.14	0.24
ν_{yx}	0.3	0.31	0.51	0.62	0.42
ν_{zx}	0.3	0.19	0.31	0.32	0.37
ν_{zy}	0.3	0.19	0.31	0.31	0.35

Table 3: Cortical bone properties: Young's moduli are indicated by Ei, i = 1, 2, 3, the shear moduli by Gij and Poisson's ratios by ν ij where i, j = 1, 2, 3, and i is not equal to j [40], [43], [44]. ISO: isotropic, TI: transversely isotropic, ORTH: orthotropic.

4.1.2 Trabecular bone

Cancellous bone generally exists only within the limits dictated by cortical bone, particularly in the epiphyseal regions of long bones. This tissue also takes the name trabecular or spongy bone, as it is made up of short struts of bone material called trabeculae, which recalls the structure of a sponge.

The architecture of cancellous bone has been difficult to characterise quantitatively. Cancellous bone is not only anisotropic but also highly porous and inhomogeneous due to the significant variation in the direction of the trabeculae architecture that occurs in any cancellous bone. Therefore, identifying the type of elastic symmetry is complicated by the inhomogeneity of the material, making it difficult to analyse the data measuring the elastic constants [40].

Normally, when the interest is joint kinematics, it suffices to interpret the proximal tibia and distal femur as rigid bodies. On the contrary, if an analysis of bone stresses and deformations on contact surfaces, it is necessary to adopt a transversely isotropic linear elastic model for cortical bone [45].

Although this material has nonlinear elastic properties even at small strains, it is frequently modelled as an isotropic material with linear elastic properties. In fact, Kabel et al. [46] showed that the use of isotropic and homogeneous properties can lead to good predictions of apparent elastic properties assuming linear elasticity.

	Kayabasi et al (2007)	Innocenti et al (2009)
Symmetry	ISO	ISO
E (GPa)	2.13	2.40
ν	0.3	0.3

Table 4: Trabecular bone's properties: Young's moduli are indicated by E, and Poisson's ratios by ν [47], [48]. ISO: isotropic.

4.2 Constitutive models of the tendons and ligaments

Tendons and ligaments, along with joint capsules, connect the bones and muscles of the joints and help guide movement and maintain joint stability. The function of tendons is to connect the muscle to the bone and to transmit tensile loads from the muscle to the bone, thus generating movement of the joint. Ligaments, on the other hand, are important structures that connect bones by guiding and limiting joint movement.

Recall that the ligaments connecting the femur, tibia, and fibula are the anterior cruciate ligament (ACL), posterior cruciate ligament (PCL), medial collateral ligament (MCL) and lateral collateral ligament (LCL). On the other hand, those involved in the patellofemoral joint are mainly the medial patellofemoral ligament, the lateral retinaculum and the patellar tendon. The latter is located anteriorly to the patellar bone and is an important structure that connects the patella to the proximal portion of the tibia [40].

Ligaments are made of a water-rich ground substance reinforced by collagen fibres. The ground substance contains proteoglycans, which, together with hyaluronic acid are able to attract water from the external environment, creating a kind of gel. The ability of the matrix to capture water molecules and thus maintain a high water content even when stretched, determines the hypothesis of incompressibility of the tissue, which is incorporated in most constitutive models. The matrix also contains a moderate number of fibroblasts, which are responsible for the synthesis of collagen molecules and constitute the fibres that provide stiffness and tensile strength to the tissue.

In general, tendons and ligaments consist of approximately 20% cellular material and 80% extracellular material; the extracellular material is further divided into approximately 30% solids and 70% water. These extracellular solids are collagen, the ground substance, and a small amount of elastin.

A "direct tendon" is a tendon that has a straight and direct course between its muscle connection and its bone connection. Instead, a ‘wraparound tendon’ is a tendon that bends around a bony pulley or threads fibrously between its muscle and bone connection. In addition to tendons, some ligaments can also be defined as wrapping or compressing against the bone. For these reasons, tendons and wrap-around ligaments are subjected to particularly high frictional forces at the wrap-around points [40].

Regarding the description of the structure of tendons and ligaments, the collagen fibres that make up the tendons have a parallel arrangement and the collagen fibres that make up the ligaments may not be completely parallel but almost parallel to each other.

In the unloaded configuration, collagen fibrils are crimped and therefore arranged in a helical or waveform pattern. As soon as a load is applied, the crimping gradually disappears as the fibrils become aligned with the loading direction. In this ‘straightening’ process, the tissue exhibits a smaller Young’s modulus than it exhibits after the crimp is removed [49].

With regard to the assignment of mechanical properties to the latter tissues considered, the literature is extensive. This is justified by the fact that ligaments and tendons are fundamental components when aiming to analyse the biomechanics of a joint such as the knee; however, they do not always turn out to be structures placed in the foreground with regard to analysis in this area.

Depending on how much attention is focused on ligaments and tendons, different models are therefore considered. *Table 5* shows the main approaches obtained from the literature.

	Constituitive model
Pianigiani et al., 2017	• Linear elastic • Isotropic
Innocenti et al., 2014	• Linear elastic • Isotropic
Peña et al., 2005	• Hyperelastic • Transversely isotropic material
Song et al., 2004	• Hyperelastic • Incompressible • Isotropic
Blankevoort et al., 1991	• Non-linear elastic

Table 5: Constitutive model of ligaments extracted from a literature review [44], [50]–[53].

The assumptions considered in each study thus lead to the consideration of multiple approaches. As highlighted in the table above, some studies, such as the one conducted by Peña et al. [50] consider the anisotropic symmetry of the material determined by the orientation of collagen fibres, while multiple other studies neglect it. Indeed, ligaments have time-dependent and history-dependent mechanical properties due to both the interaction of water with the ground substance and the intrinsic viscoelasticity of the solid phase. In fact, during loading, microstructural reorganisation processes take time to develop. Therefore, the mechanical behaviour of these tissues is strongly influenced by the strain rate and the loading time [40].

The values that emerged from the literature search of elastic moduli and Poisson moduli obtained from uniaxial tensile tests for the ligaments and tendons considered in the developed study are presented in Table 6.

A second way of classifying ligaments is based on how they are represented. A thorough literature review has shown that ligaments and tendons in finite element models can be modelled in different ways. In particular, one can have one-dimensional (1D) models using linear elements such as springs, trusses, and beams, two-dimensional (2D) models using elements such as shells or membranes, and three-dimensional (3D) models using solid elements [49].

	Reference	Material properties
Medial collateral ligament	Pianigiani et al., 2017	• E = 362 [MPa] • ν = 0.45
	Cho et al., 2020	• E = 326 [MPa]
Lateral collateral ligament	Pianigiani et al., 2017	• E = 228 [MPa] • ν = 0.45
	Cho et al., 2020	• E = 493 [MPa]
Medial patellofemoral ligament	Criscenti et al., 2015	• E = 116 [MPa]
Patellar tendon	Hashemi et al., 2005	• E = 507 [MPa] • ν = 0.45
	Blevins et al., 1994	• E = 310 [MPa]

Table 6: Ligaments properties: Young's moduli are indicated by E, and Poisson's ratios by ν [47], [48].

1D models such as springs, trusses, and beams are often used to model the mechanical role of ligaments in the knee joint. During knee movement, the fibre bundles of the knee ligaments are unevenly loaded with stresses, deformations, and mechanical properties. For this reason, a single ligament is usually not represented by a single linear element, but by two or more elements representing the different bundles of which it is composed.

Incorporating ligaments into a 3D model of the knee is achieved most naturally through the utilisation of solid elements. This methodology additionally simplifies the modelling of ligament wrapping through the implementation of surface-to-surface contact. Furthermore, this approach improves the precision of simulating stresses that encompass factors beyond pure tension, including those generated by interactions with bone structures and those in proximity to insertion regions [49].

The mechanical characteristics of ligaments exhibit a unique nature characterised by strong anisotropy and a limited ability to withstand compression. Consequently, their representation using solid elements becomes less appealing when compared with the utilisation of line elements. A middle-ground approach involves the incorporation of springs or trusses within a matrix governed by a straightforward constitutive law, such as linear isotropic elasticity or neo-Hooke hyperelasticity [54]–[56]. This method has been previously used in several research investigations, particularly in the context of 2D elements such as shells or membranes reinforced with nonlinear line elements to capture the anisotropic behaviour of ligaments. Additionally, some studies have used simplified continuum material models that neglect the anisotropy inherent in ligamentous tissue [49] [55].

In the following table, a summary of what has emerged from the literature when it comes to modelling ligament tissues in space is presented in Table 7.

	Model typology
Pianigiani et al., 2017	• One-dimensional model • One bundle
Blankevoort et al., 1991	• One-dimensional model • One bundle
Peña et al., 2005	• Three- dimensional model
Halloran et al., 2005	• Two- dimensional model • Membrane elements
Zelle et al., 2011	• Two- dimensional model • Shell and line elements

Table 7: Categories of ligament modelling emerging from the literature review [44], [50], [53], [55], [57].

4.3 Constitutive models of prosthesis materials

The material of the femoral component and tibial tray is metallic, specifically cobalt-chromium alloy (CoCr), while the material of which the tibial insert and the patellar component are manufactured is ultra-high molecular weight polyethylene (UHMWPE). According to the literature, the materials from which the knee prosthesis considered in this study is manufactured were assumed to be linear elastic, homogeneous, and isotropic [58].

The material properties, specifically Young's modulus (E) and Poisson's ratio (ν), are provided in *Table 8*.

	CoCr alloy	UHMWPE
Model	ISO	ISO
E [MPa]	240’000	685
ν	0.30	0.40

Table 8: Knee implant material properties: Young's moduli are indicated by E, and Poisson's ratios by ν [58].

Chapter 5

Materials and method

5.1 Segmentation

The segmentation process involves dividing digital images into multiple segments, called regions, or image objects. The goal of this practise is to identify objects and their boundaries in images [59]. When applied to an image stack, which is typical in medical imaging, the contours resulting from image segmentation can be used to create 3D reconstructions [60].

Digital Imaging and Communications in Medicine (DICOM) is the standard for medical imaging; in fact, it represents the output of imaging techniques such as radiography, ultrasound, computed tomography (CT), and magnetic resonance imaging (MRI). Therefore, it is a global technology standard format, for storing information from digital medical data [61].

To recreate the bone geometries on which to develop the finite element model, images obtained from CT scans of multiple patients were analysed to select a knee joint free of bone pathologies or deformities.

3D Slicer software was chosen to process the DICOM images. The latter is a free open-source software for visualisation, processing, segmentation of medical 3D images in the three cardinal anatomical planes, namely the coronal plane, the sagittal plane, and the axial plane.

The first step in analysing the available DICOM images of cadaveric legs involved selecting those that depicted a knee joint in an extended position. Therefore, images that showed even partially flexed knee or whose output resolution was not sufficient were discarded from the election.

According to the literature, a knee can be said to have neutral alignment if the hip-knee-ankle angle (HKA) is 180°. In this alignment, the line of the knee joint is inclined at an oblique angle of 3°, with an alignment in the varus of 3° in the the tibia and in valgus of 3° in the femur.

A simplified approach assumes that the joint lines are parallel to each other. Furthermore, it is necessary to specify that the mechanical femoral angle (FMA) measures 93° ± 1.5°, and the tibial angle (TMA) measures 87° ± 1.5°, with both angles measured in a medial direction [62] (Fig. 5.1).

To be able to identify the mechanical axes of the femur and tibia and to be able to measure the inclination of the joint line, it was first necessary to define the principal anatomical points of reference that would allow their measurement.

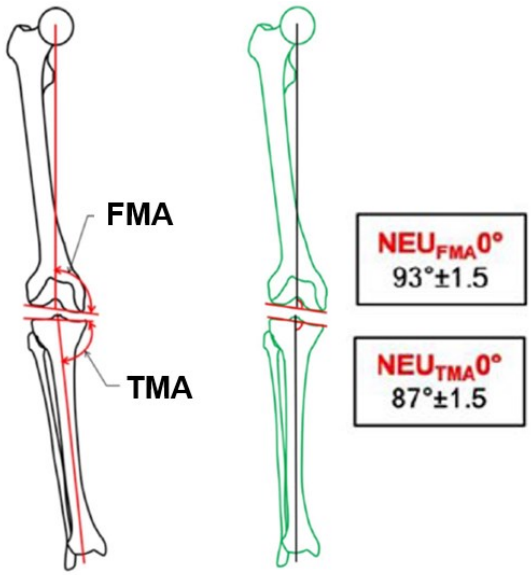

Figure 5.1: Femoral mechanical angle (FMA) and tibial mechanical angle (TMA) in neutral knee alignment [62].

For the femur, the following bony landmarks were identified:

- Femoral hip centre (FHC): centre of the ball of best fit at the femoral head;
- Femoral Knee Centre (FKC): most anterior point at the centre of the femoral notch on a caudal-cranial view of the femur, aligning the hip centre with the roof of the femoral notch;
- Posterior medial femoral condyle (FMCP): the most posterior point of the medial condyle, aligned along the mechanical axis (FMAx);
- Lateral posterior femoral condyle (FLCP): the most posterior point of the lateral condyle, aligned along the FMAx [63].

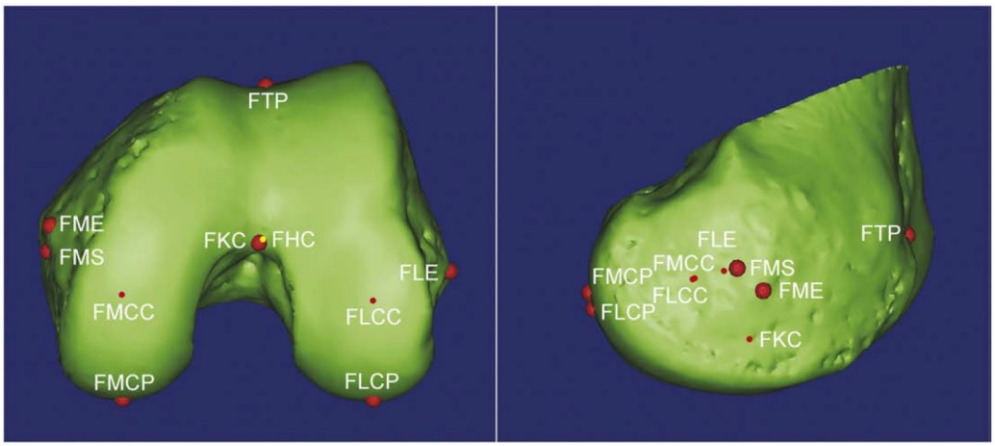

Figure 5.2: Three-dimensional model of the distal femur in axial and sagittal view showing abbreviations of the relevant bony landmarks of the bone [63].

With regard to the tibia, on the other hand, the following landmarks were considered:

- Tibial ankle centre (TAC): the centre of the circle of best fit of the tibial plafond;
- Tibial knee centre (TKC): the midpoint between the two tibial spines projected onto the bone surface;
- Centre of the medial tibial condyle (TMCC): the centre of the best-fitting circle around the edge of the cortex of the medial tibial plateau;
- Centre of the lateral tibial condyle (TLCC): the centre of the rim best positioned around the edge of the cortex of the lateral tibial plateau [63].

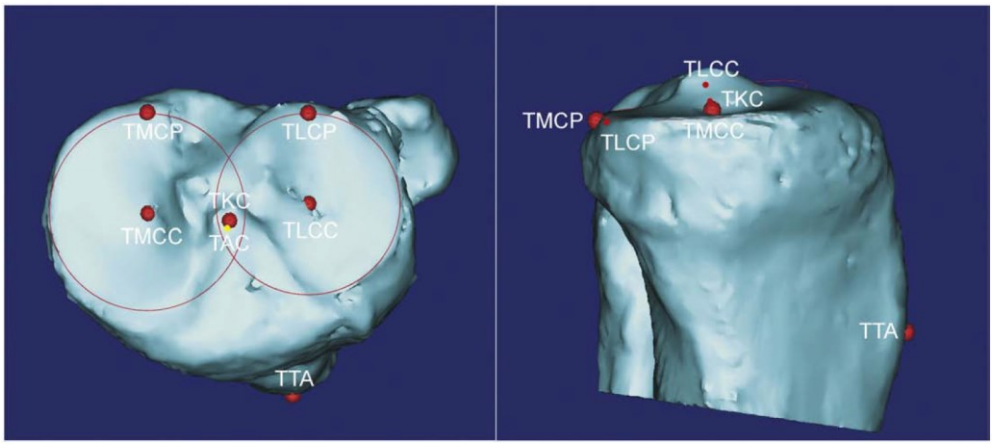

Figure 5.3: Three-dimensional model of the proximal tibia in axial and sagittal view showing abbreviations of relevant bony landmarks of the bone [63].

The femoral mechanical axis (FMAx) was defined as the line that joins the centre of the femoral knee and the centre of the femoral hip (FHC-FKC). The tibial mechanical axis (TMAx), on the other hand, was defined as the line the connects the centre of the tibial plateau and the centre of the ankle (TKC-TAC). The frontal plane of the knee was defined as the plane that contains the mechanical axes and is parallel to the joint line.

A left cadaver leg with FMA of 92.47° and TMA of 87.48° has been selected (fig 5.4) it was assumed that this limb belonged to a patient weighing about 80 kg.

The Hounsfield scale, which is a unit scale used to quantitatively describe radiodensity, can be applied, for example, to scans made with conventional computed tomography and thus allows the interpretation of differences between tissues in DICOM images. This is possible because the greyscale with which the different types of tissues in DICOM images are represented.

One of the commonly used segmentation methods is the threshold method, which recognises an image based on a Hounsfield unit (HU) threshold value and converts it into a binary image [64].

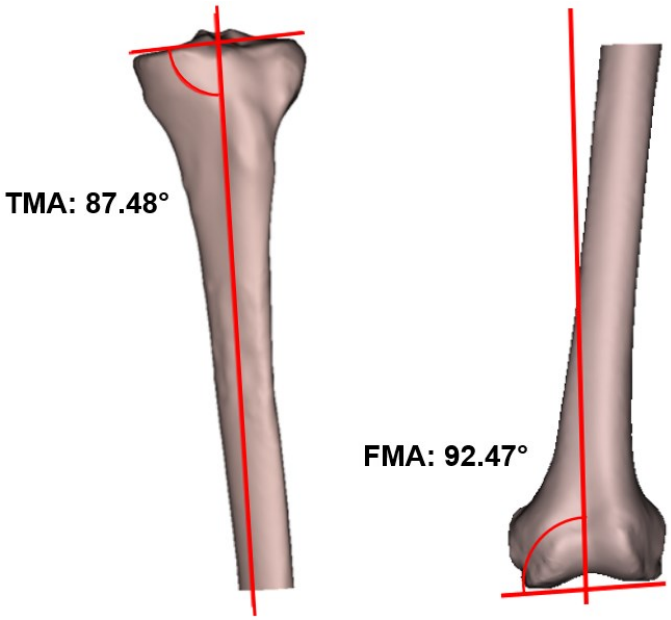

Figure 5.4: Femoral mechanical angle (FMA) and tibial mechanical angle (TMA) in the selected knee.

In this step of the study, the aim was to reconstruct cortical bone tissue. Thus, in particular, the values within which we can describe this tissue lie in a range between 130 [HU] and 1350 [HU].

However, sometimes the resulting three-dimensional image still has a lot of noise and has not been properly reconstructed.
Mesh smoothing is a technique that reduces the roughness and irregularities of a 3D mesh by adjusting the positions of selected voxels, i.e., the volumetric unit that is obtained in the three-dimensional reconstruction as a result of pixel selection in DICOM images. The smoothing technique can help remove noise, fill empty spaces, and smooth edges or sharp corners.

In this way, geometries were obtained for each bone considered for the purpose of studying the biomechanics of the tibiofemoral and patellofemoral joints, thus as described in the previous chapters, the femur, tibia and patella (Fig. 5.5).

Once the accuracy with which the bones were reconstructed was verified, it was necessary to derive the main bone landmarks, in addition to those previously extracted. This procedure was necessary to derive the reference points for the construction of the reference systems and the insertions of the tendons and ligaments.

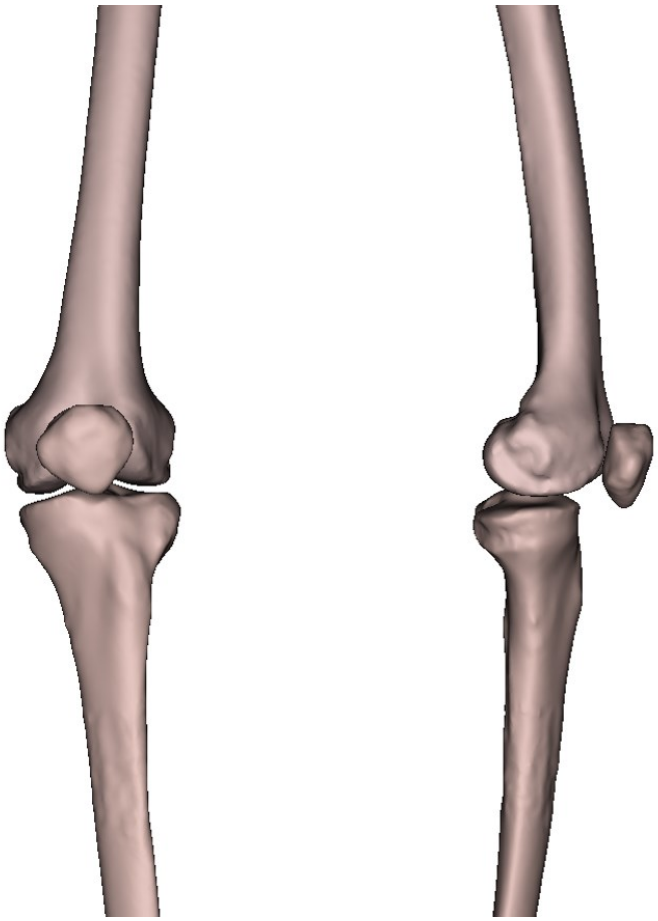

Figure 5.5: Three-dimensional reconstruction of the selected bones: femur, patella, and tibia.

In particular, the following anatomical landmarks were extracted for the construction of the reference systems:

- Femoral Hip Centre (FHC);
- Femoral Knee Centre (FKC);
- Femoral Medial Condyle Centre (FMCC): centre of the best-fit sphere to the medial condyle;
- Femoral Lateral Condyle Centre (FLCC): centre of the best-fit sphere to the lateral condyle.

For the construction of the tibia-related reference system, the previously described landmarks were extracted instead:

- Tibial Ankle Centre (CT);
- Tibial Knee Centre (TKC);
- Tibial Medial Condyle Centre (TMCC);
- Tibial Lateral Condyle Centre (TLCC).

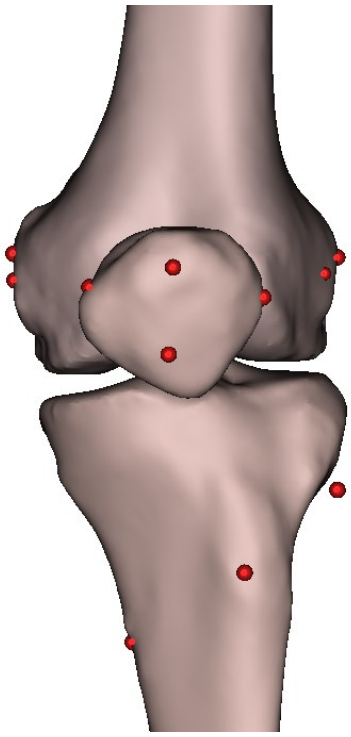

Figure 5.6: Reference points for insertion of the ligaments and tendons derived from the literature on the three-dimensional model reconstructed by segmentation.

The superficial insertion of the medial collateral ligament at the mean position of the medial femur has been considered approximately 3.2 mm proximal and 4.8 mm posterior to the medial epicondyle. Instead, the distal insertion on the tibia has been considered 60 mm distal to the joint line, anterior to the posteromedial crest of the tibia [5].

The MPFL insertion on the femur was located approximately 10.6 mm proximally and 8.8 mm posteriorly to the medial epicondyle.

With regard to the attachment at the superomedial aspect of the medial border of the patella, the insertion of the medial patellofemoral ligament was located at 41.4% of the length from the proximal tip of the patella along the total length of the patella (proximal to distal) [5], [6].

The femoral attachment of the lateral collateral ligament has been positioned in a small bony depression, approximately 1.4 mm proximal and 3.1 mm posterior to the lateral epicondyle. The distal attachment of the LCL was placed in a small depression on the lateral side of the head of the fibula, approximately 8.2 mm posterior to the head of the anterior margin of the fibula, and 28.4 mm distal to the tip of the fibular styloid [8].

In order to allow for correct application of the quadriceps load, the insertion point on the patella was considered to be on the upper pole of the patella, although the structure of the quadriceps ligament itself was not considered within the scope of the finite element model construction.

The patellar tendon was considered to extend from the apex and lower portions of the patella to the smooth upper part of the tibial tuberosity. In particular, the

proximal insertion on the patella was considered to be 12.28 mm proximal to the apex of the patella. However, it was considered in the tibial tubercle.The geometries obtained were then exported by the software as an IGS file, which is a graphic file saved in a 2D / 3D vector format based on IGES (Initial Graphics Exchange Specification), thanks to which it was possible to carry out the finite element study afterwards.

5.2 Finite elements modelling

To model the knee joint using the finite element method, Abaqus/CAE software was chosen, from Dassault Systèmes, which is software for finite element analysis and computer-aided engineering.

5.2.1 Parts

As a first step, the IGS files of each geometry were imported into the software, thus the cortical femur, cortical tibia, and patella geometries were imported.

Therefore, it was possible to reconstruct the component of the trabecular tissue by filling the hollow part of the tibia and femur geometries through a Boolean operation.

Having the parts of the bone tissue complete made it possible to develop the reference systems of the two long bones according to the literature, thus in accordance with the method explained in Grood and Suntay's 1983 study [14] presented in Chapter 2.
The three-point reference system construction method was elected; in particular, the software requires in order: the origin of the reference system, a point belonging to the X-axis, and one final point lying on the X-Y plane.
The midpoint between FMCC and FLCC was considered the origin in the femur. As regards the point lying on the X-axis, since the latter coincides with the interepicondylar axis and in the left knee this axis was considered positive in the medial direction, FMCC was taken into account. Finally, a point was chosen randomly that was of the plane orthogonal to the mechanical axis passing through the origin so that the positive direction of the Y-axis coincided with the anterior direction. The software made it possible to automatically derive the direction of the Z axis, which coincident with the mechanical and positive axis in the proximal direction. In the tibia, the origin was derived by extrapolating the midpoint between TMCC and TLCC. For the same reason that was previously described, the point on the X-axis was considered to be TMCC. For the remaining two axes, the same procedure was used as for the Y and Z axes in the femoral bone.

Two-dimensional elements were chosen to construct the ligament parts. Depending on the width and length of each ligament, the part was subdivided into an array consisting of four columns and eleven rows of four-node shell elements. The aim of the work was to analyse the kinematics and contact forces in the knee. For this reason, it was considered more appropriate to represent ligaments using two-dimensional elements as the main focus of the analysis did not lie in their mechanical behaviour, but rather they were exploited for their functions of limiting and guiding joint movement.

Furthermore, this decision was made because the literature presents multiple scenarios in which one-dimensionally modelled ligaments have been exploited, thus investigating how the biomechanics of the knee was affected by this choice.

The joint prosthesis model is a stabilised posterior (PS), which thus includes a femoral insert, tibial tray, and tibial insert made of UHMWPE in addition to the patellar component.

5.2.2 Properties

For the trabecular bone of the femur and tibia, since these are long bones, the choice of a transversely isotropic model was considered appropriate. For patellar bone, a linear elastic homogeneous model was chosen as it is also composed of a material similar to cortical bone, but an isotropic constitutive model was preferred, as the behaviour of this material can be closely approximated by such modelling as in the van Jonbergen study [65].
For trabecular bone, an isotropic linear model was selected as outlined in the previous chapter as a result of the literature analysis.
Finally, an isotropic linear elastic model was chosen for the ligaments because, as previously stated, the focus was not on mere tissue behaviour but exclusively on their comprehensive function in the model. Therefore, it was considered that this type of modelling could allow the desired development of the analysis.

The mechanical properties chosen for each material are summarised in Table 9.

Material	Properties
Cortical bone	• E_x = 11'500 [MPa] • E_y = 11'500 [MPa] • E_z = 17'000 [MPa] • G_{xy} = 3'600 [MPa] • G_{xz} = 3'300 [MPa] • G_{yz} = 3'300 [MPa] • ν_{xy} = 0.51 • ν_{xz} = 0.31 • ν_{yz} = 0.31
Cancellous bone	• E = 2'130 [MPa] • ν = 0.3
Patellar bone	• E = 15'000 [MPa] • ν = 0.3
Cobalt-Chrome alloy	• E = 240'000 [MPa] • ν = 0.3
UHMWPE	• E = 1'200 [MPa] • ν = 0.3
Lateral collateral ligament	• E = 228 [MPa] • ν = 0.45
Lateral retinaculum	• E = 100 [MPa] • ν = 0.45
Medial patellofemoral ligament	• E = 116 [MPa] • ν = 0.45
Patellar tendon	• E = 507 [MPa] • ν = 0.45
Medial colalteral ligament	• E = 362 [MPa] • ν = 0.45

Table 9: Summary of the mechanical properties of the materials used in the study. Young's moduli are indicated by E_i = 1, 2, 3, the shear moduli by G_{ij} and Poisson's ratios by ν_{ij} where i, j = 1, 2, 3, and i is not equal to j.

5.2.3 Assembly

In order to create the complete model of the joint, the components were assembled together. In particular, the ligaments were positioned with the help of the insertion points obtained in the segmentation software, following the instructions described in the previous paragraph.

When comparing the various sizes of prostheses, a 6 tibia and femur prosthesis was chosen to simulate the implant.

To avoid notching the femoral bone, it was considered appropriate to consider the posterior reference methodology to establish the reference position of the femoral component in both mechanical and kinematic alignment models.

The positioning of the implants was then carried out, following the literature. Thus, going back to what has been explained in Chapter 3: in the mechanical alignment model, it consisted of positioning the femoral and tibial components orthogonally with respect to their corresponding mechanical axes; conversely, in the kinematic alignment, resection was performed parallel to the joint line.

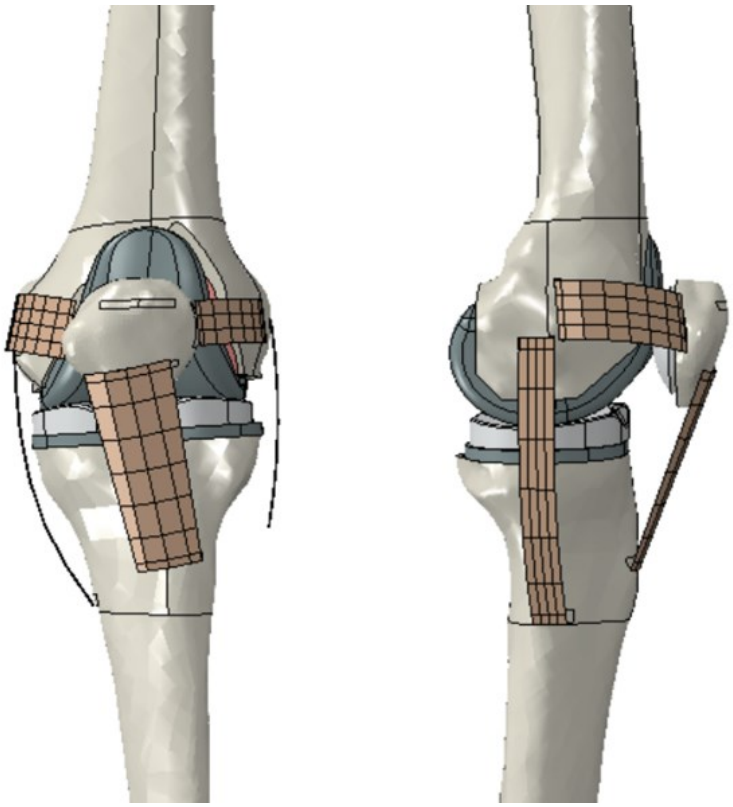

Figure 5.7: Total model of mechanical alignment TKA in full extension. Anterior view and lateral view.

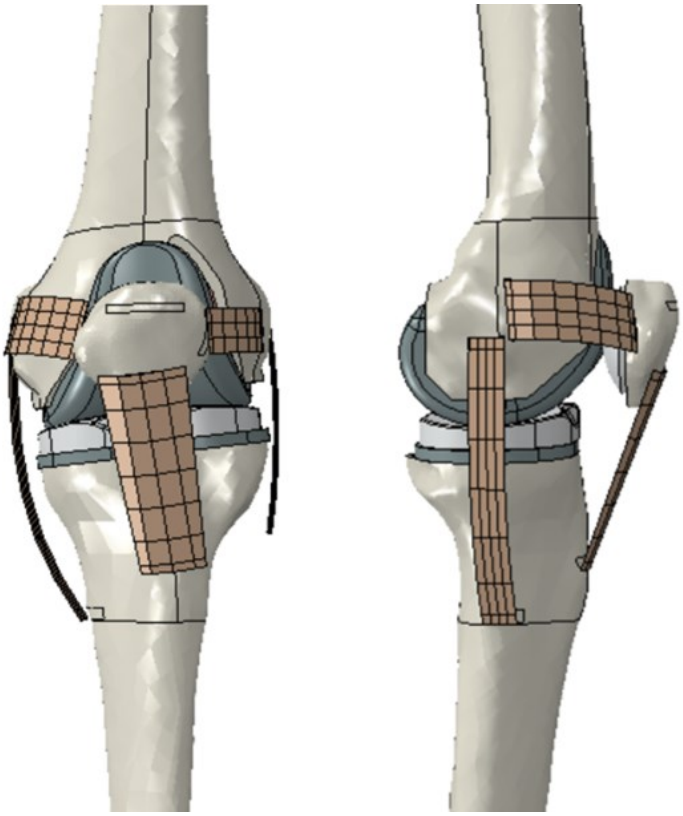

Figure 5.8: Total model of kinematic alignment TKA in full extension. Anterior view and lateral view.

5.2.4 Constraints

To simulate the fixation of the implant to the bone, a tie constraint was applied. The three interfaces where this kind of constraint was applied were the interface between the femoral component and the distal femur, the interface between the tibial tray and proximal tibia, and the finally between the patella and patellar component. This constraint typology was also applied to the interface between the tibial insert and the tibial component to avoid displacements that could lead to errors in the analysis, such as high strains.

For the ligaments and patellar tendon, a coupling constraint was applied between their insertion areas on the femur, tibia and patella and the respective portion of each ligament involved in anchoring, respectively. In detail, this constraint couples the motion of a set of nodes on a surface, in this case bone, to the motion of a reference node of the ligament, preventing reciprocal translations but allowing rotations. The following is an example of constraints involving ligament insertions, specifically in the model of kinematic alignment (Fig. 5.9).

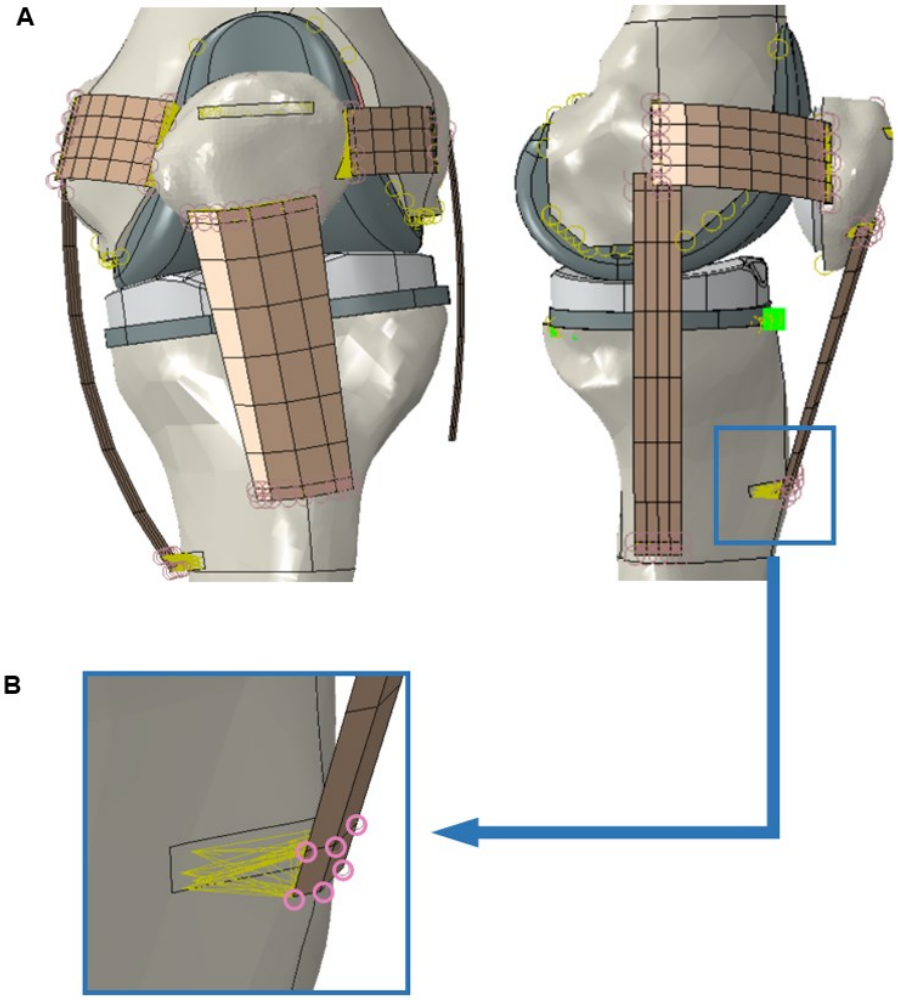

Figure 5.9: Representation of coupling constraints in frontal and lateral view (A). Magnification of the coupling between the selected nodes of the patellar tendon geometry and the insertion surface on the tibial tuberosity (B).

A tibial reference point (Constraint_tibia) was created, located 5 mm downward from the distal tibial surface. The distal part of the tibia was coupled to this reference point, where the axial load was applied to the knee joint.

For the femur, the centre of flexion-extension rotation (Flexion_centre) was identified along the transepicondylar axis. The inner surface of the femoral component was coupled to this point at which the femur was imposed.

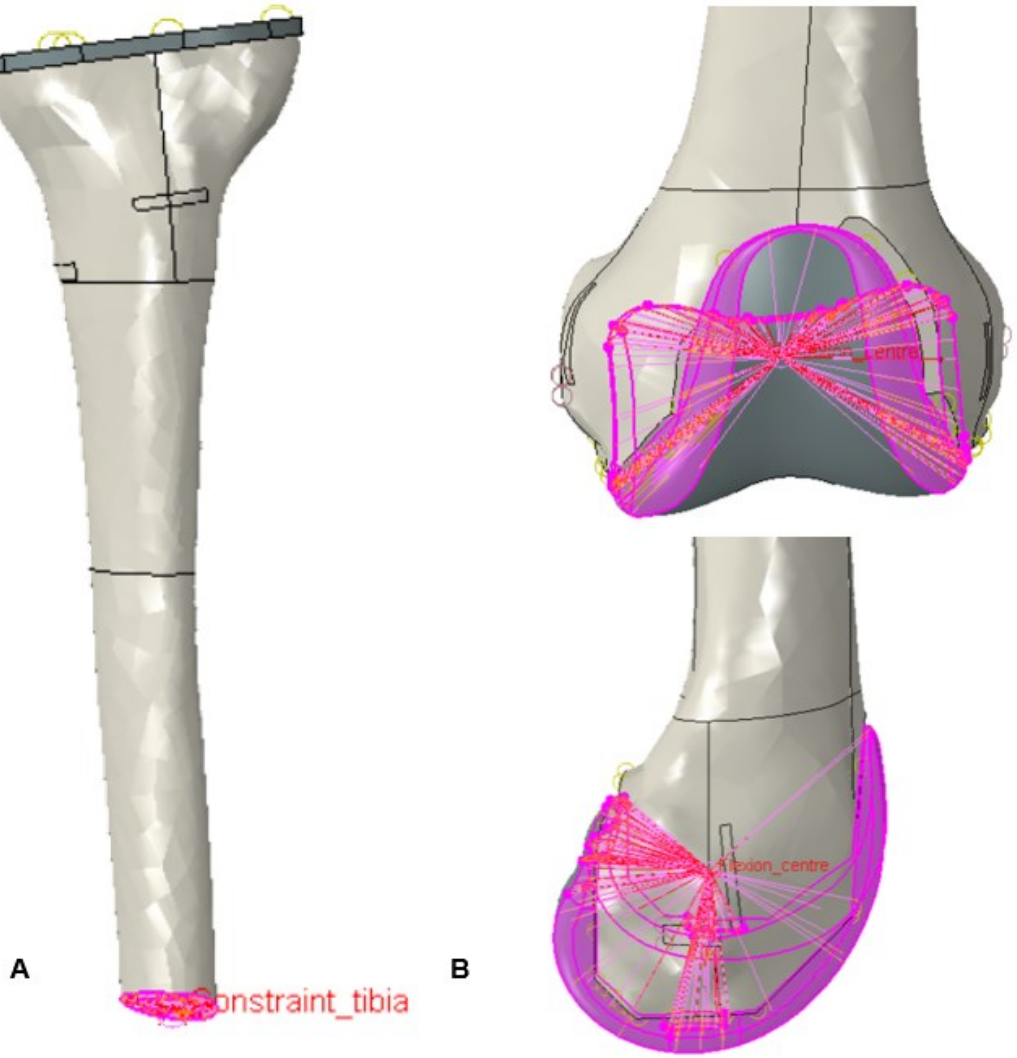

Figure 5.10: Representation of the coupling constraint in the distal section of the tibia with the reference point on which the boundary conditions will be applied (A). Representation of the coupling constraint of the femur with the reference point on which the rotation will later be applied. Represented in frontal view, top, and lateral view, bottom (B).

5.2.5 Loads

To simulate the action of the quadriceps, a load of 570 N was applied to the proximal surface of the patella. This load was not imposed constantly, but rather applied according to a linear trend that increased with degrees of flexion as described in the literature. The direction of the force during the entire flexion movement is parallel to the anatomical axis of the femur, thus following the direction of the main bundles of the muscles that make up the quadriceps [66].

Since wrapping was not modelled on the quadriceps tendon, it appeared necessary to apply a load in the anteroposterior direction to the patella in order to limit instability and thus excessive relative displacements in the patellofemoral articulation. Therefore, a load of 900 [N] was applied in the posterior direction.

Finally, to simulate the physiological load during a squat movement in a joint subjected to TKA, according to the literature, a load of 2.1 time BW emerges in the knee articulation. Therefore, following the assumptions made initially regarding the weight of the selected patient, a load of approximately 1700 [N] was plausible. In this hypothesis, this load was applied to the distal reference point of the tibia, as mentioned in the previous paragraph, as assumed in the study by Jan Victor [66].

Each load was applied in a linear increase trend as the degrees of flexion increased, as justified by the literature.

5.2.6 Prestrain of the ligaments

In the context of our research, we applied thermal loading to model the initial strain behaviour of the ligaments. This modelling process involves the utilization of a thermal expansion coefficient (α) with a negative value, inducing the material to contract when subjected to a fictious increasing temperature. The relationship is mathematically expressed as:

$$\varepsilon^{th} = \alpha\,(\Theta - \Theta^0)$$

Here, ε^{th} is the thermal strain experienced by the ligaments, α denotes the thermal expansion coefficient, Θ represents the current temperature (set at 1 K in our models), and Θ^0 is the reference temperature (set at 0 K). Under these specific conditions, the previous equation is simplified as:

$$\varepsilon^{th} = \alpha$$

This equation illustrates the effect of temperature changes on thermal strain of the ligaments, with α serving as a parameter governing this behaviour. Such a modelling plays a crucial role in our investigation of the mechanical response of the tendon and ligaments to thermal variations.

The following table shows the different values of ε^{th}, taken from the literature, which were considered for different tissues [53].

Ligament	ε^{th}
Medial collateral ligament	-0.04
Lateral collateral ligament	-0.05
Medial patellofemoral ligament	-0.06
Lateral retinaculum	-0.03

Table 10: Values of ε^{th} for the ligaments considered in the model [53].

5.2.7 Boundary conditions

For the femur, the boundary conditions were applied to the centre of rotation. The femur was then constrained in the flexion-extension direction, allowing exclusively 120 degrees of rotation around that axis, leaving the varus-valgus rotations free and constraining the remaining four degrees of freedom.

In contrast, the tibia was left free for proximal-distal translation because the axial load was applied at the reference point distal to this bone. To compensate for the degrees of freedom constrained to the femur and to allow the knee to possess the six physiological degrees of freedom, only the varus-valgus rotations were constrained, which were free as anticipated for the femur.

5.2.8 Mesh

The femur and tibial models underwent partitioning to establish a more refined mesh in the regions of specific interest, while a coarser mesh was employed in the proximal femur and distal tibia. These areas of interest are primarily concentrated near the joint, focussing on the interface between the bone and the prosthesis.
In the context of the tibia, two perpendicular planes were established along its axis. The initial plane was positioned 50 mm from the most proximal point of the joint interface, while the subsequent plane was located at a distance of 70 mm from the preceding partition. This process ultimately led to the creation of three distinct partitions within the tibia.
The femur, on the other hand, was divided into three segments employing two planes that were perpendicular to its mechanical axis. These planes were located at distances of 55 mm and 135 mm, respectively, from the most distal point of the bone.
The same mesh was used for the patella as in the partitions near the tibia and femur joints. Similarly, for all elements of the prosthesis, the mesh elements were assigned so that there was coherence at the bone-prosthesis interface.

For bone and prosthesis geometries, 4-node linear tetrahedrons (C3D4) were used. For ligaments, S4R elements were used instead. These elements are 4-node curved shells with finite membrane strains.

The mesh of the mechanical alignment model was found to have 168,103 elements, divided into 166,167 C3D4 elements and 1,936 S4R elements. For the kinematic model, on the other hand, the total was 170,703 elements, of which 168,767 were C3D4 elements and 1,936 were S4R elements.

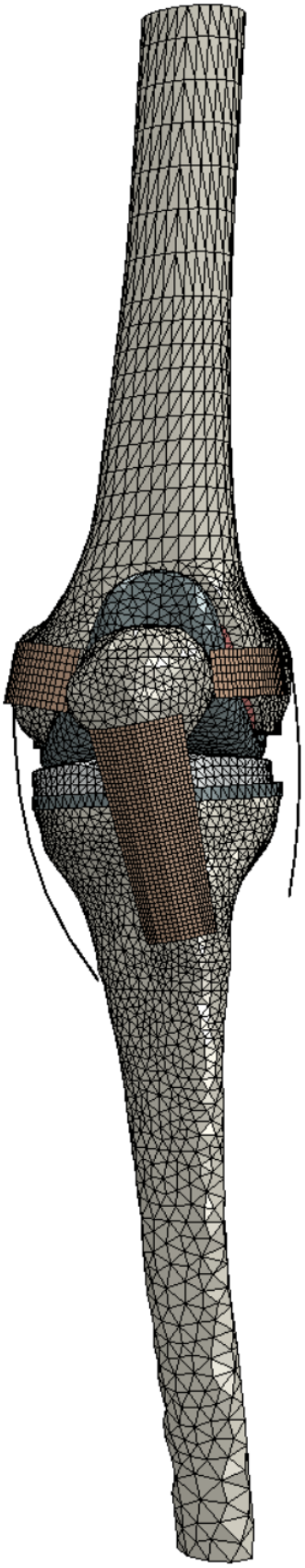

Figure 5.11: Front view of the mesh of the entire joint model with the prosthesis applied according to mechanical alignment.

5.2.9 Simulation

The aim of the study was to analyse the mechanical behaviour of the two types of knee implant alignment during a squat movement. For that purpose, it was first necessary to simulate the prestrain of the ligaments as described above, for a time lapse of 0.5 s. Secondly, the squat movement was implemented by imposing a flexion of the joint of 120 degrees over a time range of 5.3 s starting from the reference extended position according to the course shown in the following graph.

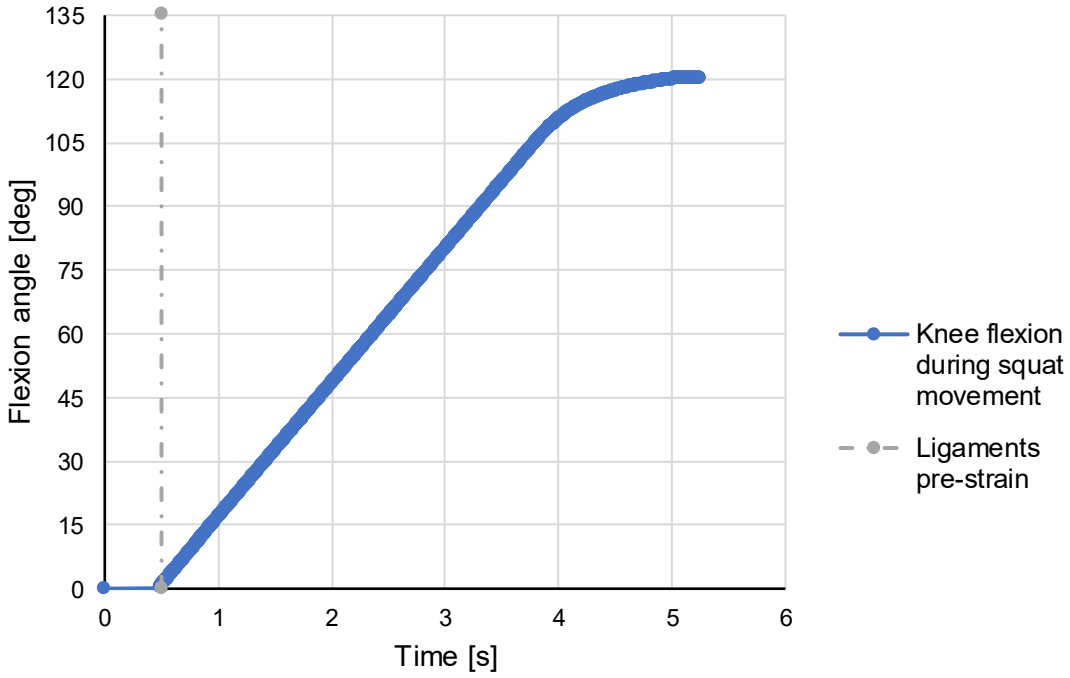

Figure 5.12: Evolution of rotation over time to implement knee flexion.

The explicit solution method was considered as it is a dynamic procedure developed to model high-speed events. Since the minimum stable time increment is usually very small, most problems require a large number of increments. An advantage of this procedure is the greater ease with which it solves complicated contact problems. Furthermore, when models become very large, the explicit procedure requires fewer system resources than the implicit procedure [67].

In this study, a relatively quick movement as a squat, averaging 1 to 2 seconds, could have caused convergence problems with the simulation. By choosing this method and considering a longer period of the movement, approximately three times the duration of a normal squat movement, it was possible to converge the analysis.

Chapter 6

Results and discussion

6.1 Analysed outputs

To perform a biomechanical analysis of both the tibiofemoral and patellofemoral joints, the variables considered and consequently extracted from each model were given as detailed below:

- mediolateral translation of the patella;
- anteroposterior translation of the femur;
- internal-external rotation of the femur;
- contact area in the tibiofemoral and patellofemoral joints;
- contact force in the tibiofemoral and patellofemoral joints;
- longitudinal deformation of the lateral and medial collateral ligaments.

6.2 Kinematic Analysis

6.2.1 Kinematics of the patellofemoral joint

For both developed models, the one concerning mechanical alignment and the one concerning kinematic alignment, the data regarding the patellofemoral joint were analysed starting from 30 degrees of flexion.

The graph shows the mediolateral translation of the patella during a knee squat movement. On the x-axis, the flexion angle of the knee measured in degrees is reported, while on the y-axis, the translation of the patella is shown in millimetres, referring to the translation on the global reference system of the model.

Taking first into account the model that simulates mechanical alignment, it can be seen that from the position of 10.85 mm, at the moment of contact engagement with the femoral trochlea, at 30 degrees of flexion, the patella translates laterally by approximately 1.22 mm. Subsequently, it can be observed that with a homogeneous tendency, it begins to translate medially approximately when the knee reaches 35 degrees of flexion. The position in which the patella is located, when the knee reaches 90 degrees of flexion, tends to stabilise until 105 degrees of flexion, which corresponds to a medial translation of approximately 7.5 mm with respect to the initial position of the sesamoid bone.

Similarly, we proceeded to analyse the data extracted from the kinematic alignment model. We recall that the same prosthesis was placed following the two different approaches although applied to the same bone geometries. Similarly, in the mechanical model, there is a slight initial lateral translation of about 1.65 mm at the moment of engagement. However, following this, a sharp medial translation of approximately 4.47 mm can be seen, up to 45 degrees of flexion, and then translating again in the lateral direction by 1.2 mm until the knee reaches 60

degrees of flexion. From that point on, the patella translates approximately linearly in a medial direction until it reaches a position of 5.49 mm medially in relation to the initial positioning.

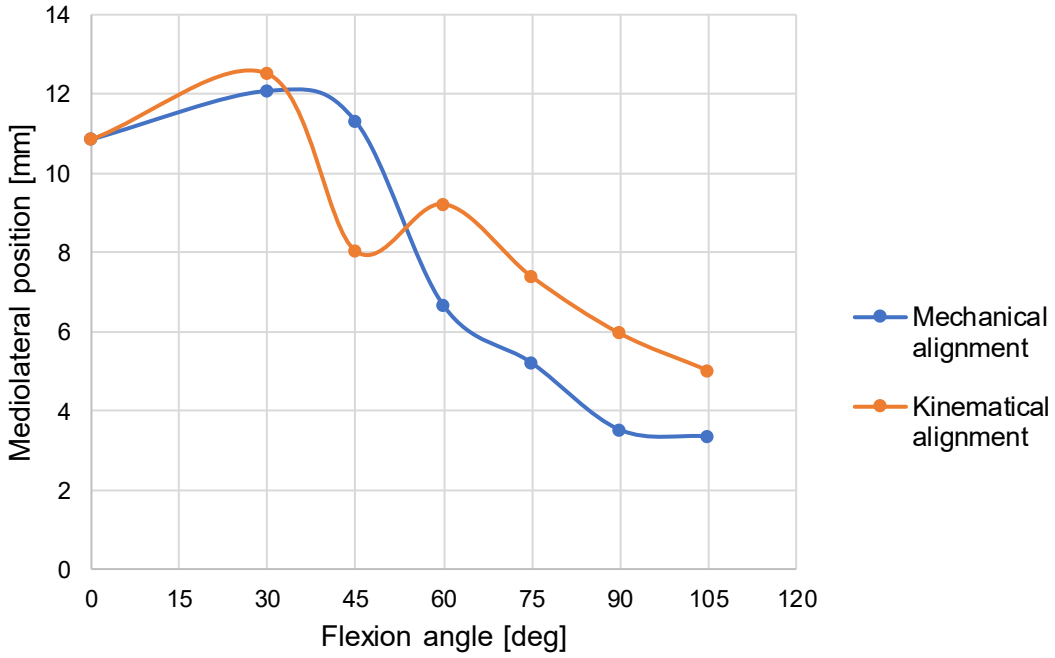

Figure 6.1: Mediolateral patella translation in the two TKA models. The mechanical alignment model is displayed in blue and in orange the kinematic alignment model.

6.2.2 Kinematics of the tibiofemoral joint

To assess the anteroposterior translation of the femur, the position of such bone with respect to the global reference system was first evaluated.

Taking into account the position of the epicondyles, medial and lateral, the behaviour of the bone in the two models was compared between the initial and final position in the squat movement. It emerges at first glance how the two models experience different translations, which are analysed in detail below.

Considering first the mechanical model, it can be seen that medially it undergoes a negligible translation, of 1.88 mm. On the contrary, in the lateral department, a significant evolution in the position of the epicondyle can be seen, as it translates anteriorly by 15.47 mm.

Taking into account the kinematic motion, the behaviour, as anticipated, is different. In fact, it is possible to observe how the trend of the medial and lateral translations, respectively, is reversed. As far as the medial epicondyle is concerned, it undergoes an appreciable anterior translation of 9.18 mm. In contrast, the corresponding lateral translates anteriorly by approximately only 3.37 mm.

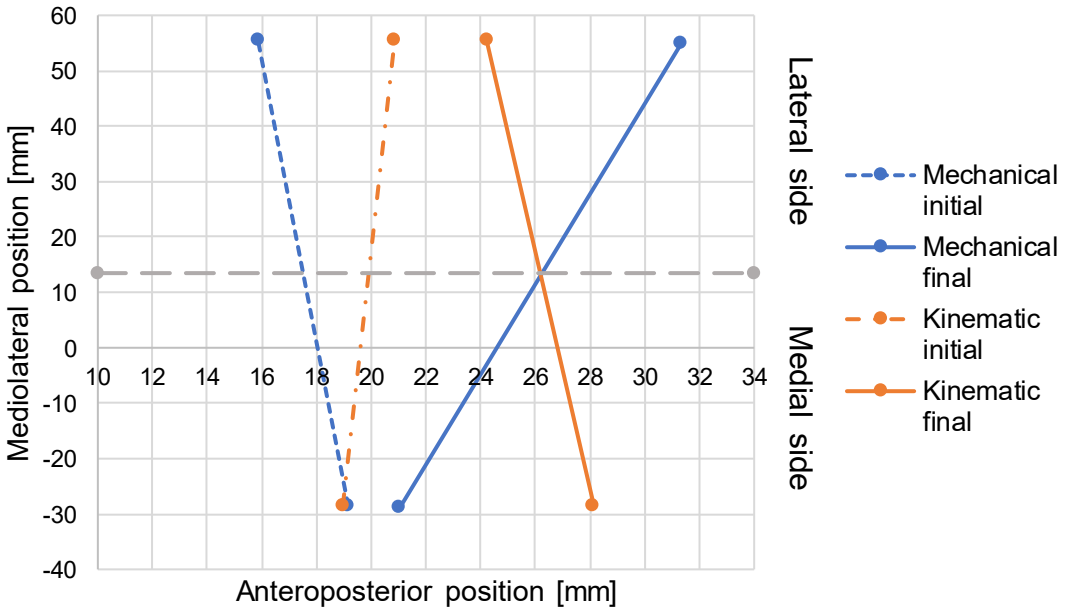

Figure 6.2: Position of the femoral epicondyles at the initial (dashed line) and final instant (solid line) instants of squat movement. In the positive values of the y-axis, the lateral component of the femur is located, and in the negative values the medial component. The mechanical alignment model is shown in blue, and in orange is the kinematic alignment model.

One separate comparison of the medial and lateral components was then analysed. Taking into account first the trend of medial anteroposterior translation, it can be seen that both models undergo anterior translation. In particular, when analysing the values in the range of flexion movement between 15 and 105 degrees, the medial component undergoes a clearly greater anterior translation in the kinematic model, in agreement with what was shown previously. Specifically, the anterior translation trend in the mechanical alignment model undergoes an increase up to 60 degrees of knee flexion and then progressively slows down, inducing the medial component to an overall anterior displacement of approximately 1.6 mm in this range. On the other hand, immediately undergoes a rapid increase in the anterior translation trend up to the last datum taken into consideration at 105 degrees of flexion. At this point, the anterior translation, with respect to the moment in which the knee is flexed by 15 degrees, is approximately 5.7 mm.

Taking into account now the lateral component, the difference in trend between the two models also stands out. In the kinematic model, the lateral translation is minimal; in fact, in the same range of flexion considered above, a slow increase in trend is evident, culminating in a total translation of 1.26 mm. As for the corresponding in the mechanical model, the increase is slow and constant up to 75 degrees of flexion, where the tendency between the two models is comparable. Thereafter, however, there is an abrupt increase of 8.33 mm in the anterior translation.

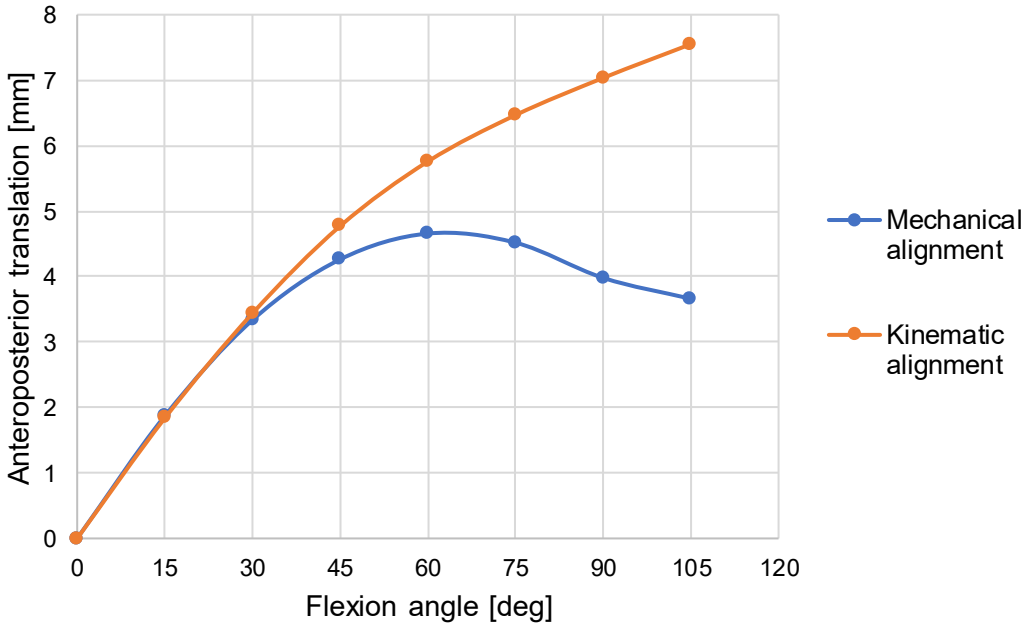

Figure 6.3: Translation of the anteroposterior medial femur condyle translation in the two TKA models. In blue is the mechanical alignment model and in orange, the kinematic alignment model.

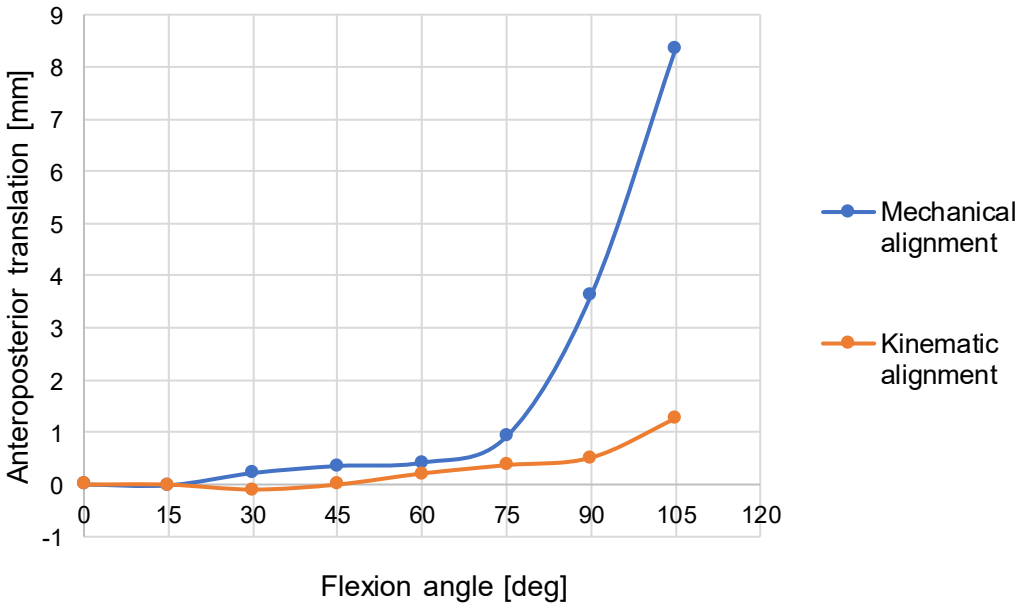

Figure 6.4: Anteroposterior lateral femur condyle translation in the two TKA models. In blue is the mechanical alignment model and in orange, the kinematic alignment model.

Finally, with regard to tibiofemoral joint kinematics, a kinematic analysis was conducted on the internal-external rotation of the femur with respect to the tibia. In this case, a similar trend is denoted in both models. In fact, it emerges that up to 60 degrees of flexion an external rotation is present; in this instance in fact the medial component translates anteriorly in both models with respect to the tibia in contrast to the respective lateral one. From the latter-mentioned angular value, the trend of both turns toward an internal rotation. In the mechanical alignment model, the overall rotation is less; in fact, an overall negligible external rotation of 0.10 degrees results. In contrast, analysing the kinematic model at 105 degrees of flexion, the joint is at an overall 1.66 degrees of intra-rotation.

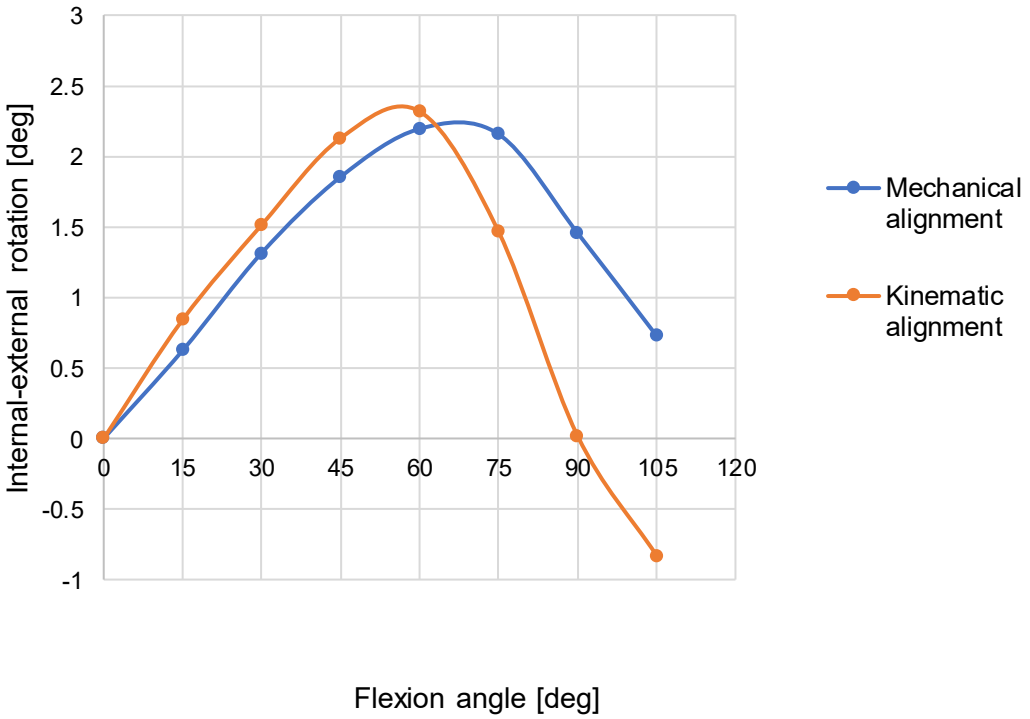

Figure 6.5: Internal-external femoral rotation in the two TKA models. Negative values represent internal rotation, and positive values external rotation. In blue is the mechanical alignment model and in orange, the kinematic alignment model.

6.3 Joint contact analysis

6.3.1 Patellofemoral joint contact

In this section, the contact of the patellofemoral joint is analyzed by comparing the contact area and the contact force between the femoral insert and the patellar UHMWPE component over a flexion range of 30 to 105 degrees. This range was considered because the patella makes contact with the femoral trochlea around 30 degrees of knee flexion, as mentioned earlier.

Qualitatively analysing the graph, we see in the data extracted from both models a rapid increase in contact area up to 60 degrees of flexion, although greater in the kinematic model. Indeed, this variable reaches 61.6 mm² at 60 degrees of flexion in the kinematic model versus the maximum peak of 54.8 mm² at about 64 degrees of flexion in the mechanical counterpart. After reaching this limit, in the kinematic model, it decreases slightly to 56.3 mm² at 75 degrees of flexion and then increases approximately linearly to a maximum of 76.0 mm² near the end of the range at 105 degrees of flexion.

In the mechanical model, on the contrary, after reaching the maximum contact area at 64.6 degrees of flexion, the contact area gradually decreases to 34.3 mm² at 90 degrees of flexion to remain at a comparable value of 37.4 mm² at 105 degrees of flexion.

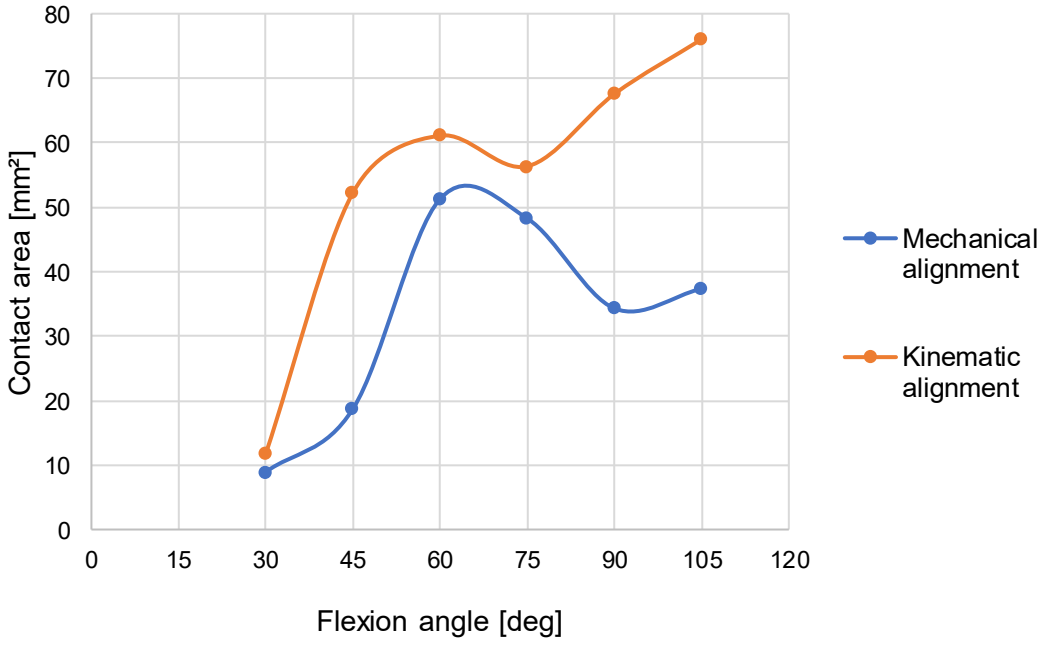

Figure 6.6: Patellofemoral contact area in the two TKA models. In blue is the mechanical alignment model and in orange, the kinematic alignment model.

Analysing now the contact force of the joint, we see an increase in force along with an increment in the flexion angle. The contact force in this case is greater in the mechanical model. Despite this, the course of this variation is consistent in the two models for a considerable part of the flexion. In the first range, between 30 and 60

degrees of flexion, the contact force increases rapidly, although less markedly in the kinematic model. Between 60 and 75 degrees of flexion, a plateau occurs in both models, with each value increasing by a slight amount of 33.7 N in the mechanical model and 37.0 N in the kinematic alignment model. The mechanical model peaks at 946.0 N of patellofemoral contact force at 90 degrees and then decreases marginally to 931.1 N at 105 degrees of flexion. On the contrary, the kinematic model reaches a maximum value of 819.6 N at 105 degrees of flexion after an approximately linear increase from 75 degrees of flexion.

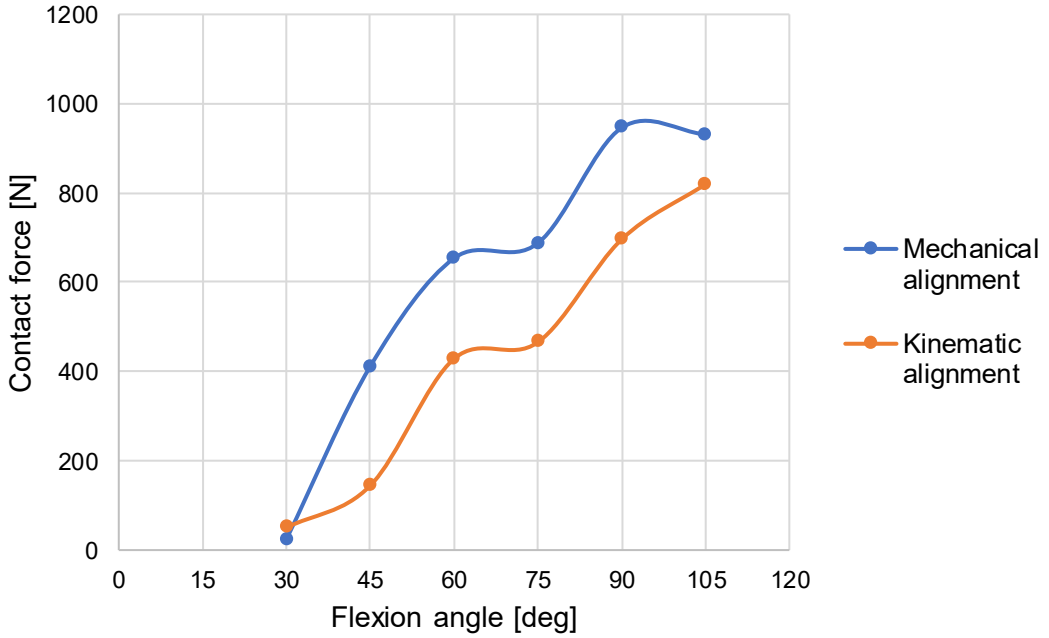

Figure 6.7: Patellofemoral contact force in the two TKA models. In blue is the mechanical alignment model and in orange, the kinematic alignment model.

Putting the data of contact areas and contact forces together now, it can be seen from the images shown in Figure 6.8 that the values of the contact pressures are comparable. In the mechanical model, it can be seen that after a higher contact pressure prevails in the medial component, the higher values move medially, reaching a peak at the end of the flexion. In contrast, the pressure in the kinematic model at 45 ° is lower. Subsequently, at 75 ° of flexion, the maximum value is found on the medial side of the patellar component. Finally, at 105 ° of flexion, as in the mechanical model, although to a lesser extent, the variable peak of the considered is in the medial section.

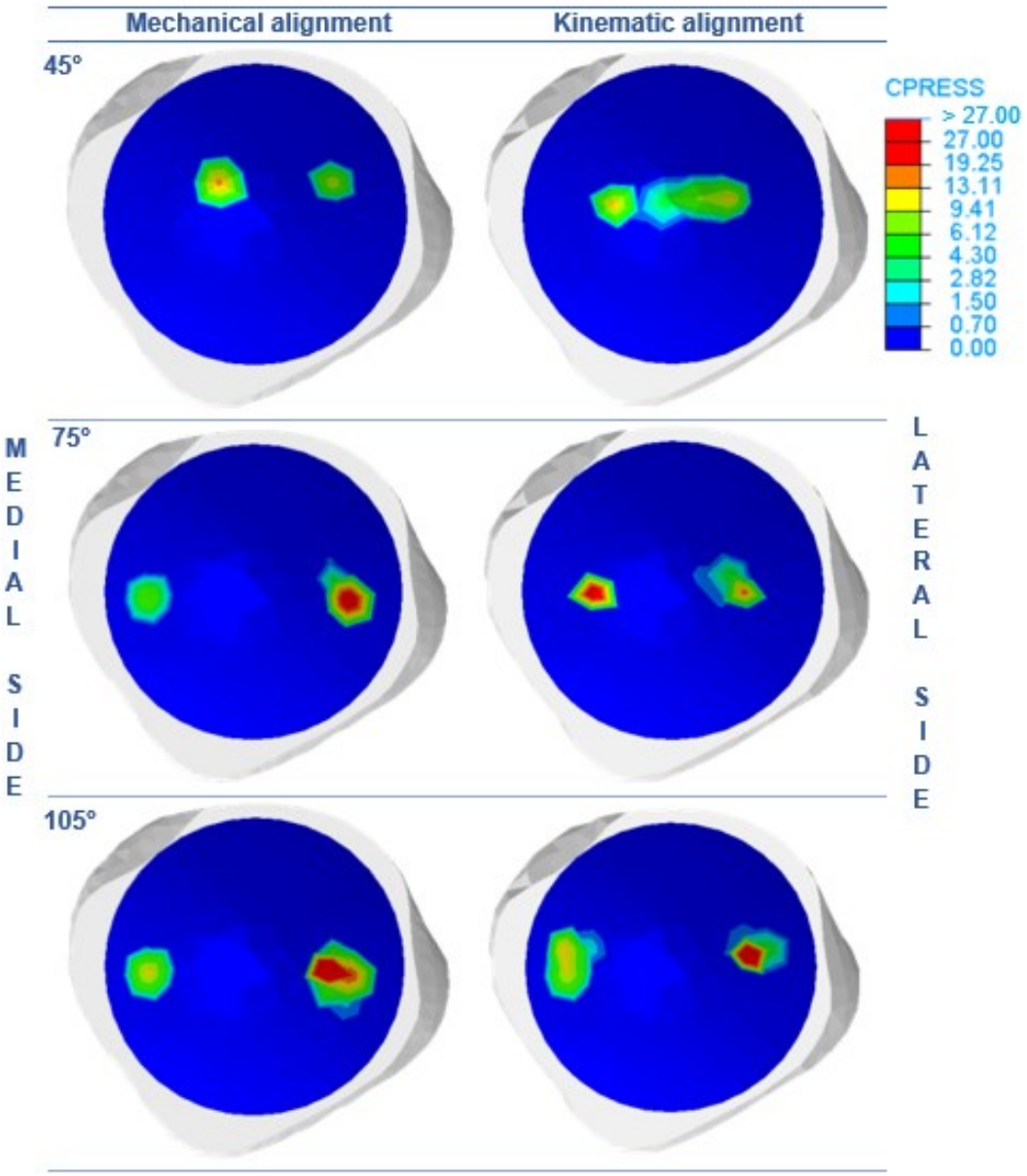

Figure 6.8: Patellofemoral contact pressure in the two TKA models. On the left, the mechanical alignment model and right side, the kinematic alignment model. Values in the legend are given in Megapascals [MPa].

6.3.2 Tibiofemoral joint contact

In the present section, the joint contact between the tibial insert and the femoral component in the respective joint is analysed, thus considering only the tibial plateau and not the post-cam contact of the posterior stabilised (PS) prosthesis.

First, the data regarding the contact area in the joint were extrapolated. Again, a similar behaviour of the two curves can be seen, which is analysed below.

At 15 degrees of flexion, values of 106.6 and 103.8 mm² are recorded for the mechanical and kinematic models, respectively. The model simulating mechanical alignment TKA proceeds, like its kinematic counterpart, with an increase of approximately 26 mm² over the initial value of the range considered. Thereafter, however, the joint contact area of the mechanical model decreases until it reaches approximately 122.6 mm², and then increases again until it peaks at 60 degrees of flexion, with a value of 145.9 mm². From this value, it decreases evenly until it hits the final value of the range at 105 degrees of flexion, which is 110.6 mm². The corresponding value in the kinematic model, on the other hand, after the value reached while the knee is flexed by 30 degrees, increases slightly in the first place to the value of 132.9 mm² at 45 degrees of flexion. Again, as in the other model, the maximum joint contact peak occurs at 60 degrees of flexion with a higher value. Indeed, in the kinematic model, the contact area reaches 158.6 mm². Once the peak is reached, this decreases to 141.0 mm² at 75 degrees of flexion before remaining approximately stable until 90 degrees, with a negligible decrease of approximately 4 mm². In the last range, between 90 and 105 degrees of flexion, the contact area undergoes a rapid decrease, greater than in the mechanical model where it achieves a minimum value of 79.8 mm².

Afterwards, the graph in the above-described ranges and the joint contact force is analysed. In contrast to the variable described above, throughout the range of motion, the force values for mechanical alignment are greater than their kinematic counterparts. Starting from a comparable value between the two models of approximately 1350 N, both undergo a rapid increase of 1230 N for the mechanical model and 846 N for the kinematic model, respectively. In the latter model, the force decreases slightly in a gradual progression until it reaches a local value of approximately 2001 N at 75 degrees of flexion. Then it increases linearly until it achieves a maximum value of 2467 N at 105 degrees of flexion. As far as the mechanical model is concerned, it hits the minimum value in the central area of the movement, before the second model, thus at 60 degrees of flexion, reaching 2534 N. From that rotational situation, the force developed at the interface between the components increases, reaching a maximum of 2868 N at 90 degrees of flexion, then diminishing to 2629 N at 105 degrees of flexion.

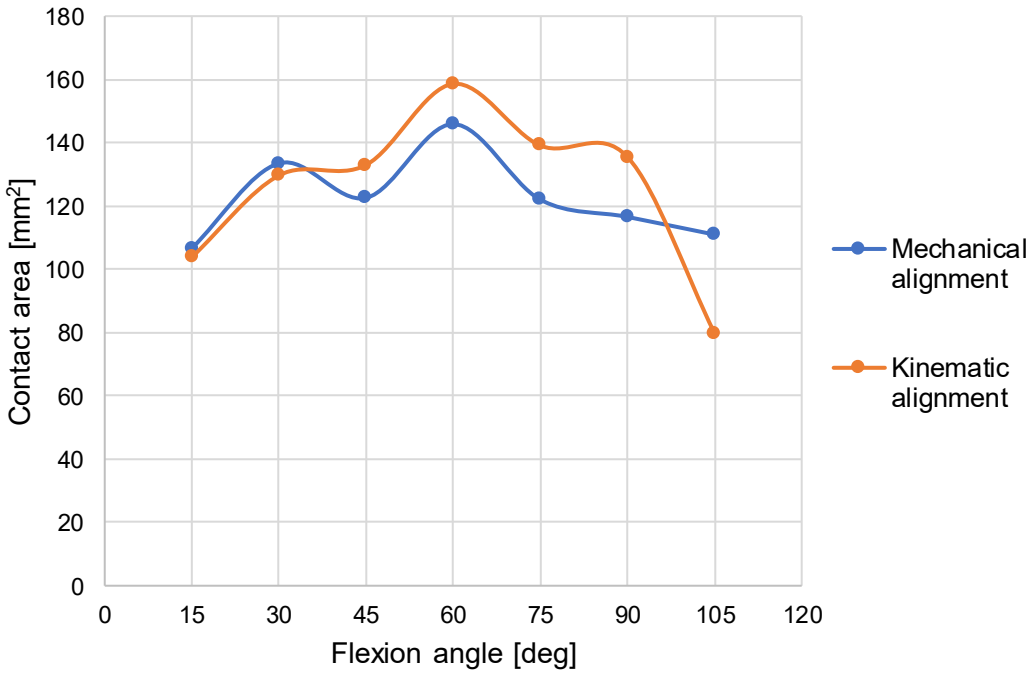

Figure 6.9: Tibiofemoral contact area in the two TKA models. In blue is the mechanical alignment model and in orange, the kinematic alignment model.

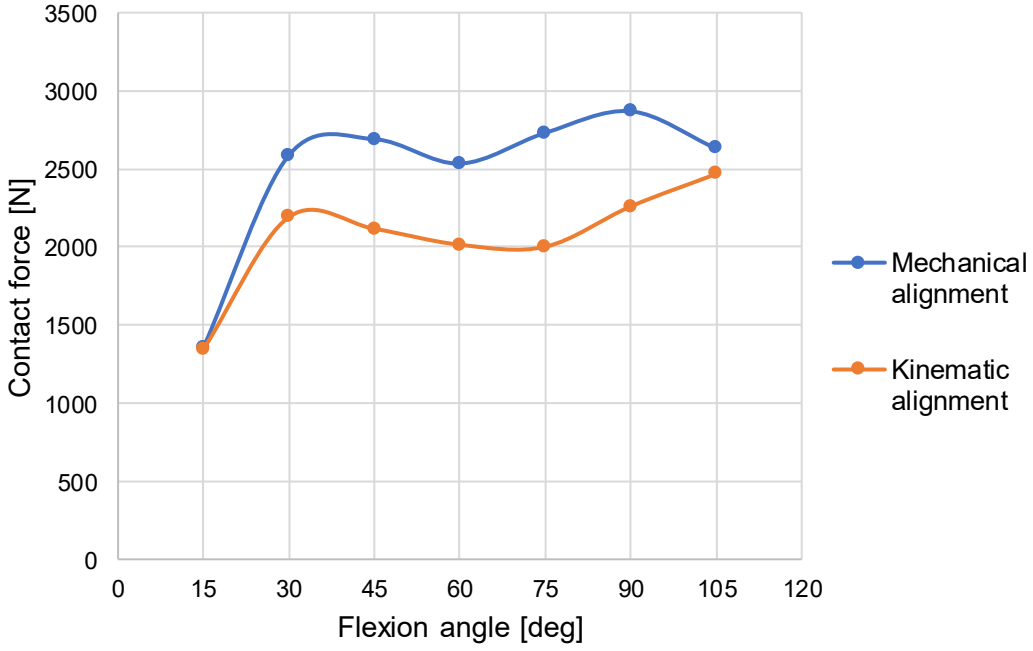

Figure 6.10: Tibiofemoral contact force in the two TKA models. In blue is the mechanical alignment model and in orange, the kinematic alignment model.

Analysing then how the contact pressure on the tibial insert varies, it is possible to evaluate the distribution of the contact between the femoral component and the polyethylene component as well as to establish the kinematics qualitatively.

It is noticeable, in fact, to note how in the mechanical model a greater contact pressure emerges in the medial area in contrast to a more uniform distribution present in the kinematic model.

In agreement with the contact area and contact force data in both models, the peak contact pressures on both sides tended to rise with increased flexion.

Finally, qualitatively, the evidence from the kinematic analysis is confirmed. It can be seen that there is less external rotation in the mechanical model than in the kinematic model, comparing the data.

With regard to the anteroposterior translations, it can be highlighted that in this instance, considering the relative movements of the two geometries, in both there is a major posterior translation of the lateral component to the disadvantage of the medial.

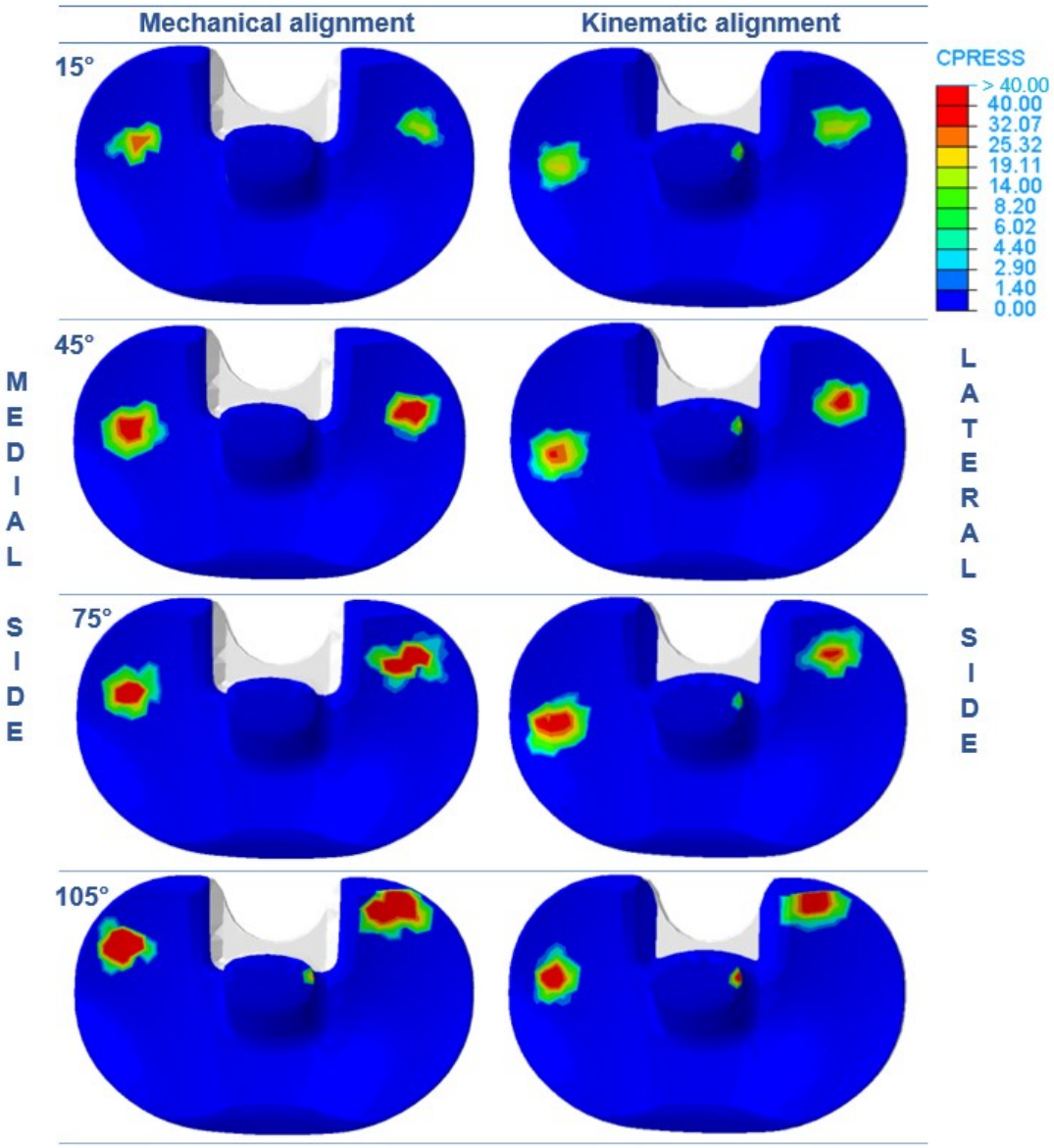

Figure 6.11: Tibiofemoral contact pressure in the two TKA models. On the left, the mechanical alignment model, and right side, the kinematic alignment model. Values in the legend are given in Megapascals [MPa].

6.4 Analysis of collateral ligaments strain

Data are derived from the analysis of ligament deformations in the longitudinal direction of the bundle. The analysis evolved by focusing in particular on the central area of the ligaments in order to reduce possible influences of inconsistent ligament deformations in the areas close to the proximal and distal insertions.

6.4.1 Medial collateral ligament strain

After an imposed pre-strain of - 4 % at 5 degrees of flexion, the MCL showed strain changes of < 3 % over the entire flexion range in the kinematic model. In this particular model, a minimum peak is reached at 75 degrees of flexion, where the ligament undergoes a longitudinal deformation of - 3 %. Beyond that flexion angle, relaxation ensued, corresponding to approximately 0.5 % deformation. Therefore, a total change of - 2.58 % in longitudinal ligament deformation is achieved.

Analysing now the mechanical model, following the pre-strain, congruent with the previous model shown, the deformation increases negatively in an approximately linear manner up to 75 degrees of flexion, reaching - 11 % deformation, thus a change of approximately - 7 % from the value of the initial pre-strain. Subsequently, at that point, the deformation continues to increase, although it slows down considerably. In fact, it can be seen that at the final instant of the range considered, it undergoes a further variation of only - 0.9 %, thus reaching a strain of - 7.9 % with respect to the initial value of the squat movement.

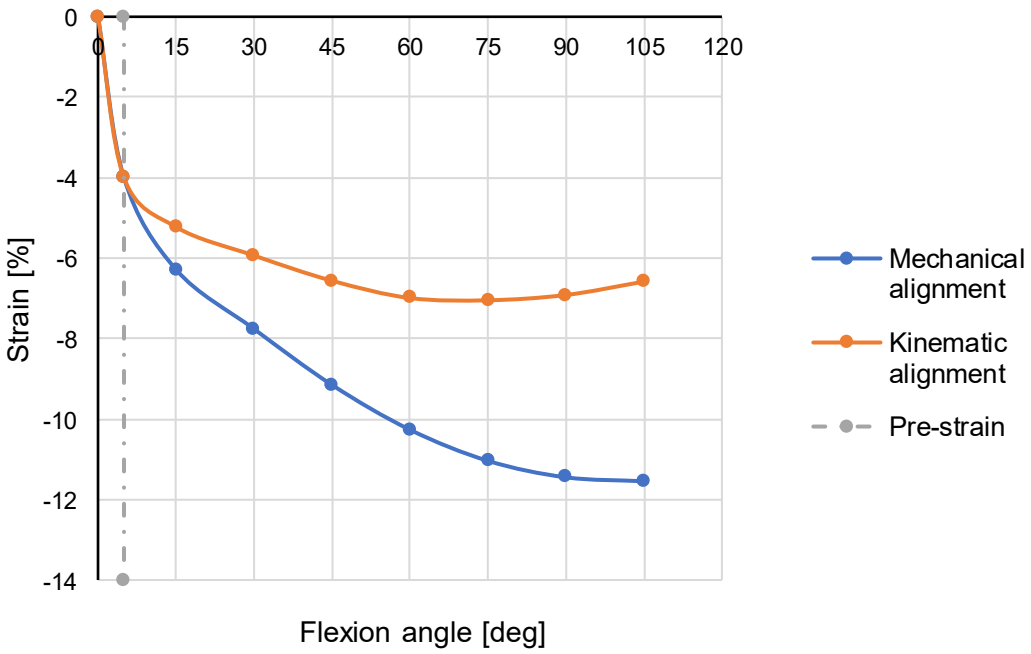

Figure 6.12: Variation in MCL percentage strain in the two TKA models. In blue, the mechanical alignment model, and in orange, the kinematic alignment model.

6.4.2 Lateral collateral ligament strain

In contrast to the medial counterpart, where the strain differences are usually greatest near the extension and reduce when the knee flexes, the lateral collateral ligament behaves differently. In fact, after an imposed prestrain of - 5 % up to 5 degrees of flexion, the ligament tends to relax in both models, remaining almost isometric for the greater part of the flexion range up to 90 degrees of flexion during the squat. The course of the curves remains comparable throughout the squat movement, with a 1 % greater difference for the mechanical model.

In the range between 90 degrees and 105 degrees of flexion in both models, the ligaments begin to contract again, undergoing a change in longitudinal strain of another- 0.4 %. Compared to the initial prestrain value, it can be seen that in the mechanical model, the LCL contracts by 0.5 % overall, while in the kinematic alignment model it contracts by 1.4 % overall.

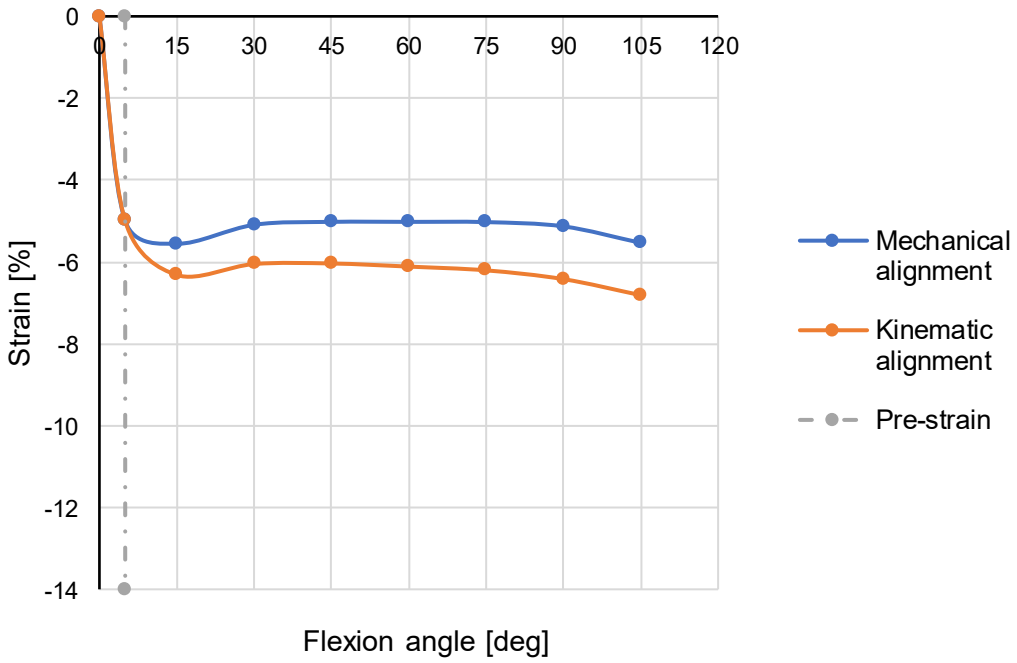

Figure 6.13: Variation in the LCL percentage strain in the two TKA models. In blue, the mechanical alignment model, and in orange, the kinematic alignment model.

6.5 Discussion

It is crucial to note that underlying the following considerations is the fact that the comparison between these two types of surgical application of a knee prosthesis is conditioned by the circumstance that in the kinematic alignment model, a prosthesis designed for the purpose of application in a mechanical alignment surgery is applied; a practice commonly used in the operating room. Thus, although the biomechanics resulting from a squat movement are naturally different, these differences are also influenced by this aspect of the prosthesis.

6.5.1 Kinematics

Different kinematics emerge in the two model types. It can be seen that the initial positions of the femur are compatible with the type of alignment. The kinematic model tends to realign the condyles, thus tending to be more physiological, with lateral contact anterior to medial.

In the kinematic model there is a behaviour consistent with the physiological one in that an extra-rotation movement, so called medial-pivot, is noticeable, during the squat movement, in fact a notable lateral translation emerges in contrast to the medial component, which translates with respect to the tibia only in the last range of flexion degrees.

With regard to patellofemoral kinematics, an instability in the kinematic model emerges from the analysis of the mediolateral translations. This can possibly be traced back to the concept that the prosthesis was not designed for this type of application. Consequently, the geometry of the femoral trochlear groove does not correspond as well as possible to the physiological one, probably inducing the highlighted instability. The concept of patellar maltracking was observed during flexion also in the study by Ishikawa et al. [68], which found a range of values comparable to the current study with consistent instability at 45° of flexion (Fig 6.14).

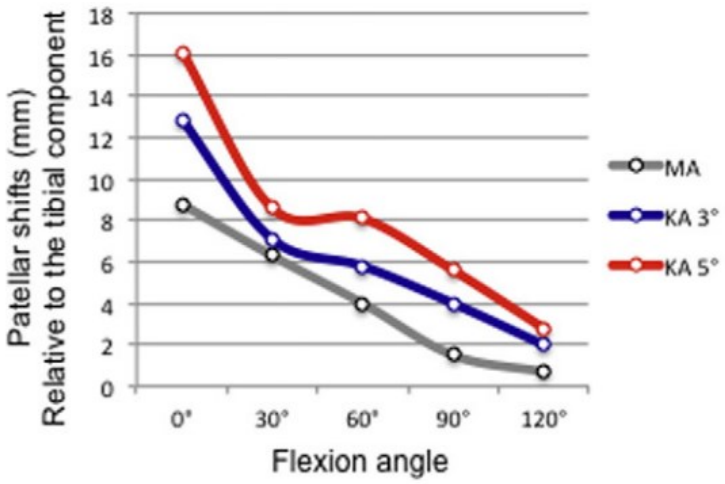

Figure 6.14: Diagrams showing patellar displacements during flexion in the three models in the study by Ishikawa et al 2015. MA: mechanical alignment, KA: kinematic alignment [68].

Comparing the values that emerged from the analysis, it is possible to find a match between the values of the shift, hence of the mediolateral translation of the patella, with regard to what was found in the mechanical model. In particular, according to the data from the 2018 study by Stephen et al. [69], the trend follows that of a native knee. This confirms the hypothesis mentioned earlier regarding the non-physiological instability found in the kinematic alignment model.

Among patellofemoral complications, patellar maltracking is a major problem that causes subluxation with increased polyethylene wear. Previous studies have shown that internally rotated femoral and tibial components cause patellar maltracking [70].

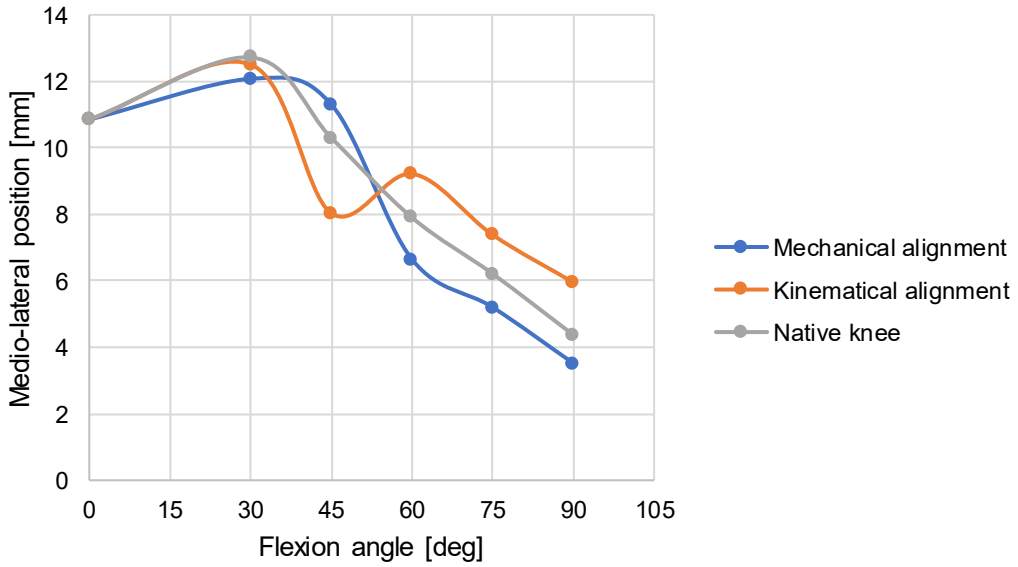

Figure 6.15: Comparison between patellar shift in the two TKA models with the mediolateral translation in a native knee. The mechanical alignment model is displayed in blue, in orange the kinematic alignment model, and in grey the native knee data from Stephen et al. [69].

6.5.2 Articular contact

In the context of the kinematic alignment model, a larger joint contact area is usually observed. This is due to the fact that a more natural inclination of the joint line makes the tibiofemoral interface of the prosthesis more congruent.

This concept is, in fact, consistent with the outcome of the current study in that in the mechanical model, the contact area is always lower than its kinematic counterpart. This therefore allows for a greater distribution of stresses, which is reflected in the lower tibiofemoral contact force throughout the flexion range considered.

6.5.3 Ligaments strain

As emerged from Bowman and Sekiya's study [71] around 30 degrees, the LCL becomes progressively slack, and its role in varus stability begins a transition to neighbouring structures. This concept is also reflected in the data extracted in the current study in that from just over 20 degrees of flexion the longitudinal strain decreases in both models.

The behaviour of the lateral collateral ligament that became slacker with increased flexion is also reflected in the study by Delport et al. [72], which demonstrates, in agreement with the current study, an approximate isometry of this ligament.

In terms of the medial collateral ligament, however, it is possible to note a clear difference between the two models in that it can be hypothesised that the neutral position of the prosthesis, at the level of the tibiofemoral joint strains more in the mediolateral direction respect to the same ligament in the kinematic alignment model. The latter, in fact, results in a strain that is more compatible with the physiological one, in a way that is in agreement with the ultimate aim of this technique.

Conclusions

In summary, the biomechanical advantages associated with kinematically aligned total knee arthroplasty (TKA) remain a subject of ambiguity. As elucidated earlier, a significant challenge within the kinematic alignment approach relates to the limited availability of implants specifically tailored for this method.

Currently, kinematically aligned total knee arthroplasties rely predominantly on conventional implants designed for mechanical alignment.

Generally, the implant configured with a kinematic alignment demonstrated a closer approximation to the average anatomical configuration compared to the model employing mechanical alignment. The findings of this study indicate that achieving a close alignment of the joint line with its natural position could yield superior clinical outcomes in the context of kinematically aligned TKA.

However, it should be noted that patellofemoral instability persists as prominent issue in kinematically aligned models and it is among the primary factors for necessitating a review of the design of TKA. Consequently, the adoption of kinematically aligned TKA with conventional implants designed for mechanical alignment can increase the risk of encountering patellofemoral joint complications.

It is essential to acknowledge the limitations of this study. First, the TKA system utilized in this investigation featured a femoral component and Posterior Stabilized (PS) tibial insert design, which could affect the biomechanical behaviour of the knee joint if an alternative prosthesis design was used. Conversely, although a computational model cannot fully replicate the intrinsic conditions of soft tissues, it does offer the advantage of facilitating comparisons between different alignment techniques under dynamic conditions, a feat unattainable in cadaver studies or fluoroscopic examinations, which do not permit intra-individual alignment comparisons.

In conclusion, kinematically aligned TKA demonstrates appreciable tibiofemoral kinematics. These results suggest that kinematically aligned TKA leads to knee kinematics that closely approximate physiological norms, thus contributing to improved clinical outcomes in comparison to mechanically aligned TKA. However, it is important to recognise that the patellofemoral joint kinematics exhibits notable weaknesses following kinematically aligned TKA. This aspect could potentially compromise the longevity of implants, particularly when commonly used prostheses are used within the kinematic alignment framework. The use of these computational models holds promise in improving our understanding of knee joint function, influenced by the choice of prosthesis and the alignment approach adopted by surgeons.

Acronyms

1D:	One-Dimensional
2D:	Two-Dimensional
3D:	Three-Dimensional
ACL:	Anterior Cruciate Ligament
AR:	Anterior Reference
CoCr:	Cobalt-Chrome Alloy
CR:	Cruciate Retaining Impant
CT:	Computed Tomography
DICOM:	Digital Imaging and Communications in Medicine
DOF:	Degree of Freedon
FEA:	Finite Elementanalysis
FEM:	Finite Element Method
FHC:	Femoral Hip Centre
FKC:	Femoral Knee Centre
FLCP:	Lateral Posterior Femoral Condyle
FMA:	Femoral Mechanical Angle
FMAx:	Femoral Mechanical Axis
FMCP:	Posterior Medial Femoral Condyle
HKA:	Hip-Knee-Ankle Angle
ISO:	Isotropic
KA:	Kinematic Alignment
LCL:	Lateral Collateral Ligament
LR:	Lateral Patellar Retinaculum
MA:	Mechanical Alignment
MCL:	Medial Collateral Ligament
MPFL:	Medial Patellofemoral Ligament
MRI:	Magnetic Resonance Imaging
OA:	Osteoarthritis
ORTH:	Orthotropic
PCL:	Posterior Cruciate Ligament

PMMA:	Polymethyl Methacrylate
PR:	Posterior Reference
PS:	Posterior Stabilised Implant
PT:	Patellar Tendon
QT:	Quadriceps Tendon
ROM:	Range of Motion
sMCL:	Superficial Medial Collateral Ligament
TAC:	Tibial Ankle Centre
TI:	Transversely Isotropic
TKA:	Total Knee Arthroplasty
TKC:	Tibial Knee Centre
TLCC:	Centre of The Lateral Tibial Condyle
TMA:	Tibial Mechanical Angle
TMAx:	Tibial Mechanical Axis
TMCC:	Centre of The Medial Tibial Condyle
UHMWPE:	Ultrahigh Molecular Weight Polyethylene

Bibliography

[1] F. Flandry and G. Hommel, “Normal Anatomy and Biomechanics of the Knee,” 2011. [Online]. Available: www.sportsmedarthro.com

[2] B. Innocenti, F. Galbusera, and E. Bori, *Human Orthopaedic Biomechanics: Fundamentals, Devices and Applications*. Mara Connor, 2022.

[3] S. Standring, *Gray’s Anatomy. The Anatomical Basis of Clinical Practice* , 40th ed., vol. 2. Elsevier, 2008.

[4] F. H. Netter, *Atlas of human anatomy*, 7th ed. Philadelphia: Elsevier, 2019.

[5] R. Koshi, *Cunningham’s manual of pactical anatomy - Upper and lower limbs*, 16th ed., vol. Volume 1. Oxford: Oxford University Press, 2017.

[6] G. Criscenti *et al.*, “Material and structural tensile properties of the human medial patello-femoral ligament,” *J Mech Behav Biomed Mater*, vol. 54, pp. 141–148, Feb. 2016, doi: 10.1016/j.jmbbm.2015.09.030.

[7] R. F. LaPrade, A. H. Engebretsen, T. V. Ly, S. Johansen, F. A. Wentorf, and L. Engebretsen, “The anatomy of the medial part of the knee,” *Journal of Bone and Joint Surgery*, vol. 89, no. 9, pp. 2000–2010, 2007, doi: 10.2106/JBJS.F.01176.

[8] E. W. James, C. M. Laprade, and R. F. Laprade, “Anatomy and Biomechanics of the Lateral Side of the Knee and Surgical Implications,” 2015. [Online]. Available: www.sportsmedarthro.com

[9] E. W. James, C. M. Laprade, and R. F. Laprade, “Anatomy and Biomechanics of the Lateral Side of the Knee and Surgical Implications,” 2015. [Online]. Available: www.sportsmedarthro.com

[10] D. Lee, D. Stinner, and H. Mir, “Quadriceps and patellar tendon ruptures,” *J Knee Surg*, vol. 26, no. 5, pp. 301–308, Oct. 2013, doi: 10.1055/s-0033-1353989.

[11] M. Golman *et al.*, “Rethinking Patellar Tendinopathy and Partial Patellar Tendon Tears: A Novel Classification System,” *American Journal of Sports Medicine*, vol. 48, no. 2, pp. 359–369, Feb. 2020, doi: 10.1177/0363546519894333.

[12] S. Standring, *Gray’s Anatomy. The Anatomical Basis of Clinical Practice*, 40th ed., vol. 2. London: Elsevier, 2008.

[13] A. R. Markes, J. D. Hodax, and C. B. Ma, “Meniscus Form and Function,” *Clinics in Sports Medicine*, vol. 39, no. 1. W.B. Saunders, pp. 1–12, Jan. 01, 2020. doi: 10.1016/j.csm.2019.08.007.

[14] E. S. Grood and W. J. Suntay, “A Joint Coordinate System for the Clinical Description of Three-Dimensional Motions: Application to the Knee 1,” 1983. [Online]. Available: http://biomechanical.asmedigitalcollection.asme.org/

[15] J. H. Naendrup, J. P. Zlotnicki, C. I. Murphy, N. K. Patel, R. E. Debski, and V. Musahl, “Influence of knee position and examiner-induced motion on the kinematics of the pivot shift,” *J Exp Orthop*, vol. 6, no. 1, Dec. 2019, doi: 10.1186/s40634-019-0183-7.

[16] O. Brantigan and A. Voshell, “The mechanics of the ligaments and menisci of the knee joint,” *J Bone Joint Surg.*, vol. 23, pp. 44–66, 1941.

[17] V. Pinskerova and P. Vavrik, “Knee anatomy and biomechanics and its relevance to knee replacement,” in *Personalized Hip and Knee Joint Replacement*, Springer International Publishing, 2020, pp. 159–168. doi: 10.1007/978-3-030-24243-5_14.

[18] D. D. D’lima, B. J. Fregly, S. Patil, N. Steklov, and C. W. Colwell, “Knee joint forces: prediction, measurement, and significance,” La Jolla, CA, USA, 2012.

[19] G. L. Smidt, “BIOMECHANICAL ANALYSIS OF KNEE FLEXION AND EXTENSION,” *J. Biomechanics.* , vol. 6, pp. 79–92, 1973.

[20] J. G. Betts, K. A. Young, J. A. Wise, E. Johnson, B. Poe, and D. H. Kruse, *Anatomy and Physiology*, OpenStax. Houston, Texas, 2013. Accessed: Aug. 19, 2023. [Online]. Available: https://openstax.org/books/anatomy-and-physiology

[21] A. A. Amis, W. Senavongse, and A. M. J. Bull, “Patellofemoral kinematics during knee flexion-extension: An in vitro study,” *Journal of Orthopaedic Research*, vol. 24, no. 12, pp. 2201–2211, Dec. 2006, doi: 10.1002/jor.20268.

[22] R. Sergio, P. Stefano, and M. Matteo, “Patello-femoral replacement,” in *Personalized Hip and Knee Joint Replacement*, Springer International Publishing, 2020, pp. 233–242. doi: 10.1007/978-3-030-24243-5_20.

[23] C. T. Lim, A. Bershadsky, and M. P. Sheetz, “Mechanobiology,” *Journal of the Royal Society Interface*, vol. 7, no. SUPPL. 3. Royal Society, Jun. 06, 2010. doi: 10.1098/rsif.2010.0150.focus.

[24] S. Roberts *et al.*, “Ageing in the musculoskeletal system: Cellular function and dysfunction throughout life,” *Acta Orthop*, vol. 87, pp. 15–25, Dec. 2016, doi: 10.1080/17453674.2016.1244750.

[25] L. Sharma, “Osteoarthritis of the Knee,” *New England Journal of Medicine*, vol. 384, no. 1, pp. 51–59, Jan. 2021, doi: 10.1056/NEJMcp1903768.

[26] T. Brabant and D. Stichtenoth, “Medikamentöse arthrosetherapie im alter,” *Z Rheumatol*, vol. 64, no. 7, pp. 467–472, Oct. 2005, doi: 10.1007/s00393-005-0778-5.

[27] C. Jiang, Z. Liu, Y. Wang, Y. Bian, B. Feng, and X. Weng, “Posterior cruciate ligament retention versus posterior stabilization for total knee arthroplasty: A meta-analysis,” *PLoS One*, vol. 11, no. 1, Jan. 2016, doi: 10.1371/journal.pone.0147865.

[28] A. Aprato, S. Risitano, L. Sabatini, M. Giachino, G. Agati, and A. Massè, “Cementless total knee arthroplasty,” *Annals of Translational Medicine*, vol. 4, no. 7. AME Publishing Company, Apr. 01, 2016. doi: 10.21037/atm.2016.01.34.

[29] R. A. Malinzak *et al.*, “The effect of rotating platform TKA on strain distribution and torque transmission on the proximal tibia,” *Journal of Arthroplasty*, vol. 29, no. 3, pp. 541–547, Mar. 2014, doi: 10.1016/j.arth.2013.08.024.

[30] N. Poirier, P. Graf, and F. Dubrana, “Mobile-bearing versus fixed-bearing total knee implants. Results of a series of 100 randomised cases after 9 years follow-up,” *Orthopaedics and Traumatology: Surgery and Research*, vol. 101, no. 4, pp. S187–S192, Feb. 2015, doi: 10.1016/j.otsr.2015.03.004.

[31] “Design, Shape, and Materials of Total Knee Replacement,” Musculoskeletalkey.com. Accessed: Aug. 23, 2023. [Online]. Available: https://musculoskeletalkey.com/design-shape-and-materials-of-total-knee-replacement/

[32] S. K. Kulkarni, M. A. R. Freeman, J. C. Poal-Manresa, J. I. Asencio, and J. J. Rodriguez, “The patellofemoral joint in total knee arthroplasty: Is the design of the trochlea the critical factor?,” *Journal of Arthroplasty*, vol. 15, no. 4, pp. 424–429, 2000, doi: 10.1054/arth.2000.4342.

[33] B. K. Daines and D. A. Dennis, “Gap balancing vs. measured resection technique in total knee arthroplasty,” *Clinics in Orthopedic Surgery*, vol. 6, no. 1. Korean Orthopaedic Association, pp. 1–8, 2014. doi: 10.4055/cios.2014.6.1.1.

[34] S. Lustig, E. Sappey-Marinier, C. Fary, E. Servien, S. Parratte, and C. Batailler, “Personalized alignment in total knee arthroplasty: Current concepts,” *SICOT-J*, vol. 7. EDP Sciences, 2021. doi: 10.1051/sicotj/2021021.

[35] Y. Minoda, “Alignment techniques in total knee arthroplasty,” *Journal of Joint Surgery and Research*, vol. 1, no. 1, pp. 108–116, Dec. 2023, doi: 10.1016/j.jjoisr.2023.02.003.

[36] D. S. Hungerford and K. A. Krackow, “Total Joint Arthroplasty of the Knee.” [Online]. Available: http://journals.lww.com/clinorthop

[37] E. Sappey-Marinier *et al.*, “Kinematic versus mechanical alignment for primary total knee arthroplasty with minimum 2 years follow-up: A systematic review,” *SICOT J*, vol. 6, 2020, doi: 10.1051/sicotj/2020014.

[38] S. Nojiri *et al.*, “Which is better? Anterior or posterior referencing for femoral component position in total knee arthroplasty,” *Journal of Orthopaedic Surgery*, vol. 29, no. 1, 2021, doi: 10.1177/23094990211002325.

[39] A. Completo, F. Fonseca, C. Relvas, A. Ramos, and J. A. Simões, “Improved stability with intramedullary stem after anterior femoral notching in total knee arthroplasty,” *Knee Surgery, Sports Traumatology, Arthroscopy*, vol. 20, no. 3, pp. 487–494, Mar. 2012, doi: 10.1007/s00167-011-1557-2.

[40] S. Cowin and S. Doty, *Tissue Mechanics*. New York: Springer, 2007.

[41] R. Popescu, E. G. Haritinian, and S. Cristea, “Relevance of finite element in total knee arthroplasty - Literature review,” *Revista Chirurgia*, vol. 114, no. 4, pp. 437–442, 2019, doi: 10.21614/chirurgia.114.4.437.

[42] S. C. Cowin and M. M. Mehrabadi, “Identification of the elastic symmetry of bone and other materials,” 1989.

[43] T. L. Norman, G. Thyagarajan, V. C. Saligrama, T. A. Gruen, and J. D. Blaha, “Stem surface roughness alters creep induced subsidence and ‘taper-lock’ in a cemented femoral hip prosthesis,” 2001.

[44] S. Pianigiani, D. Croce, M. D. ’ Aiuto, W. Pascale, and B. Innocenti, “Sensitivity analysis of the material properties ofdifferent soft-tissues: implications for a subject-specific knee arthroplasty,” *Muscles, Ligaments and Tendons Journal* , vol. 7, pp. 546–557, 2017.

[45] T. M. Keaveny, E. F. Morgan, G. L. Niebur, and O. C. Yeh, “BIOMECHANICS OF TRABECULAR BONE,” 2001. [Online]. Available: www.annualreviews.org

[46] J. Kabel, B. Van Rietbergen, M. Dalstra, A. Odgaard, and R. Huiskes, “The role of an e!ective isotropic tissue modulus in the elastic properties of cancellous bone,” 1999.

[47] O. Kayabasi and B. Ekici, “The effects of static, dynamic and fatigue behavior on three-dimensional shape optimization of hip prosthesis by finite element method,” *Mater Des*, vol. 28, no. 8, pp. 2269–2277, 2007, doi: 10.1016/j.matdes.2006.08.012.

[48] B. Innocenti, E. Truyens, L. Labey, P. Wong, J. Victor, and J. Bellemans, “Can medio-lateral baseplate position and load sharing induce asymptomatic local bone resorption of the proximal tibia? A finite element study,” *J Orthop Surg Res*, vol. 4, no. 1, 2009, doi: 10.1186/1749-799X-4-26.

[49] F. Galbusera *et al.*, “Material models and properties in the finite element analysis of knee ligaments: A literature review,” *Frontiers in Bioengineering and Biotechnology*, vol. 2, no. NOV. Frontiers Media S.A., 2014. doi: 10.3389/fbioe.2014.00054.

[50] E. Peña, B. Calvo, M. A. Martínez, and M. Doblaré, “A three-dimensional finite element analysis of the combined behavior of ligaments and menisci in the healthy human knee joint,” *J Biomech*, vol. 39, no. 9, pp. 1686–1701, 2006, doi: 10.1016/j.jbiomech.2005.04.030.

[51] Y. Song, R. E. Debski, V. Musahl, M. Thomas, and S. L. Y. Woo, “A three-dimensional finite element model of the human anterior cruciate ligament: A computational analysis with experimental validation,” *J Biomech*, vol. 37, no. 3, pp. 383–390, 2004, doi: 10.1016/S0021-9290(03)00261-6.

[52] B. Innocenti, Ö. F. Bilgen, L. Labey, G. H. Van Lenthe, J. Vander Sloten, and F. Catani, “Load sharing and ligament strains in balanced, overstuffed and understuffed UKA. A validated finite element analysis,” *Journal of Arthroplasty*, vol. 29, no. 7, pp. 1491–1498, 2014, doi: 10.1016/j.arth.2014.01.020.

[53] L. Blankevoort, J. H. Kuiper, R. Hijiskes+, and H. J. Grootenboer~, “ARTICULAR CONTACT IN A THREE-DIMENSIONAL MODEL OF THE KNEE,” 1991.

[54] C. W. Clary, C. K. Fitzpatrick, L. P. Maletsky, and P. J. Rullkoetter, “The influence of total knee arthroplasty geometry on mid-flexion stability: An experimental and finite element study,” *J Biomech*, vol. 46, no. 7, pp. 1351–1357, Apr. 2013, doi: 10.1016/j.jbiomech.2013.01.025.

[55] J. P. Halloran, A. J. Petrella, and P. J. Rullkoetter, “Explicit finite element modeling of total knee replacement mechanics,” *J Biomech*,

vol. 38, no. 2, pp. 323–331, Feb. 2005, doi: 10.1016/j.jbiomech.2004.02.046.

[56] J. Zelle, S. A. W. Van de Groes, M. C. de Waal Malefijt, and N. Verdonschot, “Femoral loosening of high-flexion total knee arthroplasty: The effect of posterior cruciate ligament retention and bone quality reduction,” *Med Eng Phys*, vol. 36, no. 3, pp. 318–324, 2014, doi: 10.1016/j.medengphy.2013.11.015.

[57] J. Zelle, D. Janssen, J. Van Eijden, M. De Waal Malefijt, and N. Verdonschot, “Does high-flexion total knee arthroplasty promote early loosening of the femoral component?,” *Journal of Orthopaedic Research*, vol. 29, no. 7, pp. 976–983, Jul. 2011, doi: 10.1002/jor.21363.

[58] E. Bori and B. Innocenti, “Biomechanical Analysis of Femoral Stem Features in Hinged Revision TKA with Valgus or Varus Deformity: A Comparative Finite Elements Study,” *Applied Sciences (Switzerland)*, vol. 13, no. 4, Feb. 2023, doi: 10.3390/app13042738.

[59] L. Shapiro and G. Stockman, *Computer vision*. Washington, 2000.

[60] S. Zachow, M. Zilske, and H.-C. Hege, “3D reconstruction of individual anatomy from medical image data: Segmentation and geometry processing,” 2007.

[61] C. E. Kahn, J. A. Carrino, M. J. Flynn, D. J. Peck, and S. C. Horii, “DICOM and Radiology: Past, Present, and Future,” *Journal of the American College of Radiology*, vol. 4, no. 9, pp. 652–657, 2007, doi: 10.1016/j.jacr.2007.06.004.

[62] M. T. Hirschmann, L. B. Moser, F. Amsler, H. Behrend, V. Leclercq, and S. Hess, “Phenotyping the knee in young non-osteoarthritic knees shows a wide distribution of femoral and tibial coronal alignment,” *Knee Surgery, Sports Traumatology, Arthroscopy*, vol. 27, no. 5, pp. 1385–1393, May 2019, doi: 10.1007/s00167-019-05508-0.

[63] J. Victor, D. Van Doninck, L. Labey, B. Innocenti, P. M. Parizel, and J. Bellemans, “How precise can bony landmarks be determined on a CT scan of the knee?,” *Knee*, vol. 16, no. 5, pp. 358–365, Oct. 2009, doi: 10.1016/j.knee.2009.01.001.

[64] J. R. Leach, V. L. Rayz, M. R. K. Mofrad, and D. Saloner, “An efficient two-stage approach for image-based FSI analysis of atherosclerotic arteries,” *Biomech Model Mechanobiol*, vol. 9, no. 2, pp. 213–223, Apr. 2010, doi: 10.1007/s10237-009-0172-3.

[65] H. P. W. van Jonbergen, B. Innocenti, G. L. Gervasi, L. Labey, and N. Verdonschot, “Differences in the stress distribution in the distal femur between patellofemoral joint replacement and total knee replacement:

A finite element study," *J Orthop Surg Res*, vol. 7, no. 1, Jun. 2012, doi: 10.1186/1749-799X-7-28.

[66] J. Victor, "A COMPARATIVE STUDY ON THE BIOMECHANICS OF THE NATIVE HUMAN KNEE JOINT AND TOTAL KNEE ARTHROPLASTY," 2009.

[67] *ABAQUS/CAE User's Manual*. 2000.

[68] M. Ishikawa, S. Kuriyama, H. Ito, M. Furu, S. Nakamura, and S. Matsuda, "Kinematic alignment produces near-normal knee motion but increases contact stress after total knee arthroplasty: A case study on a single implant design," *Knee*, vol. 22, no. 3, pp. 206–212, Jun. 2015, doi: 10.1016/j.knee.2015.02.019.

[69] J. Stephen, A. Alva, P. Lumpaopong, A. Williams, and A. A. Amis, "A cadaveric model to evaluate the effect of unloading the medial quadriceps on patellar tracking and patellofemoral joint pressure and stability," *J Exp Orthop*, vol. 5, no. 1, Dec. 2018, doi: 10.1186/s40634-018-0150-8.

[70] S. Nakamura, K. Shima, S. Kuriyama, K. Nishitani, H. Ito, and S. Matsuda, "Tibial Tubercle-Trochlear Groove Distance Influences Patellar Tilt After Total Knee Arthroplasty," *Journal of Arthroplasty*, vol. 34, no. 12, pp. 3080–3087, Dec. 2019, doi: 10.1016/j.arth.2019.07.038.

[71] K. F. Bowman and J. K. Sekiya, "Anatomy and Biomechanics of the Posterior Cruciate Ligament, Medial and Lateral Sides of the Knee," 2010. [Online]. Available: www.sportsmedarthro.com

[72] H. Delport, L. Labey, B. Innocenti, R. De Corte, J. Vander Sloten, and J. Bellemans, "Restoration of constitutional alignment in TKA leads to more physiological strains in the collateral ligaments," *Knee Surgery, Sports Traumatology, Arthroscopy*, vol. 23, no. 8, pp. 2159–2169, Aug. 2015, doi: 10.1007/s00167-014-2971-z.